Measuring Facets of Polyhedra to Predict Usefulness in Branch-and-cut Algorithms

A Thesis
Presented to
The Academic Faculty

by

Braden K. Hunsaker

In Partial Fulfillment
of the Requirements for the Degree
Doctor of Philosophy in the
Program in Algorithms, Combinatorics, and Optimization

Georgia Institute of Technology
July 2003

Measuring Facets of Polyhedra to Predict Usefulness in Branch-and-cut Algorithms

Approved by:

Professor Ellis L. Johnson, Co-advisor

Professor Richard Duke

Professor Craig A. Tovey, Co-advisor

Professor Martin Savelsbergh

Professor Shabbir Ahmed

Date Approved 8/18/2003

ACKNOWLEDGEMENTS

My advisors, Craig Tovey and Ellis Johnson, have made tremendous impacts on my life. Craig, thanks for many valuable conversations on academic and non-academic matters. I can't tell you how much I've learned from you. Ellis, thanks for being there when I most needed some guidance. You've shown me new ways to look at problems, providing invaluable insight into the questions I've pursued. For both of you, I may have learned the most just from the examples you've set as researchers, advisors, and kind concerned people.

Thanks to the members of my committee—Shabbir Ahmed, Richard Duke, and Martin Savelsbergh—for providing thoughtful feedback and suggestions as I began to write the dissertation. Thanks to Lisa Evans for sharing her data and her insights on cyclic group and knapsack shooting experiments. Thanks to Jan Karel Lenstra for bringing the first reference to Kuhn's shooting experiment to my attention.

I have very much enjoyed my time at Georgia Tech, thanks mostly to the excellent faculty, staff, and students. In particular, Gary Parker is ISyE's best asset from a graduate student's point of view. Dr. Parker was always ready to talk to me in times of stress. His frank counsel and support is much appreciated. I also want to thank Martin Savelsbergh, who not only taught several of my favorite classes, but also worked with me on my first article to appear in print and recommended me for a rewarding summer internship.

I have made a number of lifelong friends in my time here and will particularly miss our semi-regular lunch crowd, which came up with solutions for several of the world's problems.

I want to thank all my family—immediate, extended, step, and in-law—for your love and support. In particular, my parents Chad Hunsaker and Kirsten Flamand and my siblings Justin and Krystal have been tremendously supportive throughout my life.

Finally, I want to thank my wife, Amanda. Your support, love, and confidence in me has made an enormous difference in my life. Thanks for your patience and for helping me to become a better person. I can't wait to start the next phase of our life together.

TABLE OF CONTENTS

ACKNOWLEDGEMENTS iii

LIST OF TABLES viii

LIST OF FIGURES xi

SUMMARY xiii

I INTRODUCTION 1

1.1 Background on branch-and-cut algorithms for integer programming . . . 1

1.1.1 Linear programming and polyhedral theory 2

1.1.2 Integer programming 4

1.2 Purpose and scope of this dissertation 6

1.3 Literature review 9

1.3.1 Measures of facets 9

1.3.2 Computational studies 11

1.3.3 Size of the branch-and-bound tree 11

1.4 Additional background 12

1.4.1 Chvátal-Gomory inequalities and rank 13

1.4.2 Complexity and asymptotic notation 14

1.4.3 Probability 14

1.4.4 Graph theory 15

1.4.5 Polyhedra and polarity 16

1.5 Structure of this dissertation 18

II POSSIBLE MEASURES OF FACETS AND CUTTING PLANES . 20

2.1 Explanation of each measure 20

2.1.1 Best-case improvement in the objective value when the facet is added to a given relaxed polyhedron 20

2.1.2 Shooting experiment size 21

2.1.3 Chvátal-Gomory rank 22

2.1.4 Facet volume 22

2.1.5 Probability of an integer optimum when the facet is added to a given relaxed polyhedron 23

2.1.6 Other possible measures 23
2.2 Measures make use of different information 23
2.3 Measuring non-facetial cutting planes 24
2.4 Fundamental theory of the best-case improvement ratio, the shooting experiment, and Chvátal-Gomory rank 24
2.4.1 Best-case improvement applied to anti-blocking polyhedra 25
2.4.2 The shooting experiment 26
2.4.3 Computational determination of Chvátal-Gomory rank 28
III POLARITY RELATIONSHIP BETWEEN THE SHOOTING EXPERIMENT AND PROBABILITY OF OPTIMALITY 30
3.1 Central polarity relationship 30
3.2 Complexity results 32
3.3 Examples of the polar relationship 35
3.3.1 Chinese postman and odd-cut problems 36
3.3.2 Minimum spanning set and partition polyhedra 37
3.4 The shooting experiment and probability of integrality 38
IV CYCLIC GROUP AND KNAPSACK POLYHEDRA 40
4.1 Performing the shooting experiment 41
4.1.1 Application to the master packing knapsack problem 42
4.1.2 Determining the shooting point 43
4.2 A partial order on the shooting experiment sizes 45
4.2.1 Definitions 46
4.2.2 Lemmas and Proof 47
4.2.3 Example results 49
4.3 Best-case improvement 51
4.4 Facet volume 52
4.4.1 Sampling points in a simplex uniformly 52
4.4.2 Master cyclic group problems 53
4.4.3 Master packing knapsack problems 54
4.5 Chvátal-Gomory rank 55
4.6 Number of tight inequalities 55

4.7 An empirical measure of usefulness 55
4.8 Comparing the measures 57
4.8.1 Example tables of measures 57
4.8.2 Correlation between measures 58
4.8.3 Summary results 59
4.8.4 Tables of Correlations 61
V MATCHING POLYTOPES 81
5.1 Analysis of the shooting experiment 82
5.2 Best-case improvement 87
5.3 Chvátal-Gomory rank 88
5.4 Performing the shooting experiment 89
5.5 Complexity of odd-set constraints 90
5.5.1 Complexity 91
5.5.2 Fractionality 98
5.6 Computational results 106
5.7 Summary 108
VI NODE-PACKING POLYTOPES 109
6.1 Facets and valid inequalities for node packing 109
6.2 Computational study by Nemhauser and Sigismondi 110
6.3 Shooting experiment 111
6.4 Best-case improvement 113
6.5 Chvátal-Gomory rank 115
6.6 Lifted odd-hole inequalities 116
6.6.1 Shooting experiment 116
6.6.2 Best-case improvement 120
6.7 Summary 120
VII EXPONENTIAL SIZE BRANCH-AND-BOUND TREES 122
7.1 Statement of the result 122
7.2 Properties of the random instances 125
7.3 Instances almost always possess the properties 126

7.4 Instances that satisfy the properties require exponential trees 129
7.4.1 Lifted coefficients are small 129
7.4.2 The ratio of cover size to sum of coefficients 132
7.4.3 Chvátal's class of problems requires an exponential tree even in the presence of simple lifted cover inequalities 134
7.5 Summary 136

VIII CONTRIBUTIONS AND FUTURE RESEARCH 138

8.1 Summary of contributions 138
8.2 Conclusions 140
8.3 Possible future research 141
8.3.1 Specific questions 141
8.3.2 Theoretical relationships between measures 142
8.3.3 General extensions 142

APPENDIX A — TESTS OF STATISTICAL SIGNIFICANCE FOR MEASURES USED ON KNAPSACK AND CYCLIC GROUP POLYHEDRA 144

APPENDIX B — MEASUREMENTS OF CYCLIC GROUP AND KNAPSACK POLYHEDRA 147

REFERENCES 172

VITA 175

LIST OF TABLES

1	Parameters required for each measure	23
2	Shooting point candidates for the knapsack polytope for $n = 9$	44
3	Alternate shooting point trials for $n = 9$	45
4	Interior shooting points based on the "moving average"	45
5	Facets of the master packing knapsack polytope with $n = 9$	50
6	Facets of the master cyclic group polyhedron with $n = 10, r = 9$	50
7	Measures for the packing knapsack polytope with $n = 9$	57
8	Measures for the cyclic group polyhedron with $n = 10, r = 9$	57
9	Pairwise concordance of knapsack measures	59
10	Pairwise concordance of cyclic group measures	61
11	Concordance of measures for knapsack polytope with $n = 6$	62
12	Concordance of measures for knapsack polytope with $n = 7$	63
13	Concordance of measures for knapsack polytope with $n = 8$	64
14	Concordance of measures for knapsack polytope with $n = 9$	65
15	Concordance of measures for knapsack polytope with $n = 10$	66
16	Concordance of measures for knapsack polytope with $n = 11$	67
17	Concordance of measures for knapsack polytope with $n = 12$	68
18	Concordance of measures for knapsack polytope with $n = 13$	69
19	Concordance of measures for knapsack polytope with $n = 14$	70
20	Concordance of measures for the cyclic group polyhedron with $n = 7, r = 6$	71
21	Concordance of measures for the cyclic group polyhedron with $n = 8, r = 7$	71
22	Concordance of measures for the cyclic group polyhedron with $n = 8, r = 2$	72
23	Concordance of measures for the cyclic group polyhedron with $n = 8, r = 4$	72
24	Concordance of measures for the cyclic group polyhedron with $n = 9, r = 8$	73
25	Concordance of measures for the cyclic group polyhedron with $n = 9, r = 3$	73
26	Concordance of measures for the cyclic group polyhedron with $n = 10, r = 9$	74
27	Concordance of measures for the cyclic group polyhedron with $n = 10, r = 2$	74
28	Concordance of measures for the cyclic group polyhedron with $n = 10, r = 5$	75
29	Concordance of measures for the cyclic group polyhedron with $n = 11, r = 10$	75

30 Concordance of measures for the cyclic group polyhedron with $n = 12, r = 11$ 76
31 Concordance of measures for the cyclic group polyhedron with $n = 12, r = 2$ 76
32 Concordance of measures for the cyclic group polyhedron with $n = 12, r = 3$ 77
33 Concordance of measures for the cyclic group polyhedron with $n = 12, r = 4$ 77
34 Concordance of measures for the cyclic group polyhedron with $n = 12, r = 6$ 78
35 Concordance of measures for the cyclic group polyhedron with $n = 13, r = 12$ 78
36 Concordance of measures for the cyclic group polyhedron with $n = 14, r = 13$ 79
37 Concordance of measures for the cyclic group polyhedron with $n = 14, r = 2$ 79
38 Concordance of measures for the cyclic group polyhedron with $n = 14, r = 7$ 80
39 Branch-and-bound performance of matching instances 107
40 Measures for the packing knapsack polytope with $n = 6$ 147
41 Measures for the packing knapsack polytope with $n = 7$ 148
42 Measures for the packing knapsack polytope with $n = 8$ 148
43 Measures for the packing knapsack polytope with $n = 9$ 149
44 Measures for the packing knapsack polytope with $n = 10$ 150
45 Measures for the packing knapsack polytope with $n = 11$ 151
46 Measures for the packing knapsack polytope with $n = 12$ 152
47 Measures for the packing knapsack polytope with $n = 13$ 153
48 Measures for the packing knapsack polytope with $n = 14$ 154
49 Measures for the cyclic group polyhedron with $n = 7, r = 6$ 155
50 Measures for the cyclic group polyhedron with $n = 8, r = 7$ 155
51 Measures for the cyclic group polyhedron with $n = 8, r = 2$ 156
52 Measures for the cyclic group polyhedron with $n = 8, r = 4$ 157
53 Measures for the cyclic group polyhedron with $n = 9, r = 8$ 157
54 Measures for the cyclic group polyhedron with $n = 9, r = 3$ 158
55 Measures for the cyclic group polyhedron with $n = 10, r = 9$ 158
56 Measures for the cyclic group polyhedron with $n = 10, r = 2$ 159
57 Measures for the cyclic group polyhedron with $n = 10, r = 5$ 160
58 Measures for the cyclic group polyhedron with $n = 11, r = 10$ 160
59 Measures for the cyclic group polyhedron with $n = 12, r = 11$ 161
60 Measures for the cyclic group polyhedron with $n = 12, r = 2$ 162

61 Measures for the cyclic group polyhedron with $n = 12, r = 3$ 163
62 Measures for the cyclic group polyhedron with $n = 12, r = 4$ 164
63 Measures for the cyclic group polyhedron with $n = 12, r = 6$ 164
64 Measures for the cyclic group polyhedron with $n = 13, r = 12$ 166
65 Measures for the cyclic group polyhedron with $n = 14, r = 13$ 167
66 Measures for the cyclic group polyhedron with $n = 14, r = 2$ 169
67 Measures for the cyclic group polyhedron with $n = 14, r = 7$ 170

LIST OF FIGURES

1 IP example 5

2 IP with cuts 7

3 Integer hull 8

4 Partial order for the master packing knapsack polytope with $n = 9$ 49

5 Partial order for the master cyclic group polyhedron with $n = 10, r = 9$ . . 50

6 Edges with weight zero 98

7 Optimal Solution 99

8 Edges with weight zero in the general graph 100

9 Primal Solution 100

10 Dual Solution 101

11 Partial order for the packing knapsack polytope with $n = 6$ 148

12 Partial order for the packing knapsack polytope with $n = 7$ 148

13 Partial order for the packing knapsack polytope with $n = 8$ 149

14 Partial order for the packing knapsack polytope with $n = 9$ 149

15 Partial order for the packing knapsack polytope with $n = 10$ 150

16 Partial order for the packing knapsack polytope with $n = 11$ 151

17 Partial order for the packing knapsack polytope with $n = 12$ 151

18 Partial order for the packing knapsack polytope with $n = 13$ 152

19 Partial order for the packing knapsack polytope with $n = 14$ 152

20 Partial order for the cyclic group polyhedron with $n = 7, r = 6$ 155

21 Partial order for the cyclic group polyhedron with $n = 8, r = 7$ 156

22 Partial order for the cyclic group polyhedron with $n = 8, r = 2$ 156

23 Partial order for the cyclic group polyhedron with $n = 8, r = 4$ 157

24 Partial order for the cyclic group polyhedron with $n = 9, r = 8$ 157

25 Partial order for the cyclic group polyhedron with $n = 9, r = 3$ 157

26 Partial order for the cyclic group polyhedron with $n = 10, r = 9$ 158

27 Partial order for the cyclic group polyhedron with $n = 10, r = 2$ 159

28 Partial order for the cyclic group polyhedron with $n = 10, r = 5$ 159

29 Partial order for the cyclic group polyhedron with $n = 11, r = 10$ 159

30 Partial order for the cyclic group polyhedron with $n = 12, r = 11$ 159
31 Partial order for the cyclic group polyhedron with $n = 12, r = 2$ 162
32 Partial order for the cyclic group polyhedron with $n = 12, r = 3$ 162
33 Partial order for the cyclic group polyhedron with $n = 12, r = 4$ 162
34 Partial order for the cyclic group polyhedron with $n = 12, r = 6$ 165
35 Partial order for the cyclic group polyhedron with $n = 13, r = 12$ 165
36 Partial order for the cyclic group polyhedron with $n = 14, r = 13$ 168
37 Partial order for the cyclic group polyhedron with $n = 14, r = 2$ 170
38 Partial order for the cyclic group polyhedron with $n = 14, r = 7$ 171

SUMMARY

Integer programming (IP) can be used to model a variety of industrial problems, especially those related to planning and systems design. One of the most successful ways of solving IPs has been the use of branch-and-cut algorithms, which combine a branch-and-bound framework with the use of cutting planes. This dissertation considers measures of cutting planes with the aim of predicting and understanding their usefulness in branch-and-cut. Measures considered include the volume of the facet, the shooting experiment size of the facet, the best-case improvement that the facet provides, and the Chvátal-Gomory rank of the facet.

We show that the shooting experiment size of a facet of a polyhedron is the same as the probability that the corresponding extreme point of the polar polyhedron is optimal. This result is also extended to blocking and anti-blocking pairs of polyhedra. Therefore, performing one shot of the shooting experiment on a polyhedron is polynomial-time equivalent to optimizing over the polyhedron.

In the case of master cyclic group and master knapsack polyhedra, we derive a deterministic partial order of the facets that is consistent with the order defined by their shooting experiment sizes. We evaluate several measures for 19 master cyclic group problems and 9 master knapsack problems. We find that the shooting experiment size and best-case improvement measures correlate best with empirical usefulness, as determined by the size of the branch-and-bound tree.

We also consider matching polytopes defined by complete graphs. The facets of interest for this problem are defined by odd sets of nodes. We prove that for sets up to size $o(n/\log n)$, the shooting experiment will almost always hit facets defined by larger odd sets rather than facets defined by smaller odd sets. In contrast, we show that the best-case improvement ratio is better for facets defined by smaller odd sets. Computational tests

based on the branch-and-bound tree size show that both evaluations have merit. Larger odd sets are better when all facets of a given size are used, as is the case in the shooting experiment analysis. When only a few facets are used, small odd sets are better, as suggested by best-case improvement, which is based on consideration of individual facets.

We consider node packing, a classical combinatorial optimization problem in which two primary classes of cutting planes are defined by cliques and odd holes. We show that both best-case improvement and the shooting experiment predict that cuts defined by cliques are much more useful than those defined by odd holes. These results are consistent with experimental results found by Nemhauser and Sigismondi.

Among the measures considered, the shooting experiment and best-case improvement seem to offer the best correlation with usefulness across the four problems studied. In most cases, analyses of both of these measures were tractable and agreed with empirical tests. Chvátal-Gomory rank presented conflicting predictions. For the knapsack problems, a low Chvátal-Gomory rank was weakly correlated with good empirical performance. For node packing, high Chvátal-Gomory rank was a good predictor of usefulness. On matching, Chvátal-Gomory rank did not distinguish among the facets. Taken together, these results suggest that Chvátal-Gomory rank is not a reliable predictor of facet usefulness in general.

Finally, we consider an example of the limits of facet usefulness. We extend a result of Chvátal's concerning the minimum size of a branch-and-bound tree. For certain random instances of partitioning, modeled as knapsack instances, we show that even with the use of simple lifted cover inequalities, the branch-and-bound tree will have an exponential number of nodes with high probability.

CHAPTER I

INTRODUCTION

Integer Programming (IP) deals with modeling and solving problems of maximizing or minimizing a linear function of variables subject to a set of linear constraints on the variables, with the additional requirement that some or all of the variables must take on integer values. The requirement of integrality allows variables to model yes/no or other limited-choice decisions, which makes IP useful in many planning and design problems. For example, IP can be used to determine the shortest route for a delivery vehicle, the minimum number of school buses for a school district, balanced and legal monthly schedules for airline crews, or the optimal locations for factories and warehouses. In addition, IP techniques are used for a number of classical optimization problems, such as the Traveling Salesperson Problem (TSP), node packing, and the knapsack problem.

This dissertation considers branch-and-cut, a common and effective solution method for IP. Specifically, it considers measures of cutting planes with the aim of predicting and understanding their usefulness in branch-and-cut. Section 1.1 reviews the background necessary to more fully state the focus and scope of this dissertation, which are laid out in Section 1.2. Section 1.3 reviews the relevant literature. Section 1.4 presents additional background material, and Section 1.5 describes the remaining chapters of the dissertation.

1.1 Background on branch-and-cut algorithms for integer programming

We assume that the reader is familiar with linear and integer programming, including LP duality and branch-and-cut solution methods for integer programs. This section includes a brief review of the most relevant material in linear programming, polyhedral theory, and integer programming.

We denote the set of real numbers by $\mathbf{R}$ and the set of integers by $\mathbf{Z}$. The nonnegative

real numbers and nonnegative integers are denoted $\mathbf{R}_+$ and $\mathbf{Z}_+$, respectively. We will often use matrix notation, and vectors will typically be assumed to be column vectors. We denote the transposes of matrix A and vector x by A^T and x^T.

1.1.1 Linear programming and polyhedral theory

A *linear program* (LP) is a problem of the following form: maximize (alternatively, minimize) $c^T x$ such that $x \in S$, where $c \in \mathbf{R}^n$ is a constant vector, $x \in \mathbf{R}^n$ is a variable vector, and the set $S \subseteq \mathbf{R}^n$ may be expressed by a finite set of linear equalities and inequalities in x. (Equivalently, S is the intersection of a finite set of half-spaces in $\mathbf{R}^n$.) The vector c is the *objective vector*, the value $c^T x$ is the *objective value*, and the linear equalities and inequalities are also called *constraints.*

We will often present linear programs in the following matrix notation, where vectors $c \in \mathbf{R}^n, b \in \mathbf{R}^m$, and matrix $A \in \mathbf{R}^{m \times n}$ are constant:

$$\begin{aligned} \min \quad & c^T x \\ s.t. \quad & Ax \leq b. \end{aligned}$$

Alternatively, we may use algebraic notation, such as the following:

$$\begin{aligned} \min \quad & \textstyle\sum_{j=1}^{n} c_j x_j \\ s.t. \quad & \textstyle\sum_{j=1}^{n} a_{ij} x_j \leq b_i \quad i = 1, \ldots, m. \end{aligned}$$

Linear programs often include constraints of the form $x_j \geq 0$ for some or all variables. These constraints are known as *nonnegativity constraints.* When nonnegativity constraints are present, we may refer to the set of other constraints as *non-trivial constraints.* To refer to a single linear constraint $\sum_{i=1}^{n} a_i x_i \leq a_0$, we may also use the notation (a, a_0), where $a = (a_1, a_2, \ldots, a_n)$.

The set of points that satisfy the constraints of the linear program is called the *feasible region*, which may be empty, bounded, or unbounded. Since it is the intersection of closed half-spaces, the feasible region is a *polyhedron* in $\mathbf{R}^n$. A bounded polyhedron is also called a *polytope.*

If an inequality (a, a_0) is satisfied by all points in a polyhedron P, we say that it is a *valid inequality* for P. The intersection of P and a valid inequality of P is called a *face* of

P. This intersection could be empty, a single point, a line segment, or a higher dimensional set. If the dimension of the face is one less than the dimension of P, then the face is a *facet.* If there are no redundant inequalities in the set of constraints for P, then every inequality determines a facet of P.

A face that has dimension 0 (a point) is known as a *vertex* or *extreme point* of P. Because the objective function and constraints are linear, it is true that if there is an optimal solution to the LP, then there is an optimal solution that is an extreme point of the feasible region.

In general, linear programs may be solved relatively quickly by using either a variant of the *simplex algorithm* or an *interior-point method.* Historically first, the simplex algorithm has the disadvantage that it may take super-polynomial time to solve but the advantage that it allows for quick resolves after adding a constraint or variable to the instance. Interior-point methods give rise to polynomial-time algorithms, but resolving problems after modifications is not as easy.

Every linear program has a *dual linear program.* In this context, the original linear program is called the *primal.* There is a variable in the dual for each constraint in the primal and a constraint in the dual for each variable in the primal. Specifically, the primal LP

$$\begin{aligned} \min \quad & c^T x \\ s.t. \quad & Ax \leq b \\ & x \geq 0 \end{aligned}$$

has dual LP

$$\begin{aligned} \max \quad & b^T y \\ s.t. \quad & y^T A \geq c \\ & y \geq 0. \end{aligned}$$

The LP duality theorem states that if either LP has an optimal solution, then both do and the optimal objective values are equal.

See a textbook on linear programming, such as Chvátal [9] or Bertsimas & Tsitsiklis [3], for more details.

1.1.2 Integer programming

A *mixed integer program* (MIP) is a generalization of a linear program in which one or more variables are required to take on integer values. If all variables are required to be integral, then it is a *pure integer program.* The term *integer program* is sometimes used as a synonym for mixed integer program and at other times as a synonym of pure integer program. We will generally use the term integer program in the broader sense, though the problems studied in this dissertation are all pure integer programs.

Unlike linear programs, integer programs generally have a feasible region that is not convex or even connected. The problem of solving a general integer program is NP-hard.

A common method for solving integer programs is *branch-and-bound.* The integrality requirements of the IP are relaxed and the resulting linear program, known as the *linear relaxation* or *LP relaxation*, is solved. If the resulting solution is *integer feasible*—all the integer variables have integer values—then the solution is optimal. Figure 1 shows the constraints and feasible region of an IP. The white dots are the feasible integer points, and the shaded region is the feasible region of the LP relaxation. In this example, exactly one of the vertices of the LP relaxation is integer feasible. In general, there may be no, some, or many integer feasible vertices in the LP relaxation.

If the optimal solution to the LP relaxation is not integer feasible, the problem, called the *parent*, is split into several subproblems, called *child subproblems.* This process is called *branching.* Most commonly, two subproblems are created based on an integer variable x_i that does not have an integer value in the solution. If the value of x_i is x_i^*, then one subproblem has the added constraint $x_i \leq \lfloor x_i^* \rfloor$ and the other subproblem has the added constraint $x_i \geq \lceil x_i^* \rceil$. It is clear that any optimal solution to the parent IP must be feasible for one of these subproblems. Each of these branches must be explored and may lead to further branching.

Branch-and-bound is more efficient than simply enumerating all possible solutions primarily because of *bounding.* If a given subproblem has a relaxed objective value that is no better than a currently known integer feasible solution, then this subproblem does not need to be explored any further. It is said to be *fathomed*, and its branch is said to be *pruned.*

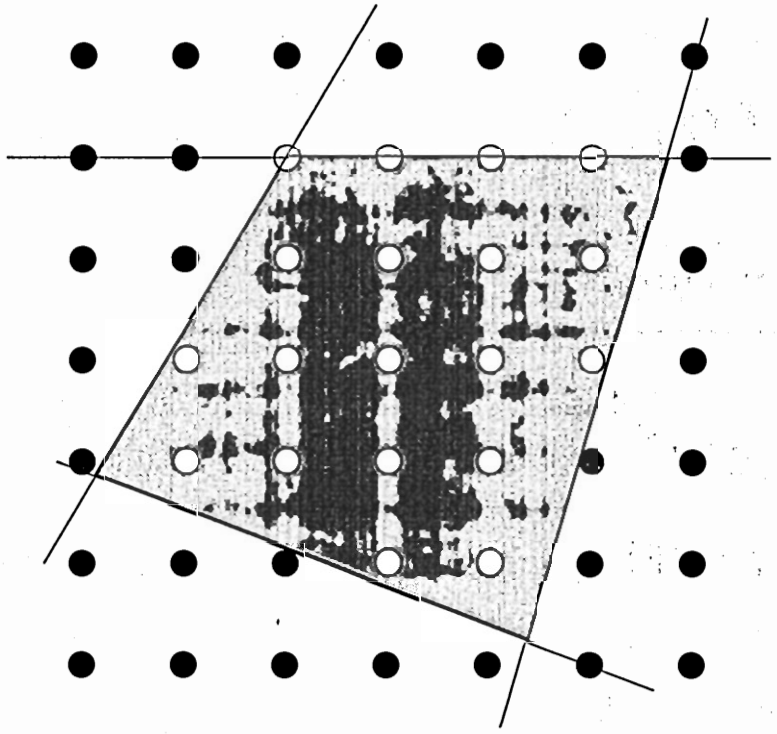

The four lines are constraints. The white dots show the IP feasible set, and the shaded area is the feasible region of the LP relaxation.

Figure 1: IP example

As the algorithm progresses, a tree is formed by the LP subproblems, which therefore are also referred to as nodes. The size and shape of this tree, as well as the efficiency of the algorithm, depend on the exact choice of rules for branching and exploring subproblems.

Because the child subproblems are closely related to their parent problem, it is much quicker to use the simplex method starting from the parent's optimal solution to solve the LP than to solve it from scratch. For this reason, simplex-based algorithms are generally used to solve the LPs in the branch-and-bound tree.

In practice, the most successful general method for solving integer programs is *branch-and-cut*. In this variant of branch-and-bound, additional *valid inequalities*, or *cutting planes*, may be added to the problem, either at the root node of the branch-and-bound tree or at other nodes. For example, Figure 1.1.2 shows additional valid inequalities added to the IP from Figure 1. These valid inequalities do not change the feasible set of the IP, but they do create a tighter LP relaxation by reducing the size of its feasible set. This may help the branch-and-bound algorithm by exposing integer solutions to the LP relaxation and by tightening the optimal value of the LP relaxation, which may allow it to be fathomed.

Figure 3 shows the tightest possible inequalities for the IP from Figure 1. The feasible set of the LP relaxation is now the same as the convex hull of the integer feasible solutions, also known as the *integer hull*. Every vertex of the LP relaxation is an integer feasible solution, so no branching will be necessary. As a consequence, the facets of the integer hull are of particular interest for use as cutting planes.

If one polyhedron contains another polyhedron, then the first is said to be a *relaxation* of the second. The term *LP relaxation* comes from the fact that the LP defines a relaxation of the integer hull.

See a textbook such as Nemhauser and Wolsey [34] or Wolsey [38] for more details on integer programming and branch-and-cut.

1.2 Purpose and scope of this dissertation

Cutting planes can benefit a branch-and-bound algorithm by more quickly exposing integer solutions and by causing nodes to be fathomed through tighter LP relaxations. The use of

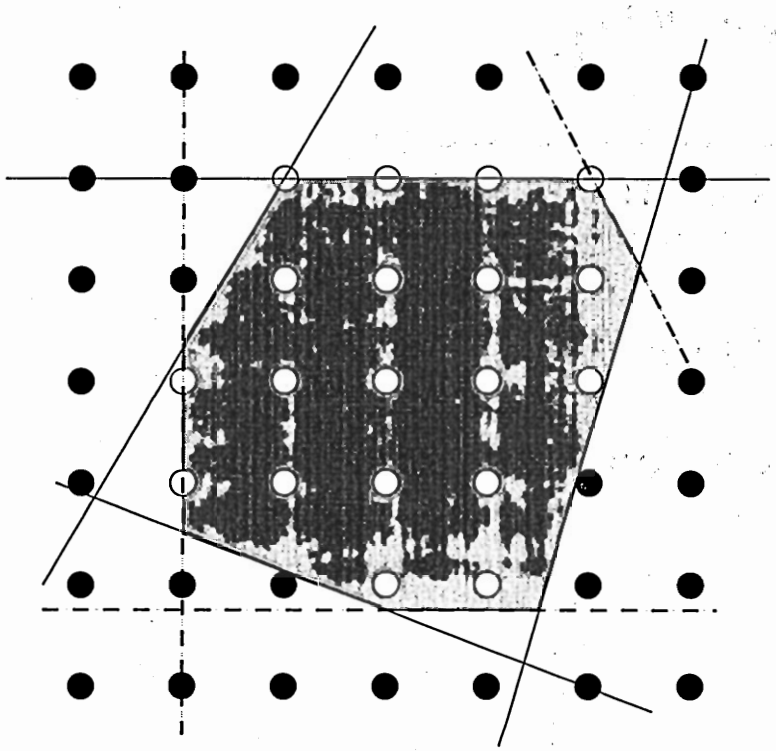

The dashed lines are cuts that have been added.

Figure 2: IP with cuts

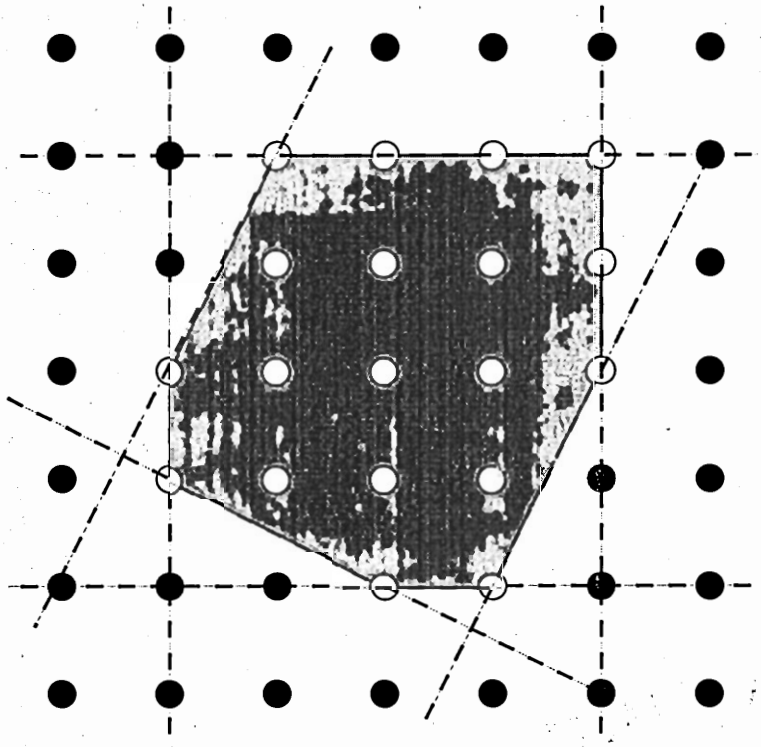

All extreme points of the LP relaxation are now integer feasible. The seven dashed lines correspond to facets of the integer hull.

Figure 3: Integer hull

each cutting plane incurs computational costs in time and memory, however. These costs result not only from the generation of the cut and the need to perform simplex pivots with more rows but also from the possibility that the cutting plane may negatively affect the sparsity of the matrix. For these reasons it is not obvious how useful a particular cutting plane or set of cutting planes will be.

This dissertation explores the question of usefulness from two points of view. The bulk of the dissertation is motivated by the desire to understand and predict the relative usefulness of different cutting planes, particularly facets, by examining ways that they can be measured. Several possible measures are considered and applied to classical IP problems, including knapsack and cyclic group problems, matching, and node packing. The tractability of analytical or empirical results for each measure is considered as well as whether the measure appears to correlate with usefulness in branch-and-cut.

Chapter 7 takes another view and considers limits on the usefulness of branch-and-cut. The main result of this chapter is a proof that a certain class of random knapsack instances requires an exponential number of branch-and-bound nodes with probability converging to 1 as the size of instance increases, even if a large class of facet-defining cuts is added.

1.3 Literature review

This section discusses prior work on measuring cuts, empirical studies of cutting planes, and limits on the minimum size of the branch-and-bound tree. Some later chapters present additional references that are specific to the topic of that chapter.

1.3.1 Measures of facets

To our knowledge, there have been only three general measures of facets/cuts proposed in the literature: a worst-case improvement measure used by Goemans [18] to analyze the graphical TSP polyhedron, the shooting experiment used by Kuhn [29, 30] for the TSP and more recently by Gomory, Johnson, and Evans [23] for cyclic group polyhedra, and the Chvátal-Gomory rank of inequalities, which stems from the work of Gomory [20] and Chvátal [7]. In addition to these, Evans [15] and Gomory and Johnson [22] considered a

"merit" function that applies only to facets of master cyclic group and master knapsack polyhedra.

For a minimization problem, Goemans [18] defined the *strength* of an inequality $ax \geq b$, where $a, b \geq 0$, with respect to a polyhedron P of blocking type as

$$\frac{b}{\min\{ax : \ x \in P\}}.$$

This definition is based on the fact that if the objective vector $c = a$, then the strength of the inequality is the ratio of the optimal objective value with the inequality present to the optimal objective value without the inequality. Goemans proved that choosing $c = a$ gives the largest such ratio. As Goemans himself pointed out, this is really a "best-case" measure, though it falls in the category known as "worst-case" analyses. This measure was used again by Goemans and Hall [19]. An advantage of Goemans's approach is that it lends some tractability to the problem. Goemans was able to evaluate the measure for quite a few of the common TSP cuts, including comb inequalities at 10/9, clique tree inequalities at 8/7, and path configuration inequalities at 4/3. A disadvantage is that the measure doesn't address typical-use considerations. Is this best-case objective function very likely? Is the cut almost as good for other objective functions or does it do poorly except on a few exceptional objective functions?

We believe the name "shooting experiment" was first used by Gomory several years ago in his work on cyclic group polyhedra, which was recently published in a paper jointly authored with Johnson and Evans [23]. Kuhn used the technique much earlier in mostly unpublished experiments on the 5-city TSP polytope from 1953 [29], with some follow-up in 1991 [30]. After selecting a point in the interior of a polytope, rays—or "shots"—are sent from that point in random directions, and the facets that they intersect are recorded. The number of rays which hit a given facet gives an estimate of its size. For the TSP, we do not have a complete description of the facets in the general case. Kuhn used an explicit list of the extreme points for the 5-city polytope to perform the shooting experiment. Gomory's use of the shooting experiment is different in that he is shooting from outside an unbounded polyhedron and one "shot" of the experiment can be performed in polynomial time on

master cyclic group polyhedra by solving an LP, even without an explicit list of the facets. This allows for better use of the shooting experiment to investigate important facets as the size of the problem increases. Additional work on cyclic group and knapsack problems appears in Evans's dissertation [15].

Gomory and Johnson [22] and Evans [15] noticed that cyclic group facets that were hit often by the shooting experiment also exhibited more degeneracy in a system of inequalities that characterizes the facets. Gomory and Johnson refer to a measure based on the amount of degeneracy as the "merit function", which they presented in a more general continuous model of cutting planes. In both references, the measure is considered because of its correlation with the shooting experiment.

1.3.2 Computational studies

There are a number of computational studies of the relative usefulness of cuts for particular problems. Nemhauser and Sigismondi [33] found that clique inequalities are much more useful than odd-hole inequalities for node-packing problems in random graphs, though for lower density random graphs odd-hole inequalities were also important. We consider their results in Chapter 6.

Aardal [1] considered many cuts for the Capacitated Facility Location (CFL) problem and found that the single most effective class was knapsack cover inequalities, even though they ignore the flow variables in the formulation. Fischetti, Gonzalez, and Toth [16] studied the orienteering problem. They did not compare performance using different cuts, but they did find that the most often violated cuts were generalized subtour elimination constraints, logical constraints linking nodes and vertices, and a new class that they call conditional cuts. Magnanti, Mirchandani, and Vachani [32] considered the two-facility loading problem, and found that cutset and 3-partition inequalities were more effective at reducing the integrality gap than arc residual capacity inequalities were.

1.3.3 Size of the branch-and-bound tree

For optimization problems, an implementation of an algorithm is generally evaluated based on the time it takes and the amount of memory it uses. These two measures depend on

many details of the implementation and are therefore not the only ways that we wish to evaluate the usefulness of facets for branch-and-cut algorithms. An additional performance measure that we have used is based on the size of the branch-and-bound tree when the facet is added at the root node. This size depends on the choice of branching variable and the node exploration strategy.

This measure has been considered previously, particularly in the context of proving that branch-and-bound will require an exponential number of nodes for certain problem instances when branching is done on variables.

Jeroslow [28] presented an instance of the knapsack problem which requires an exponential number of branch-and-bound nodes.

Chvátal [8] considered a set of random instances of the knapsack problem in which the objective coefficients were the same as the constraint coefficients and the right-hand-side was the floor of half the sum of all the coefficients. Note that this can be considered a bipartition problem in the form of a knapsack problem. Chvátal showed that with probability converging to 1, it takes exponentially many nodes to solve such a random instance by branch-and-bound. More details on Chvátal's results are given in Chapter 7.

Gu, Nemhauser, and Savelsbergh [26] also considered the knapsack problem, but with the addition of cutting planes to the algorithm. Specifically, they presented a family of instances that require an exponential number of branch-and-bound nodes even with the addition of simple lifted cover inequalities.

More recent work in proving exponential worst-case bounds in the presence of various cutting planes has been done by Dash [12], who proved worst-case exponential bounds in the presence of lift-and-project cuts, Chvátal-Gomory inequalities, and matrix cuts as described by Lovász and Schrijver.

1.4 Additional background

This section provides additional background on topics and techniques used in the dissertation, including Chvátal-Gomory inequalities, complexity, probability, graph theory, and polarity.

1.4.1 Chvátal-Gomory inequalities and rank

Chvátal-Gomory rounding is one method of using known valid inequalities to generate additional—hopefully stronger—valid inequalities. The resulting inequalities are called *Chvátal-Gomory inequalities*, which we will often abbreviate as C-G inequalities. The rounding procedure was explicitly presented by Chvátal [7] but was implicit in earlier work by Gomory [20]. See Nemhauser and Wolsey [34] or Wolsey [38], for example, for a detailed discussion of Chvátal-Gomory rounding. We present a summary for the case in which all variables are nonnegative, which is sufficient for this dissertation.

Given two inequalities $\sum_{j=1}^{n} c_{1j}x_j \leq d_1$ and $\sum_{j=1}^{n} c_{2j}x_j \leq d_2$, we say that the first *dominates* the second if $c_{1j} \geq c_{2j}$ for all j and $d_1 \leq d_2$. If an inequality is valid, then because the variables must be nonnegative, any inequality it dominates is also valid.

Let $\sum_{j=1}^{n} a_{ij}x_j \leq b_i$ be the currently known valid inequalities, where $i = 1, \ldots, m$. Let $u_1, \ldots, u_m$ be nonnegative multipliers for the inequalities. Then the linear combination

$$\sum_{j=1}^{n}\sum_{i=1}^{m}(u_i a_{ij})x_j \leq \sum_{i=1}^{m} u_i b_i \tag{1}$$

is a valid inequality.

We can round down in (1) to get a dominated inequality, which is also valid:

$$\sum_{j=1}^{n} \left\lfloor \sum_{i=1}^{m} u_i a_{ij} \right\rfloor x_j \leq \sum_{i=1}^{m} u_i b_i.$$

Since the coefficients on the left-hand-side are all integers, the sum of the left-hand-side must be integer for any integer solution x. Therefore, we can round the right-hand-side down and still have a valid inequality. That is the crucial step in the process, which allows us to generate stronger inequalities. The resulting Chvátal-Gomory inequality is

$$\sum_{j=1}^{n} \left\lfloor \sum_{i=1}^{m} u_i a_{ij} \right\rfloor x_j \leq \left\lfloor \sum_{i=1}^{m} u_i b_i \right\rfloor.$$

Once some C-G inequalities have been generated, they can be used along with the original inequalities to generate further inequalities. This iterated approach to C-G rounding leads to the idea of *Chvátal-Gomory rank*. We define the C-G rank of the initial inequalities and any inequality dominated by a nonnegative linear combination of the initial inequalities

to be 0. Any inequality which can be generated as a C-G inequality based on rank 0 inequalities—but is not rank 0 itself—has C-G rank 1. Similarly, a valid inequality has C-G rank k if it can be generated as a C-G inequality based on inequalities of rank $0, 1, \ldots, k-1$, but it is does not have rank less than k.

1.4.2 Complexity and asymptotic notation

We expect that readers are familiar with the complexity classes P and NP.

We will use the following standard notation for asymptotic behavior. Given functions $f(n)$ and $g(n)$, we say $f(n) = O(g(n))$ if there exists a constant $c > 0$ such that $f(n) \leq cg(n)$ for all sufficiently high n. We also say $f(n) = \Omega(g(n))$ if $g(n) = O(f(n))$, and $f(n) = \Theta(g(n))$ if both $f(n) = O(g(n))$ and $f(n) = \Omega(g(n))$. If the ratio $f(n)/g(n)$ goes to 0 as n increases, we say that $f(n) = o(g(n))$.

1.4.3 Probability

We expect that readers are familiar with the concept of a random variable, as well as continuous and discrete probability functions. We will use the abbreviation *iid* to refer to variables that are independent and identically distributed.

Given an event A, we denote the probability that A occurs by $P(A)$. Given an event A_n parametrized by an integer n, we say that event A_n occurs *almost always* if $P(A_n) \to 1$ as $n \to \infty$.

We will use the standard normal distribution often. The density function for the standard normal distribution is

$$f(x) = \frac{1}{\sqrt{2\pi}} e^{\frac{-x^2}{2}}.$$

If X is a standard normal random variable, then $Y = |X|$ is a positive standard normal random variable and has distribution function

$$f(y) = \begin{cases} 0, & \text{if } y < 0, \\ \frac{2}{\sqrt{2\pi}} e^{\frac{-y^2}{2}}, & \text{if } y \geq 0. \end{cases}$$

Although the normal distribution has great importance in its own right, in the context of this dissertation the importance comes from a desire to generate uniformly random points

on the unit sphere. This can be done in n dimensions by generating n coordinates as iid normal random variables with mean 0 and then scaling the resulting vector to have unit magnitude. In fact, since the direction is what we are concerned with, it is not generally important to scale the result. In either case, we say that the distribution is *spherically symmetric.* See Bryc [5], for example, for a proof of this fact.

We will make use of two standard bounds in the field of probabilistic analysis. The first is the Chernoff bound [6]. Recall that a binomial distribution is the same as the sum of iid Bernoulli trials.

Theorem 1.1 (Chernoff Bound) *Let X be a binomial random variable with parameters p, n (X may be considered the sum of n iid Bernoulli random variables with probability p that each is 1). Then $\mu \equiv E[X] = np$ and for any $\delta > 0$,*

$$P(X > (1+\delta)\mu) < \left(\frac{e^{\delta}}{(1+\delta)^{(1+\delta)}}\right)^{\mu}.$$

A slightly more general theorem is true, but this will suffice for our needs. Note that if p and δ are constants then $\mu = \Theta(n)$, and the right-hand-side above is exponentially small in n.

Another bound we will use is a Hoeffding bound [27]. There are several forms for this inequality.

Theorem 1.2 (Hoeffding Bound) *Let $X_1, X_2, \ldots, X_n$ be independent random variables with $0 \leq X_i \leq B$ for each i, where B is constant. Let $X = \sum_{i=1}^{n} X_i$ and let $\mu = E[X]$. Then for any $\delta > 0$,*

$$P(X \geq (1+\delta)\mu) \leq e^{-\frac{\delta^2\mu}{2B(1+\delta/3)}},$$

and

$$P(X \leq (1-\delta)\mu) \leq e^{-\frac{\delta^2\mu}{2B}}.$$

1.4.4 Graph theory

We expect readers are familiar with the notion of a graph, as well as the notions of adjacent nodes, paths, cycles, subgraphs, and induced subgraphs. We will typically denote a graph by $G = (V, E)$, where V is the vertex or node set of the graph and E is the edge set.

A *clique* is a set $C \subseteq V$ such that every pair of nodes in C is adjacent. A *hole* is a set $H \subseteq V$ such that the induced subgraph on H is a cycle containing all the nodes of H. An odd hole is a hole such that $|H|$ is odd.

Given a subset $S \subseteq V$, let $\delta(S) = \{\{u,v\} \in E : u \in S, v \notin S\}$ and let $\gamma(S) = \{\{u,v\} \in E : u \in S, v \in S\}$. That is, $\delta(S)$ is the set of edges in the cut defined by S, and $\gamma(S)$ is the set of edges interior to S. When $S = \{v\}$ contains a single node, we abbreviate $\delta(\{v\}) = \delta(v)$ and $\gamma(\{v\}) = \gamma(v)$.

To generate random instances of graphs, we will use the notion of a *random graph* with density p. For such a graph, the number of nodes is given ahead of time, and each possible edge is present with probability p, independently of all other edges. For example, let $n = 10$ and $p = 1/4$. There are $\binom{10}{2} = 45$ possible edges in a graph with 10 nodes. To generate a random instance, we independently include each edge with probability $1/4$.

See Bollobás [4], for example, for more information about the theory of random graphs.

We will make use of the following result about the size of the largest clique in a random graph (see [4]).

Proposition 1.3 *For a random graph with density p, given a constant $\epsilon > 0$, the size of the largest clique C' in the graph almost always satisfies*

$$\lfloor d(n,p) - \epsilon \rfloor \leq |C'| \leq \lfloor d(n,p) + \epsilon \rfloor,$$

where

$$d(n,p) = 2\log_{\frac{1}{p}} n - 2\log_{\frac{1}{p}} \log_{\frac{1}{p}} n + 1 + \log_{\frac{1}{p}}(\frac{e}{2}).$$

1.4.5 Polyhedra and polarity

Given a set of points $S \subseteq \mathbf{R}^n$, the *convex hull* of S is the set

$$\text{hull}(S) = \{\sum_{i=1}^{m} \alpha_i x_i : m \geq 1, x_i \in S, \sum_{i=1}^{m} \alpha_i = 1, \alpha_i \geq 0\}.$$

This is the smallest convex set containing S.

The *cone* generated by a set of S of vectors is

$$\text{cone}(S) = \{\sum_{i=1}^{m} \alpha_i x_i : m \geq 0, x_i \in S, \alpha_i \geq 0\}.$$

The sum of two sets S and P is $S + P = \{x + y : x \in S, y \in P\}$.

Given a set $P \subset \mathbf{R}^n$, the *polar* of P is the set

$$P^* = \{z \in \mathbf{R}^n \ : \ z^T x \leq 1 \text{ for all } x \in P\}.$$

If P is a polyhedron containing the origin, then it can be shown that P^* is also a polyhedron and that $P^{**} = P$. Moreover, if $P = \text{hull}\{x_1, \ldots, x_m\} + \text{cone}\{y_1, \ldots, y_k\}$, then

$$P^* = \{z \in \mathbf{R}^n : z^T x_i \leq 1 \text{ for } i = 1, \ldots, m, z^T y_j \leq 0 \text{ for } j = 1, \ldots, k\}.$$

That is, the extreme points and extreme rays of P are enough to specify P^*. If P is full-dimensional, then the extreme points of P are in 1-1 correspondence with the facets of P^*, and vice-versa. See Schrijver [37], for example, for proofs of these facts.

The origin plays a special role in polarity, as indicated by the above results. It is also possible to consider the polar with respect to another point in the polyhedron. Conceptually, this is done by translating the polyhedron prior to computing the polar. Equivalently, we may define the *polar of P with respect to point a* as

$$P_a^* = \{z \in \mathbf{R}^n \ : \ (z - a)^T (x - a) \leq 1 \text{ for all } x \in P\}.$$

There are special kinds of polarity for certain polyhedra. A polyhedron P is *of blocking type* if $P \subset \mathbf{R}_+^N$ and $x \in P, y \geq x \Rightarrow y \in P$. The *blocker* of P is denoted by $B(P)$ and is given by $B(P) = \{z \in \mathbf{R}^n \ : \ z^T x \geq 1\}$. Similar to polarity, $B(B(P)) = P$ as long as P is of blocking type. If P has extreme points $x_1, x_2, \ldots, x_m$ and is of blocking type, then $B(P) = \{z \in \mathbf{R}^n \ : \ z^T x_i \geq 1 \text{ for } i = 1, \ldots, m\}$. In fact, the extreme points of P correspond to the facets of $B(P)$, and vice versa.

A polyhedron P is *of anti-blocking type* if $P \subset \mathbf{R}_+^N$ and $x \in P, y \leq x \Rightarrow y \in P$. The *anti-blocker* of P is denoted by $A(P)$ and is given by $A(P) = \{z \in \mathbf{R}^n \ : \ z^T x \leq 1\}$. As before, $A(A(P)) = P$ as long as P is of anti-blocking type. If P has extreme points $x_1, x_2, \ldots, x_m$ and is of anti-blocking type, then $A(P) = \{z \in \mathbf{R}^n \ : \ z^T x_i \leq 1 \text{ for } i = 1, \ldots, m\}$. In fact, the extreme points of P correspond to the facets of $A(P)$, and vice versa.

Schrijver [37] includes an excellent presentation of polarity, including blocking and anti-blocking polyhedra.

1.5 *Structure of this dissertation*

Chapters 2 through 6 consider the possibility of measuring facets to predict their relative usefulness in branch-and-cut. Chapter 2 presents a set of candidate measures along with a discussion of their inherent similarities and differences. Measures considered include best-case improvement, shooting experiment size, probability of integrality, Chvátal-Gomory rank, and facet volume.

Chapter 3 examines some polar properties of the shooting experiment size, showing that performing the shooting experiment is equivalent to optimizing over the polar polyhedron. A consequence is that performing the shooting experiment on a polyhedron is polynomial-time equivalent to optimizing over the polyhedron.

Chapters 4, 5, and 6 apply the measures to several classical IP problems: master cyclic group and master knapsack problems, matching, and node packing, respectively.

For cyclic group and knapsack problems, a variety of measures are evaluated for comparison to one another and to an empirical measure of usefulness based on branch-and-bound tree size. In part, the results indicate that best-case improvement and the shooting experiment provide the strongest correlation to empirical usefulness for master knapsack problems.

In Chapter 5, analyses of the shooting experiment and best-case improvement on matching polytopes show that the measures make opposite predictions of facet usefulness, while Chvátal-Gomory rank fails to differentiate among the facets. Empirical results show that, in a sense, both the best-case improvement and shooting experiment predictions are correct.

Node packing polytopes are considered in Chapter 6. The results of the analysis are compared to an empirical study by Nemhauser and Sigismondi, which made use of clique inequalities and odd-hole inequalities. Analyses of the shooting experiment and best-case improvement both predict that clique inequalities are much more useful than odd-hole inequalities, consistent with the results of Nemhauser and Sigismondi.

As mentioned earlier, Chapter 7 takes a different view, looking instead at the limits of cutting-plane usefulness. The main result is a proof that a certain class of random knapsack instances almost always requires an exponential number of branch-and-bound nodes, even

if a large class of facet-defining cutting planes is added to the relaxation.

Finally, Chapter 8 summarizes the contributions of the dissertation and considers possible future research.

CHAPTER II

POSSIBLE MEASURES OF FACETS AND CUTTING PLANES

We will consider the following quantities, which can be used as measures of facets.

- Best-case improvement in the objective value when the facet is added to a given relaxed polyhedron
- Shooting experiment size
- Chvátal-Gomory rank
- Facet volume
- Probability of an integer optimum when the facet is added to a given relaxed polyhedron

Each measure is described more carefully in Section 2.1, and Section 2.2 discusses some of the inherent differences between the measures. Section 2.3 addresses the application of these measures to cutting planes that do not define facets. Finally, Section 2.4 presents best-case improvement, the shooting experiment, and Chvátal-Gomory rank in more depth.

2.1 Explanation of each measure

This section presents a formal description of each measure as well as a brief discussion of the intuition that motivates it.

2.1.1 Best-case improvement in the objective value when the facet is added to a given relaxed polyhedron

This measure was proposed by Goemans in the context of the Graphical Traveling Salesman Problem (GTSP) [18] and was used by Goemans and Hall [19] on the acyclic subgraph

polytope. The GTSP polyhedron is of blocking type and the objective is to minimize, while the acyclic subgraph polytope is of anti-blocking type and the objective is to maximize. We will only apply the best-case improvement measure to anti-blocking polytopes, so we present the second version here.

Given an anti-blocking polyhedron $Q \subseteq \mathbf{R}^n_+$ and a relaxation $P \supseteq Q$, we define the *best-case improvement* ratio of Q with respect to P to be

$$\sup_{c \in \mathbf{R}^n_+} \frac{\max\{c^T x : x \in P\}}{\max\{c^T x : x \in Q\}}.$$

In words, this is the inverse of the maximum ratio of improvement in the objective value between polyhedra P and Q.

To apply the best-case improvement measure to a single facet, we start with a relaxation P of the integer hull under consideration and let Q be the polyhedron defined by adding the facet in question to P. Alternatively, we may consider a group of facets in conjunction, in which case we add all of them simultaneously to form Q.

Intuitively, this measure indicates the most that a facet could help the objective value. Goemans referred to this as a "worst-case" measure, since it falls in the category known as worst-case analysis. It is in a sense a best-case measure, however, which is why we have chosen the term best-case improvement for use in this dissertation.

Section 2.4.1 presents best-case improvement in more detail.

2.1.2 Shooting experiment size

The shooting experiment was first considered by Kuhn in the context of the TSP [29, 30]. After selecting a point in the interior of a polytope, rays—or "shots"—are sent from that point in random directions, and the facets that they intersect are recorded. Intuitively, a facet that is hit by a large number of shots is probably "larger" and more important than a facet hit by few shots. At the time of Kuhn's investigation, computing power was limited and he did not develop or pursue the technique.

More recently, Gomory applied a similar idea to cyclic group polyhedra, developing it further and performing more extensive tests along with Johnson and Evans [23]. In this case, the originating point is external.

We will refer to the originating point as the *shooting point*, and we define the *shooting experiment size* of a facet to be the probability that a ray in a random direction will hit that facet. Note that this probability depends on the shooting point as well as the random distribution we are using. Actually performing the shooting experiment gives a Monte Carlo estimate of the shooting experiment size.

We will consider two possibilities for the distribution of directions. If all directions are of interest, then the directions will be chosen from a spherically symmetric distribution. If only nonnegative directions are of interest, then the directions will be chosen from a spherically symmetric distribution that is limited to the nonnegative orthant. See Section 1.4.3 for a method of generating such random directions.

When comparing a subset of facets or inequalities, we may also consider the shooting experiment sizes on the polyhedron defined by adding only those inequalities to the LP relaxation of the problem. Although these values are not the same as the shooting experiment sizes on the integer hull, they provide a way to compare sets of facets, especially when not all facets of the integer hull are known.

2.1.3 Chvátal-Gomory rank

The definitions of Chvátal-Gomory inequalities and their rank are given in Section 1.4.1. Since C-G rank is often considered when new inequalities are investigated, we wish to consider whether this rank can be used as an indicator of the usefulness of the inequality as well.

2.1.4 Facet volume

Let the integer polyhedron P have dimension n. Then the facets of P are polyhedra of dimension $n-1$. The volumes of these polyhedra give a direct measure of their size. Intuitively, we suspect that facets with larger volumes might be more useful than facets with smaller volumes.

Table 1: Parameters required for each measure

Measure	Relaxed polyhedron	Probability distribution	Shooting point
Best-case improvement	√		
Shooting experiment size		√	√
C-G rank	√		
Facet volume			
Probability of integrality	√	√	

2.1.5 Probability of an integer optimum when the facet is added to a given relaxed polyhedron

Given a relaxation P of an integer hull and a distribution for random objective functions, there is a well-defined probability (possibly zero) that the optimum extreme point of P is an extreme point of the integer hull. We will call this the *probability of integrality* for relaxation P and the given objective distribution. The probability of integrality is of interest because finding feasible integer solutions more quickly can significantly improve the performance of a branch-and-bound algorithm.

2.1.6 Other possible measures

Our list of candidate measures is by no means exhaustive. In Chapter 8, we mention other measures as possible subjects of future research.

2.2 Measures make use of different information

The measures described above do not all use the same information. For example, the facet volume depends only the integer hull, while the best-case improvement ratio depends on the chosen relaxation. The shooting experiment requires a shooting point, which is not needed for any other measure.

As indicated in Table 1, the measures under consideration may depend on a choice of relaxed polyhedron, a probability distribution for a vector (either the objective or a shooting direction), and/or a shooting point.

What implications do these differences have for the measures? On one hand, it may be

simpler to analyze measures for which little or no extra information is considered. Facet volume, for example, depends only on the integer hull being considered. We do not need to consider specific relaxations or the objective vector.

In practice, however, branch-and-cut is performed by starting with a relaxed polyhedron and a known objective vector. A measure that ignores these two elements may not have the same potential benefits of one that considers them. Considering the information is not always straightforward, however. What is an appropriate random distribution for objective functions? As is often the case in probabilistic analysis, when this question comes up we make simplifying assumptions that do not accurately describe real-world instances.

It is particularly significant that none of the measures under consideration makes use of an explicit objective function, even though that information is readily available during branch-and-cut. We will say more about this when we discuss potential future work in Chapter 8.

It is not the goal of this dissertation to precisely examine the effects of using or ignoring particular information. Instead, we wish to focus on the relative usefulness of the measures. For this reason, we will not pursue the issues raised in this section.

2.3 *Measuring non-facetial cutting planes*

All of the measures above can be applied to facets, but not all can be naturally applied to cutting planes that do not define facets. For example, cutting planes do not have a "facet volume" or shooting experiment size in terms of the integer hull.

It is possible to use such a measure, however, by considering a relaxation in which the cutting plane defines a facet. For example, in Chapter 6 we will consider a relaxation of the node-packing polyhedron in which only certain inequalities are present. The resulting cutting-plane measures depend on the relaxation used, of course.

2.4 *Fundamental theory of the best-case improvement ratio, the shooting experiment, and Chvátal-Gomory rank*

This section discusses the application of best-case improvement to anti-blocking polyhedra, the process of performing the shooting experiment, and our method of determining partial

information about Chvátal-Gomory rank computationally.

2.4.1 Best-case improvement applied to anti-blocking polyhedra

We assume that $P \subseteq \mathbf{R}^n_+$ is a relaxation of a polyhedron $Q \subseteq \mathbf{R}^n_+$, both of anti-blocking type. Given constant $\alpha \geq 1$, we say that P is an α-relaxation of Q if $Q \supseteq \frac{1}{\alpha}P$.

Definition 2.1 *The* best-case improvement ratio *of P relative to Q, denoted $t(P,Q)$, is the minimum value of α such that P is an α-relaxation of Q.*

It is clear that $t(P,Q) \geq 1$, and $t(P,Q) = 1$ if and only if $P = Q$. The motivation for the name "best-case improvement ratio" is given by the following proposition, due to Goemans and Hall [19]. We present our own proof of the proposition, which is more complete than that in [19].

Proposition 2.2 (Goemans, Hall) *Given P and Q as defined above,*

$$t(P,Q) = \sup_{c \in \mathbf{R}^n_+} \frac{\max\{c^T x : x \in P\}}{\max\{c^T x : x \in Q\}}.$$

Proof: If P is an α-relaxation of Q, then for any $c \in \mathbf{R}^n_+$,

$$\max\{c^T x : x \in Q\} \geq \frac{1}{\alpha} \max\{c^T x : x \in P\}.$$

Therefore,

$$\alpha \geq \frac{\max\{c^T x : x \in P\}}{\max\{c^T x : x \in Q\}}.$$

Since this holds for any nonnegative c, we have shown that

$$t(P,Q) \geq \sup_{c \in \mathbf{R}^n_+} \frac{\max\{c^T x : x \in P\}}{\max\{c^T x : x \in Q\}}.$$

Now let $\alpha = \sup_{c \in \mathbf{R}^n_+} \frac{\max\{c^T x : x \in P\}}{\max\{c^T x : x \in Q\}}$. For a contradiction, assume that P is not an α-relaxation of Q. Then there exists a point $y \in P$ such that $\frac{1}{\alpha} y \notin Q$. Therefore there exists a hyperplane $a^T x = b$ such that $a^T(\frac{1}{\alpha}y) > b$ and $a^T x \leq b$ for all $x \in Q$.

Let a' be defined by $a'_i = \max\{a_i, 0\}$. We claim a' is also a separating hyperplane. Clearly $(a')^T(\frac{1}{\alpha}y) > b$. Given $x \in Q$, let x' be defined so that $x'_i = 0$ if $a'_i = 0$ and $x'_i = x_i$

otherwise. Since $x' \leq x$, we know that $x' \in Q$, and thus $a^T x' \leq b$. But $a^T x' = (a')^T x$, so $(a')^T x \leq b$, which proves that a' is a separating hyperplane.

Since $a' \geq 0$, we may set $c = a'$, and we must have

$$\alpha \geq \frac{\max\{(a')^T x : x \in P\}}{\max\{(a')^T x : x \in Q\}}.$$

The denominator is clearly no more than b, while the numerator is at least $(a')^T y > \alpha b$. This gives

$$\alpha \geq \frac{\max\{(a')^T x : x \in P\}}{\max\{(a')^T x : x \in Q\}} > \frac{\alpha b}{b} = \alpha.$$

This contradiction proves that P is an α-relaxation of Q, so that

$$t(P,Q) \leq \sup_{c \in \mathbf{R}^n_+} \frac{\max\{c^T x : x \in P\}}{\max\{c^T x : x \in Q\}}.$$

We have already shown the reverse inequality, so this proves the proposition. ■

Definition 2.3 *For an inequality $a^T x \leq b$, its* strength relative to anti-blocking polyhedron *P is $\frac{\max\{a^T x : x \in P\}}{b}$.*

This definition is justified by the following theorem, due to Goemans and Hall [19]:

Theorem 2.4 *Let anti-blocking polyhedron Q be defined by inequalities $a_i^T x \leq b_i$ for $i = 1, \ldots, m$, where $a_i \geq 0, b_i \geq 0$ for all i. Let P be a relaxation of Q. Then*

$$t(P,Q) = \max_i \frac{d_i}{b_i},$$

where $d_i = \max\{a_i^T x : x \in P\}$. That is, $t(P,Q)$ is the strength of the strongest inequality of Q relative to P.

2.4.2 The shooting experiment

Given a shooting point z and a direction d, the points along the ray are of the form $z + td$, where $t \geq 0$ is a scalar. The distance from z to $z + td$ is $t\,||d||$.

Definition 2.5 *The value t is the* scaled shooting distance *from z to $z + td$.*

Since d is constant, the scaled shooting distance can be used to compare the distances from z to the intersections of the ray with the inequalities that define the polyhedron.

Proposition 2.6 *The scaled shooting distance from point z to inequality $\sum_{j=1}^{n} a_j x_j \leq b$, where z satisfies the inequality, is given by*

$$t = \frac{b - \sum_{j=1}^{n} a_j z_j}{\sum_{j=1}^{n} a_j d_j},$$

if this value is defined and positive.

Proof: To determine the scaled distance along the ray to the inequality, we must solve $\sum_{j=1}^{n} a_j(z_j + td_j) = b$ for t. This gives

$$\begin{aligned} \sum_{j=1}^{n} a_j(z_j + td_j) &= b \\ \sum_{j=1}^{n} a_j z_j + t\sum_{j=1}^{n} a_j d_j &= b \\ t &= \frac{b - \sum_{j=1}^{n} a_j z_j}{\sum_{j=1}^{n} a_j d_j}. \end{aligned} \tag{2}$$

Since z satisfies the inequality, the numerator of (2) is nonnegative. If z lies in the hyperplane defined by the inequality, then we may ignore it, so we may restrict attention to inequalities for which the numerator of (2) is positive. If the denominator of (2) is zero, then the direction d lies in the same hyperplane defined by a, so the inequality is never intersected. If the denominator is negative, then the ray does not intersect the inequality. Therefore, we may restrict our attention to inequalities for which t is positive. ■

Consider the case that z is inside the polyhedron. Since z is inside the polyhedron, the ray leaves the polyhedron at the first inequality that it intersects. So the facet that is hit is the one that minimizes the value of t among those for which t is positive.

Proposition 2.7 *The scaled shooting distance from point z to inequality $\sum_{j=1}^{n} a_j x_j \geq b$, where z does not satisfy the inequality, is given by*

$$t = \frac{b - \sum_{j=1}^{n} a_j z_j}{\sum_{j=1}^{n} a_j d_j},$$

if this value is defined and positive.

Proof: The derivation of the equation is the same as in the previous proof.

Since z does not satisfy the inequality, the numerator is positive. If the denominator is zero, then the direction d lies in the same hyperplane defined by a, so the inequality is never intersected. If the denominator is negative, then the ray does not intersect the inequality. Therefore, we may restrict our attention to inequalities for which t is positive. ■

In the case of blocking polyhedra, we are interested in an external shooting point, the origin. The ray enters the polyhedron when it intersects the *last* inequality. Therefore, the facet that is intersected is the one that maximizes the value of t.

This general approach to the shooting experiment will be used in several later chapters.

2.4.3 Computational determination of Chvátal-Gomory rank

In general, it is not easy to determine the Chvátal-Gomory rank of an inequality. For some well-known facets, the rank or bounds on the rank have been determined. This is not the case for master cyclic group or knapsack facets, however, so we have devised a computational approach to determine those facets that have Chvátal-Gomory rank 1.

Consider the following IP:

$$\begin{aligned} \max \quad & c^T x \\ s.t. \quad & a_i^T x \leq b_i \quad i = 1, 2, \ldots, m \\ & x \geq 0 \\ & x \text{ integer} \end{aligned}$$

where $x, c, a_i \in \mathbf{R}^n, b_i \in \mathbf{R}$. The standard LP relaxation is found by removing the integrality requirement.

As discussed in Section 1.4.1, Rank 1 C-G inequalities are of the form

$$\sum_{j=1}^{n} \left\lfloor \sum_{i=1}^{m} u_i a_{ij} \right\rfloor x_j \leq \left\lfloor \sum_{i=1}^{m} u_i b_i \right\rfloor,$$

where $u_i \in \mathbf{R}_+$.

Assume we are presented with a candidate inequality $f^T x \leq g$ with $f \in \mathbf{Z}^n, g \in \mathbf{Z}$. If this is a rank 1 C-G inequality, then there exist nonnegative u_i such that $\sum_{i=1}^{m} u_i a_{ij} \geq f_j$

for all j and such that $\sum_{i=1}^{m} u_i b_i < g + 1$. We can determine this with the following LP:

$$\begin{array}{lrcll} \min & b^T u & & & \\ s.t. & \sum_{i=1}^{m} u_i a_{ij} & \geq & f_j & j = 1, \ldots, n \\ & u_i & \geq & 0 & i = 1, \ldots, m \end{array}$$

If the optimal objective value is less than $g + 1$, then the inequality is rank 1. Otherwise it is not. Note that the value g is not present in the LP itself.

CHAPTER III

POLARITY RELATIONSHIP BETWEEN THE SHOOTING EXPERIMENT AND PROBABILITY OF OPTIMALITY

This chapter presents connections between the shooting experiment and polyhedral analysis. These connections stem from a polarity relationship between performing the shooting experiment and optimizing over a polyhedron. See Section 1.4.5 for a review of polarity. A consequence of these connections is a polar relationship between two measures: the shooting experiment and the probability of integrality.

3.1 Central polarity relationship

Definitions for polarity are given in Section 1.4.5.

Theorem 3.1 *Let $P \subset R^n$ be a polyhedron containing the origin. Let c be an objective vector with dimension n. Let $P = \text{hull}\{0, x_1, x_2, \ldots, x_m\} + \text{cone}\{y_1, y_2, \ldots, y_\ell\}$. Let P^* be the polar of P, so that $P^* = \{z \in R^n \mid z^T x_i \leq 1$ for $1 \leq i \leq m, z^T y_j \leq 0$ for $1 \leq k \leq \ell\}$.*

Then x_j is an optimal extreme point of P for objective vector c if and only if $z^T x_j \leq 1$ defines a facet of P^* that is hit by the ray from the origin in direction c.

Proof: We will first show that the distance from the origin to the hyperplane $z^T x_i = 1$ along ray c is given by $\frac{||c||}{c^T x_i}$. The vector that gives this distance is a multiple αc of c. We must solve $(\alpha c)^T x_i = 1$ for α, which gives $\alpha = 1/(c^T x_i)$. Thus, the distance is $||\alpha c|| = \alpha||c|| = ||c||/(c^T x_i)$, as claimed.

Now assume that x_j is an optimal extreme point of P for objective vector c. Then $c^T x_j \geq c^T x_i \ \forall i$ and $c^T y_k \leq 0 \ \forall k$. The second set of inequalities indicates that direction c goes into the interior of P^* even if some constraints contain the origin. Then we have

$||c||/(c^T x_j) \leq ||c||/(c^T x_i)$ $\forall i$, which means that the first constraint of P^* intersected in the direction of c is $z^T x_j \leq 1$.

It is clear that each of the implications in the above paragraph is in fact an "if and only if" relation, which proves the theorem. ■

Theorem 3.1 states that performing the shooting experiment on the polar P^* with the origin as the shooting point gives the same information as solving the optimization problem on P. If we wish to use a shooting point other than the origin, then the result would apply to the polar of P with respect to that point.

As discussed in Section 1.4.5, two other types of polarity exist for blocking and anti-blocking polyhedra. Similar results apply in these cases. For a blocking polyhedron P, let $B(P)$ be its blocker. For an anti-blocking polyhedron P, let $A(P)$ be its anti-blocker.

Theorem 3.2 *Given a blocking polyhedron P and a nonnegative objective vector c for minimization, x_j is an optimal extreme point of P if and only if $z^T x_j \geq 1$ defines a facet of $B(P)$ that is intersected by the ray from the origin in direction c.*

Proof: As in the proof of Theorem 3.1, the distance to the constraint defined by x_j is $\frac{||c||}{c^T x_j}$. In this case, however, a facet that is hit must maximize this value, since the origin is not in the polyhedron.

If x_j is an optimal extreme point, then $c^T x_j \leq c^T x_i$ for all i. Thus, $\frac{||c||}{c^T x_j} \geq \frac{||c||}{c^T x_i}$ for all i, so the facet defined by x_j is hit. The converse is clear. ■

Theorem 3.3 *Given an anti-blocking polyhedron P and a nonnegative objective vector c for maximization, x_j is an optimal extreme point of P if and only if $z^T x_j \leq 1$ defines a facet of $A(P)$ that is intersected by the ray from the origin in direction c.*

Proof: The argument is the same as in the proof of Theorem 3.1 in the case that there are no extreme rays y_k. ■

Note that in the blocking and anti-blocking cases, it is not possible to consider a shooting point other than the origin, since the blocker or anti-blocker is only defined with respect to

the origin. If a shooting point inside the polyhedron is used, however, then Theorem 3.1 can be applied using a traditional polar polyhedron.

3.2 Complexity results

We will distinguish between *solving the shooting experiment*, by which we mean determining the shooting experiment size of one or more facets, and *performing the shooting experiment*, by which we mean determining the facet that is hit by a shot in an arbitrary direction.

We do not know the complexity of solving the shooting experiment. We know of no efficient methods to determine the shooting experiment size, and the problem has strong similarities to computing the volume of a polytope, which is known to be #P-hard. For this reason, we speculate that solving the shooting experiment may also be #P-hard. To our knowledge this is an open question.

In contrast, we can use the polar relationship of Theorem 3.1 to relate the complexity of performing the shooting experiment to the complexity of optimizing.

Theorem 3.4 *There exists an algorithm* OPT *such that given input* (n, L, SHOOT, c)*, where*

- n *and* L *are positive integers*
- SHOOT *is an algorithm that performs the shooting experiment on a polyhedron* $P \in \mathbf{R}^n$ *defined by linear inequalities of size at most* L
- c *is a rational vector with* n *coordinates,*

then OPT *optimizes over polyhedron* P *with objective* c*, in time polynomially bounded by* n, L*, the size of* c*, and the running time of* SHOOT.

Proof: Performing the shooting experiment provides a way to separate: Given a point x which may or may not lie in the polyhedron P, perform the shooting experiment from point q in the direction $x - q$. This identifies a facet (a, a_0). Check whether $ax \leq a_0$ to determine whether $x \in P$. The running time of this separation algorithm is polynomial in n, L, x and the running time of SHOOT.

By the polynomial-time equivalence of separation and optimization, we conclude that optimizing can be done in time as indicated in the theorem. See Schrijver [37] for details of how the ellipsoid algorithm is used to prove this equivalence. ■

Theorem 3.5 *There exists an algorithm* SHOOT *such that given input* (n, L, OPT, d)*, where*

- n *and* L *are positive integers*
- OPT *is an optimization algorithm for a polyhedron* $P \in \mathbf{R}^n$ *defined by linear inequalities of size at most* L
- d *is a rational vector with* n *coordinates,*

then SHOOT *performs the shooting experiment on polyhedron* P *in direction* d*, in time polynomially bounded by* n, L*, the size of* d*, and the running time of* OPT.

Proof: Optimizing over P is the same as performing the shooting experiment in P^*. By Theorem 3.4, we can optimize over P^* in time polynomially bounded by n, L, the size of d, and the running time of OPT. This algorithm also performs the shooting experiment on P. ■

By restricting to nonnegative objective vectors and nonnegative points x, Theorems 3.4 and 3.5 may be applied to blocking and anti-blocking polyhedra as well, as the following corollaries indicate.

Corollary 3.6 *There exists an algorithm* OPT *such that given input* (n, L, SHOOT, c)*, where*

- n *and* L *are positive integers*
- SHOOT *is an algorithm that performs the shooting experiment on a polyhedron* $P \in \mathbf{R}^n_+$ *of blocking type, defined by linear inequalities of size at most* L
- c *is a nonnegative rational vector with* n *coordinates,*

then OPT *optimizes over polyhedron* P *with objective* c*, in time polynomially bounded by* n, L*, the size of* c*, and the running time of* SHOOT.

Corollary 3.7 *There exists an algorithm* SHOOT *such that given input* (n, L, OPT, d), *where*

- n *and* L *are positive integers*
- OPT *is an optimization algorithm for a polyhedron* $P \in \mathbf{R}^n_+$ *of blocking type, defined by linear inequalities of size at most* L
- d *is a nonnegative rational vector with* n *coordinates,*

then SHOOT *performs the shooting experiment on polyhedron* P *in direction* d, *in time polynomially bounded by* n, L, *the size of* d, *and the running time of* OPT.

Proof of Corollaries 3.6 and 3.7: Performing the shooting experiment provides a way to separate. Given a point $x \geq 0$, we can shoot in direction x and test x against the inequality hit. The rest of the proof is the same as the proofs of Theorems 3.4 and 3.5 with $B(P)$ replacing P^*. ■

Corollary 3.8 *There exists an algorithm* OPT *such that given input* (n, L, SHOOT, c), *where*

- n *and* L *are positive integers*
- SHOOT *is an algorithm that performs the shooting experiment on a polyhedron* $P \in \mathbf{R}^n_+$ *of anti-blocking type, defined by linear inequalities of size at most* L
- c *is a nonnegative rational vector with* n *coordinates,*

then OPT *optimizes over polyhedron* P *with objective* c, *in time polynomially bounded by* n, L, *the size of* c, *and the running time of* SHOOT.

Corollary 3.9 *There exists an algorithm* SHOOT *such that given input* (n, L, OPT, d), *where*

- n *and* L *are positive integers*
- OPT *is an optimization algorithm for a polyhedron* $P \in \mathbf{R}^n_+$ *of anti-blocking type, defined by linear inequalities of size at most* L

- *d is a nonnegative rational vector with n coordinates,*

then SHOOT *performs the shooting experiment on polyhedron P in direction d, in time polynomially bounded by n, L, the size of d, and the running time of* OPT.

Proof of Corollaries 3.8 and 3.9: The proof is identical to the proof of Corollaries 3.6 and 3.7 with $A(P)$ replacing $B(P)$. ■

The proofs of Theorems 3.4 and 3.5 have several additional consequences:

- Optimization over the polyhedron P is polynomial-time equivalent to optimization over P^* (or $B(P)$ or $A(P)$, as appropriate).
- Performing the shooting experiment with respect to one shooting point is polynomial-time equivalent to performing the shooting experiment with respect to any other shooting point, as long as both are interior points of P (for the general polar case).
- Performing the shooting experiment is polynomial-time equivalent to separating.

One direction of the last equivalence is perhaps not obvious, since separation merely requires the identification of any violated inequality, while performing the shooting experiment gives, in a sense, a most-violated inequality.

A consequence of Theorem 3.4 is that we can perform the shooting experiment in polynomial time only for problems that are in P. It is unlikely, therefore, that the shooting experiment would be an efficient tool for deciding the relative importance of facets "on the fly" during computation, since the problem being solved is presumably not in P. This does not rule out the potential value of the shooting experiment as a tool for analyzing and better understanding polyhedra, however.

3.3 Examples of the polar relationship

In this section we consider two examples that illustrate the results of the previous sections. First we consider the Chinese postman problem and the odd-cut problem, whose polyhedra form a blocking pair. Next we consider the spanning set and partition problems, which also form a blocking pair.

3.3.1 Chinese postman and odd-cut problems

Given a graph $G = (V, E)$, let $T \subseteq V$ such that $|T|$ is even. The *Chinese postman problem* on G with set T is

$$\begin{array}{lrcll} \min & c^T x & & & \\ s.t. & \sum_{e \in \delta(v)} x_e & \equiv & |T \cap \{v\}| \pmod 2 & \forall v \in V \\ & x_e & \geq & 0 & \forall e \in E \\ & x_e & & \text{integer} & \forall e \in E \end{array}$$

The set of edges with $x_e = 1$ is called a *postman set.*

The name "postman" comes from the special case in which T is the set of nodes with odd degree (that is, nodes with an odd number of incident edges). In this case, the graph represents the streets that a postman must deliver mail to, and the optimal postman set leads to the shortest walk that traverses every edge in the graph. Specifically, the postman set shows those edges that must be traversed twice in an optimal walk.

It is called the Chinese postman problem after Mei-ko Kwan [31], who gave necessary and sufficient conditions for a postman set to represent an optimal solution.

The modular congruence in the Chinese postman problem does not lend itself naturally to polyhedral analysis, but we can still consider the convex hull of integer feasible solutions. Note that by increasing any value x_e by 2 in a feasible integer solution, we get another feasible integer solution. Therefore, the integer hull of the Chinese postman problem is of blocking type.

Edmonds and Johnson [13] showed that this integer hull is given by

$$\begin{array}{rcll} \sum_{e \in \delta(S)} x_e & \geq & 1 & \forall S \subset V, |S \cap T| \text{ odd} \\ x_e & \geq & 0 & \forall e \in E \end{array} \tag{3}$$

An edge set $\delta(S)$ where $S \subseteq V, |S \cap T|$ odd is called an *odd cut.*

From the description above, it is clear that the blocker for (3) has extreme points that correspond to the odd cuts. Specifically, consider the points in $\mathbf{R}^n$ whose coordinates match the coefficients of an odd-cut constraint. The blocker of (3) is the polyhedron formed by the convex hull of these points along with all points that are greater than or equal to a point in the convex hull. We call this the *odd-cut polyhedron.*

Corollary 3.10 *Performing the shooting experiment on the Chinese postman polyhedron with the origin as the shooting point may be accomplished by minimizing over the odd-cut polyhedron.*

Proof: This follows from the proof of Theorem 3.5, but the point here is to confirm it directly.

Shooting from the origin, it is not possible to hit a nonnegativity facet, so we are concerned only with the facets defined by odd cuts. Using the analysis of Section 2.4.2, the distance in direction d to the facet defined by the set S is given by

$$\frac{||d||}{\sum_{e \in \delta(S)} d_e}.$$

Since we are shooting from an exterior point, the facet hit is the one with the greatest distance. Since the numerator is constant, this can be found by minimizing the denominator above.

That is, the facet that is hit corresponds to the minimum odd cut where the direction d is used as the objective vector. ■

Of course, the result is also true with the polyhedra switched: shooting on the odd cut polyhedron may be accomplished by minimizing over the Chinese postman polyhedron.

The proof of Theorem 3.5 also indicates that the complexity of the Chinese postman problem and odd-cut problem must be the same. In fact, both problems are in P, which means that we can also perform the shooting experiment on either polyhedron in polynomial time.

3.3.2 Minimum spanning set and partition polyhedra

Another example of a blocking polyhedron comes from the minimum spanning set problem. The variables in this problem correspond to edges in the graph under consideration, so that 0-1 points represent edge subsets of the graph. The polyhedron is the blocking polyhedron whose extreme points are exactly the 0-1 points that define spanning trees. If the objective vector is nonnegative, then minimizing over this polyhedron will always yield a minimum spanning tree.

Let $S_1, S_2, \ldots, S_k$ with $k \geq 2$ represent a partition of V. That is, $S_i \cap S_j = \emptyset$ for all $i \neq j$ and $S_1 \cup S_2 \cup \cdots \cup S_k = V$. Let $\delta(S_1, \ldots, S_k) = \{\{u, v\} \in E : u \in S_i, v \in S_j, i \neq j\}$. Fulkerson [17] showed that the spanning set polyhedron is given by the following system:

$$\begin{aligned} \textstyle\sum_{e \in \delta(S_1, S_2, \ldots, S_k)} x_e &\geq k - 1 \quad \forall \text{ partitions } S_1, S_2, \ldots, S_k \\ x_e &\geq 0 \qquad \forall e \in E \end{aligned}$$

The first set of inequalities are called *partition inequalities.*

From the form above, the vertices of the blocker of the minimum spanning tree polyhedron have values $x_e = \frac{1}{k-1}$ for $e \in \delta(S_1, \ldots, S_k)$ and $x_e = 0$ otherwise, corresponding to partitions of V. The blocker is formed by taking the convex hull of these points and all points that are greater than or equal to a point in the convex hull. We will call this the *partition polyhedron.*

Using Theorem 3.5, we know that we can perform the shooting experiment on the partition polyhedron by finding a minimum spanning tree, which can be done in polynomial time. Conversely we can perform the shooting experiment on the spanning set polyhedron by finding a minimum partition. As a consequence of the proof of Theorem 3.5, this must be possible in polynomial time. In fact, Cunningham [11] showed that it is possible to find the optimal partition in polynomial time by solving a polynomial number of network flow problems.

3.4 The shooting experiment and probability of integrality

The probability of integrality is a measure that is the sum of probabilities of optimality for certain extreme points. Therefore, Theorem 3.1 provides a relationship between the probability of integrality and the shooting experiment, provided that we use the same distribution for the random vectors in each case.

Corollary 3.11 *Let a random objective vector be taken from a spherically symmetric distribution. Then the probability that an extreme point x_i of a polyhedron P is optimal equals the shooting experiment size of the corresponding facet of P^*.*

Corollary 3.12 *Let P be a polyhedron that is a relaxation of an integer hull, and let a random objective vector be taken from a spherically symmetric distribution. Then the probability of integrality is the same as the sum of the shooting experiment sizes of the facets of P^* that correspond to feasible integral extreme points of P.*

Corollary 3.12 indicates a clear relationship between these two measures, but the consequences of that relationship are less clear. When examining the probability of integrality we also want to understand the possible changes when additional cutting planes are added to P. In that case P^* changes by adding additional extreme points, which causes some facets to be replaced with new ones. What does the shooting experiment mean in that context? To more fully understand this relationship, it would be necessary to explore the dynamics of this interplay between changing polyhedra. This is a possible area of future research.

CHAPTER IV

CYCLIC GROUP AND KNAPSACK POLYHEDRA

Gomory studied group problems in his work with corner polyhedra for integer programs. He developed a shooting experiment in order to study their facetial structure [23]. The *master cyclic group problem* with n variables and right-hand-side r is

$$\begin{aligned} \min \quad & c^T x \\ s.t. \quad & x_1 + 2x_2 + \ldots + nx_n \equiv r \pmod{n+1} \\ & x \in Z_+. \end{aligned}$$

The term "master" refers to the fact that all integer coefficients $1, 2, \ldots, n-1$ are present in the congruence. Although there is no natural LP relaxation, the integer hull is formed as usual by taking the convex hull of all integer solutions to the modular congruence. Given an integer feasible point $(x_1, \ldots, x_i, \ldots, x_n)$, we may find another feasible integer point $(x_1, \ldots, x_i + n, \ldots, x_n)$ in any coordinate direction, so the polyhedron has a recession cone equal to the nonnegative orthant. That is, starting at a point x in the polyhedron, all directions in the nonnegative orthant remain in the polyhedron.

There is a close relationship between master cyclic group polyhedra and master knapsack polyhedra. This relationship was considered by Aráoz, Evans, Gomory, and Johnson [2]. The *master packing knapsack problem* with n variables is

$$\begin{aligned} \max \quad & c^T x \\ s.t. \quad & x_1 + 2x_2 + \ldots + nx_n \leq n \\ & x \geq 0 \\ & x \in Z. \end{aligned}$$

In this case, the LP relaxation is formed as usual. We call the non-trivial inequality in the formulation the *defining inequality* for the knapsack.

In this chapter we consider many of the measures from Chapter 2 applied to master cyclic group and master packing knapsack polyhedra. Section 4.1 discusses performing the shooting experiment to obtain a Monte Carlo estimate of the shooting experiment size. Section 4.2 presents a deterministic partial ordering of the facets that is consistent with the ordering determined by their shooting experiment sizes. Sections 4.3 through 4.6 describe four other measures used: best-case improvement, facet volume, Chvátal-Gomory rank, and a measure based on the polyhedral characterization of the facets. Section 4.7 presents an empirical measure of usefulness based on the size of the branch-and-bound tree. Section 4.8 presents a summary of the results, including a discussion of correlations between the measures for each polyhedron. The data itself appears for reference in Appendix B.

4.1 Performing the shooting experiment

Gomory [21] showed that the facets of the master cyclic group polyhedron with dimension n and right-hand-side $r \neq 0$ are of the form $\sum_{i=1}^{n} \pi_i x_i \geq \pi_r$, where the coefficients π_i are given by the extreme rays of the following cone:

$$\begin{aligned} \pi_i + \pi_j &\geq \pi_k, \quad 1 \leq i,j,k \leq n-1, i+j \equiv k \pmod{n} \\ \pi_i + \pi_j &= \pi_r, \quad 1 \leq i,j \leq n-1, i+j \equiv r \pmod{n} \\ \pi_i &\geq 0, \quad 1 \leq i \leq n. \end{aligned} \tag{4}$$

The first set of inequalities are called *subadditivity constraints*, and the set of equations are called *complementarity constraints*. Scaling the coefficients does not change the facet, so it is also possible to add a scale factor such as $\pi_r = 1$ to the above system. In that case, the facets correspond to the extreme points of the resulting polytope. The case for $r = 0$ is slightly different, and we will not consider it in this dissertation.

Shooting from the origin in direction given by vector d, we can determine the distance to each inequality based on Proposition 2.7. For the inequality (π, π_r), t is given by

$$t = \frac{\pi_r}{\sum_{i=1}^{n} \pi_i d_i},$$

and the facet that is hit is the one that maximizes this value.

Therefore, as Gomory showed, it is possible to perform the shooting experiment on a cyclic group polyhedron by solving the following LP:

$$\begin{array}{lrcl} \min & \sum_{i=1}^{n} d_i \pi_i & & \\ s.t. & \pi_i + \pi_j & \geq & \pi_k, \quad 1 \leq i,j,k \leq n-1, i+j \equiv k \pmod{n} \\ & \pi_i + \pi_j & = & \pi_r, \quad 1 \leq i,j \leq n-1, i+j \equiv r \pmod{n} \\ & \pi_i & \geq & 0, \quad i = 1, \ldots, n \\ & \pi_r & = & 1. \end{array} \tag{5}$$

To calculate a Monte Carlo estimate of the shooting experiment size, we iteratively generate random directions d to serve as the objective vector and solve (5). If facet A is hit X_A times during n trials, then $\frac{X_A}{n}$ is an estimate of its shooting experiment size.

The data for the shooting experiment performed on cyclic group polyhedra was provided by Lisa Evans and appears along with other measures in Appendix B.

When comparing the results for two facets, it is important to know whether the difference between them is statistically significant. The test we used for statistical significance appears in Appendix A.

4.1.1 Application to the master packing knapsack problem

By using the relationship between cyclic group and knapsack polyhedra, it is possible to perform the shooting experiment on master knapsack polyhedra in a similar way.

Aráoz et al. [2] showed that the facets of the master packing knapsack polytope—other than nonnegativity—have the form $\sum_{i=1}^{n} \rho_i x_i \leq \rho_n$, where ρ is given by the extreme rays of the following polyhedron:

$$\begin{array}{rcl} \rho_i + \rho_j & \leq & \rho_{i+j}, \quad 1 \leq i,j,i+j \leq n \\ \rho_i + \rho_{n-i} & = & \rho_n, \quad 1 \leq i \leq n-1 \\ \rho_i & \geq & 0, \quad 1 \leq i \leq n. \end{array} \tag{6}$$

Note the similarity to (4), except that superadditivity constraints have replaced subadditivity constraints, and there is no modularity.

Shooting from the origin, the distance to the hyperplane (ρ, ρ_n) is $\frac{\rho_n ||d||}{\sum_{i=1}^{n} \rho_i d_i}$. In this case, it is the nearest inequality that is hit, so we can perform the shooting experiment by fixing

ρ_n and maximizing the denominator:

$$\begin{array}{lrcll} \max & \sum_{i=1}^{n} d_i\rho_i & & & \\ s.t. & \rho_i + \rho_j & \leq & \rho_{i+j}, & 1 \leq i,j,i+j \leq n \\ & \rho_i + \rho_{n-i} & = & \rho_n, & 1 \leq i \leq n-1 \\ & \rho_i & \geq & 0, & 1 \leq i \leq n \\ & \rho_n & = & 1. & \end{array} \tag{7}$$

Thus, we can perform the shooting experiment in polynomial time on both cyclic group and knapsack polyhedra.

4.1.2 Determining the shooting point

In the case of the knapsack polytope, it is not clear that the origin is the best point to use as the shooting point. Advantages of using the origin include that only nonnegative directions are needed and that all such directions will intersect non-trivial facets.

Shooting from another point in the polytope is also possible, however. Let z be the point we wish to shoot from. Then using Proposition 2.6, for facet (ρ, ρ_n) the scaled distance t is

$$t = \frac{\rho_n - \sum_{i=1}^{n} \rho_i z_i}{\sum_{i=1}^{n} \rho_i d_i}. \tag{8}$$

Note that some directions will never intersect a particular hyperplane. In that case the value for t will be negative, so by maximizing t we will correctly avoid these inequalities. Since z is constant, we can scale ρ so that the numerator of (8) is constant and then maximize the denominator as before:

$$\begin{array}{lrcll} \max & \sum_{i=1}^{n} d_i\rho_i & & & \\ s.t. & \rho_i + \rho_j & \leq & \rho_{i+j}, & 1 \leq i,j,i+j \leq n \\ & \rho_i + \rho_{n-i} & = & \rho_n, & 1 \leq i \leq n \\ & \rho_i & \geq & 0, & i = 1,\ldots,n \\ & \rho_n - \sum_{i=1}^{n} \rho_i z_i & = & 1. & \end{array} \tag{9}$$

This gives the first non-trivial inequality intersected, but it is possible that a nonnegativity facet was in fact intersected first. This possibility can be checked directly.

Table 2: Shooting point candidates for the knapsack polytope for $n = 9$

Description	x_1	x_2	x_3	x_4	x_5	x_6	x_7	x_8	x_9
Origin	0	0	0	0	0	0	0	0	0
Centroid estimate	0.971	0.461	0.312	0.225	0.164	0.142	0.121	0.108	0.100
Moving average	0.281	0.255	0.213	0.203	0.150	0.150	0.138	0.141	0.136
Defining ineq.	0.016	0.032	0.047	0.063	0.079	0.095	0.111	0.126	0.142

Selection of the shooting point z has a significant impact on the shooting experiment sizes. Intuitively, if we shoot from a point that is near a particular facet, then that facet will be hit more often than it otherwise would be.

We considered several possibilities for the shooting point for knapsack polytopes:

- the origin
- the centroid of the polytope (estimated)
- the moving average of points hit by shots
- a point halfway between the origin and the defining inequality

The centroid was estimated as the average of a set of random points generated uniformly in the polytope. The "moving average" was found by shooting from the origin a number of times and taking the average of the points where those shots intersected the boundary of the polytope. This average point was used as the new shooting point, and the process was repeated until the "moving average" point appeared to stabilize.

These possible points were tested on knapsacks of sizes $n = 9, 10, 11$, and 12. As an example, Table 2 shows the points that were considered for $n = 9$ and Table 3 indicates the sample results for these points.

The results for these different choices are largely similar. The most significant differences occur in the number of times the defining inequality was hit and in the number of times the nonnegativity inequalities were hit.

Shooting from the origin, in particular, did not hit the defining inequality as much as we expected, given its clear importance to the polytope. The moving average seemed to

Table 3: Alternate shooting point trials for $n = 9$

Facet	Origin	Centroid	Moving Average	Defining Inequality
0 0 0 0 1 1 1 1 1	313	187	437	1130
0 0 0 1 1 2 2 2 2	181	36	289	541
0 0 1 1 2 2 3 3 3	133	4	67	120
0 0 2 3 3 4 6 6 6	119	6	190	229
0 1 1 2 2 3 3 4 4	104	11	377	126
0 1 2 2 4 4 5 6 6	60	2	58	39
0 1 2 3 3 4 5 6 6	32	2	86	36
0 2 3 4 5 6 7 9 9	30	1	70	34
1 2 3 4 5 6 7 8 9	28	32176	1104	76
nonnegativity	0	67575	7322	97669

Table 4: Interior shooting points based on the "moving average"

n	"Moving average" shooting point
6	0.444 0.282 0.236 0.201 0.187 0.190
7	0.435 0.278 0.250 0.185 0.178 0.152 0.158
8	0.330 0.324 0.216 0.194 0.181 0.164 0.142 0.136
9	0.281 0.255 0.213 0.203 0.150 0.150 0.138 0.141 0.136
10	0.270 0.250 0.195 0.174 0.165 0.140 0.137 0.126 0.126 0.121
11	0.261 0.229 0.208 0.172 0.149 0.138 0.124 0.125 0.117 0.112 0.118
12	0.234 0.230 0.185 0.173 0.137 0.135 0.124 0.120 0.115 0.106 0.108 0.109
13	0.179 0.196 0.138 0.179 0.112 0.135 0.124 0.107 0.104 0.101 0.111 0.119 0.101
14	0.141 0.152 0.149 0.154 0.140 0.111 0.175 0.116 0.096 0.098 0.094 0.096 0.096 0.094

offer the best contrast with the origin in that the defining inequality was hit a great deal, but not so often as to overshadow the differences among other facets. For this reason, we consider only shooting from the origin and shooting from the moving average interior point in the full results of Section B. The points used for each value of n should be viewed as heuristic values. They are given in Table 4.

The data for shooting from the origin was provided by Lisa Evans, while tests for shooting from interior points were performed by the author.

4.2 A partial order on the shooting experiment sizes

In addition to the Monte Carlo estimate, we may compute a deterministic partial order on the facets of a master cyclic group polyhedron or master packing knapsack polytope that is

consistent with the total order determined by their shooting experiment sizes. Although the results of this section can be applied to either problem, we present them using the notation of the knapsack problem.

Let the inequality $\sum_{i=1}^{n} a_i x_i \leq a_n$ be denoted simply by the vector $a = (a_1, a_2, \ldots, a_n)$. Assume that the facet is scaled so that $a_n = 1$ and define $\tilde{a} = (a_1, a_2, \ldots, a_{\lfloor n/2 \rfloor})$ (that is, the first half of the vector).

Definition 4.1 *Given facets a and b, we say that $a \succ b$ if for every facet $c \notin \{a, b\}$,*

$$(\tilde{a} - \tilde{c})^T(\tilde{a} - \tilde{b}) \geq (\tilde{c} - \tilde{b})^T(\tilde{a} - \tilde{b}).$$

Theorem 4.2 *The partial order of Definition 4.1 is consistent with the total order determined by the shooting experiment sizes of the facets.*

To prove Theorem 4.2, we will use several definitions and lemmas. First note that the use of partial vectors $\tilde{a}, \tilde{b}$, and $\tilde{c}$ does not sacrifice any information about the facets. The value $a_n = 1$, and if $n/2$ is an integer, $a_{n/2} = 1/2$. By the complementarity constraints of (6), we know that $a_{n-i} = 1 - a_i$, so it is possible to reconstruct a from $\tilde{a}$.

4.2.1 Definitions

Consider two facets a and b. Their shooting experiment sizes are defined as probabilities on the space of directions $d \in \mathbf{R}^n_+$, where the coordinates of d are iid positive normal values, as discussed in Section 1.4.3. Let $m = \lfloor \frac{n-1}{2} \rfloor$. Just as $\tilde{a}, \tilde{b} \in \mathbf{R}^m$, we will find it more convenient to consider a space of direction vectors in $\mathbf{R}^m$. Define the map $\varphi(d) = \hat{d} \equiv (d_{n-1} - d_1, d_{n-2} - d_2, \ldots, d_{n-m} - d_m)$.

Note that $\hat{d}$ is a random vector, and each coordinate is iid with mean zero. Also, even though many vectors d map to the same vector $\hat{d}$, $\hat{d}$ allows us to compare facets just as d did. Since $a_n = b_n = 1$, the scaled shooting distance to facet a in direction d is $\frac{1}{a^T d}$. The same is true for b, of course, so we can determine which facet is intersected first by comparing $a^T d$ and $b^T d$, or by considering the difference $a^T d - b^T d = (a - b)^T d$. It is easy to confirm that because of complementarity $(a - b)^T d = (\tilde{b} - \tilde{a})^T \hat{d}$. Thus, d intersects a first if $(\tilde{b} - \tilde{a})^T \hat{d} > 0$ and b first if $(\tilde{b} - \tilde{a})^T \hat{d} < 0$.

The map φ takes many directions d to a single $\hat{d}$, so the inverse φ^{-1} is a set function. That is, $\varphi^{-1}(\hat{d}) = \{d \in \mathbf{R}^n_+ : \varphi(d) = \hat{d}\}$. We will also consider φ and φ^{-1} acting on sets in the obvious way.

Given a subset $T \subseteq \mathbf{R}^n_+$, let $P(T)$ be the probability that a random direction d falls in T. For $S \subseteq \mathbf{R}^m$, define $P(S) = P(\varphi^{-1}(S))$. This is the probability of a direction d such that $\varphi(d) \in S$.

For ease of exposition, we will refer to a vector $\hat{d} \in \mathbf{R}^m$ as a direction and say that $\hat{d}$ intersects facet a before facet b when we mean that any direction d such that $d \in \varphi^{-1}(\hat{d})$ intersects a before b. This is well-defined, since $(a-b)^T d = (\tilde{b} - \tilde{a})^T \hat{d}$ for any $d \in \varphi^{-1}(\hat{d})$.

Let $A \subseteq \mathbf{R}^m$ be the set of directions $\hat{d}$ that hit facet a. For any facet $i \notin \{a, b\}$, let A_i be the set of directions $\hat{d}$ such that facet a is intersected before facet i or facet b. Then $A_i \supseteq A$, but the reverse is not necessarily true, since some directions in A_i may hit a facet other than a, b, or i. Define B and B_i similarly.

It is clear that $A = \cap_i A_i$ and $B = \cap_i B_i$, where the intersections are taken over all facets i other than a and b.

4.2.2 Lemmas and Proof

We will call the plane $(\tilde{b} - \tilde{a})^T \hat{d} = 0$ the ab-plane. We already noted that direction $\hat{d}$ intersects a before b if $(\tilde{b} - \tilde{a})^T \hat{d} > 0$ and b before a if $(\tilde{b} - \tilde{a})^T \hat{d} < 0$.

Given a point $\hat{d} \in \mathbf{R}^m$, let $\hat{d}'$ be the image of the point reflected across the ab-plane. For set $S \subseteq \mathbf{R}^m$, let $S' = \{\hat{d}' : \hat{d} \in S\}$ be the image of S reflected across the ab-plane.

Lemma 4.3 *For any set $S \in \mathbf{R}^m$, $P(S) = P(S')$.*

Proof: We have $P(S') = P(\varphi^{-1}(S')) = P(\{d : \varphi(d) \in S'\})$. Reflecting $\varphi(d)$ across the ab-plane may be viewed as changing the sign of a single coordinate in a suitable basis. This is equivalent to exchanging two coordinates in d-space. Given $d \in \mathbf{R}^n_+$, let d' be the point defined by this mapping, so that $\forall d \in \varphi^{-1}(\hat{d}), \varphi(d') = \hat{d}'$.

From the spherical symmetry of the distribution of directions in $\mathbf{R}^n$, exchanging two coordinates gives a point with the same probability density. Therefore $P(\{d : \varphi(d) \in S'\}) =$

$P(\{d' : \varphi(d) \in S'\})$. Noting that the condition $\varphi(d) \in S'$ is the same as $\varphi(d') \in S$, we have

$$P(\{d' : \varphi(d) \in S'\}) = P(\{d' : \varphi(d') \in S\}) = P(\varphi^{-1}(S)) = P(S).$$

This completes the proof that $P(S') = P(S)$. ■

Lemma 4.4 *If* $(\tilde{a} - \tilde{c})^T(\tilde{a} - \tilde{b}) \geq (\tilde{c} - \tilde{b})^T(\tilde{a} - \tilde{b})$, *then* $B'_c \subseteq A_c$.

Proof: Change from the standard basis to an orthonormal basis in which the first coordinate is in the direction $\tilde{b} - \tilde{a}$, which is normal to the ab-plane. For a point $\hat{d}$ and facet $\tilde{a}$, let $\bar{d}$ and $\bar{a}$ be the vectors expressed in the new basis.

Because the ab-plane is normal to the first coordinate direction, $\bar{d}'$ is found by simply changing the sign of the first coordinate of $\bar{d}$. Also, $(\tilde{b} - \tilde{a})^T\hat{d} > 0$ if and only if $\bar{d}_1 > 0$.

Consider sets A_c and B'_c. We have

$$\begin{aligned} A_c &= \{\hat{d} : (\tilde{b} - \tilde{a})^T\hat{d} > 0, (\tilde{c} - \tilde{a})^T\hat{d} > 0\} \\ &= \{\bar{d} : \bar{d}_1 > 0, (\bar{c} - \bar{a})^T\bar{d} > 0\} \\ B'_c &= \{\hat{d} : (\tilde{b} - \tilde{a})^T\hat{d}' < 0, (\tilde{c} - \tilde{b})^T\hat{d}' > 0\} \\ &= \{\bar{d} : \bar{d}_1 > 0, (\bar{c} - \bar{b})^T\bar{d}' > 0\}. \end{aligned}$$

Examining the last condition in each of the above, we have

$$(\bar{c} - \bar{a})^T\bar{d} = (\bar{c}_1 - \bar{a}_1)\bar{d}_1 + \sum_{i=2}^{m}(\bar{c}_i - \bar{a}_i)\bar{d}_i \tag{10}$$

and

$$\begin{aligned} (\bar{c} - \bar{b})^T\bar{d}' &= (\bar{c}_1 - \bar{b}_1)\bar{d}'_1 + \sum_{i=2}^{m}(\bar{c}_i - \bar{b}_i)\bar{d}'_i \\ &= (\bar{c}_1 - \bar{b}_1)(-\bar{d}_1) + \sum_{i=2}^{m}(\bar{c}_i - \bar{b}_i)\bar{d}_i \\ &= (\bar{b}_1 - \bar{c}_1)\bar{d}_1 + \sum_{i=2}^{m}(\bar{c}_i - \bar{b}_i)\bar{d}_i \end{aligned} \tag{11}$$

Note that $\bar{a}$ and $\bar{b}$ must agree on all coordinates except the first, since $\bar{b} - \bar{a}$ has zeros in all other coordinates. Thus $\bar{a}_i = \bar{b}_i$ for $i = 2, 3, \ldots, m$, and the summation terms in (10) and (11) are equal.

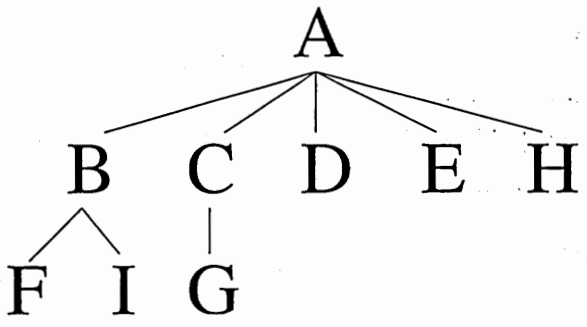

Figure 4: Partial order for the master packing knapsack polytope with $n = 9$

We are given that $(\tilde{a} - \tilde{c})^T(\tilde{a} - \tilde{b}) \geq (\tilde{c} - \tilde{b})^T(\tilde{a} - \tilde{b})$, or equivalently $(\tilde{a} - \tilde{c})^T(\tilde{b} - \tilde{a}) \leq (\tilde{c} - \tilde{b})^T(\tilde{b} - \tilde{a})$. This means that the component of $\tilde{a} - \tilde{c}$ in direction $\tilde{b} - \tilde{a}$ is less than the corresponding component of $\tilde{c} - \tilde{b}$. In terms of the new basis, we conclude that

$$\begin{aligned} \bar{a}_1 - \bar{c}_1 &\leq \bar{c}_1 - \bar{b}_1 \\ \bar{c}_1 - \bar{a}_1 &\geq \bar{b}_1 - \bar{c}_1. \end{aligned}$$

Thus, the coefficient of $\bar{d}_1$ in (10) is greater than the coefficient of $\bar{d}_1$ in (11) while all other coefficients are the same in both equations. Since $\bar{d}_1 > 0$, we conclude that the set of directions $\bar{d}$ for which (10) is positive is a superset of the set for which (11) is positive. This proves that $B'_c \subseteq A_c$. ■

We are now ready to prove Theorem 4.2.

Proof of Theorem 4.2: If $A \succ B$, then $(\tilde{a} - \tilde{c})^T(\tilde{a} - \tilde{b}) \geq (\tilde{c} - \tilde{b})^T(\tilde{a} - \tilde{b})$ for all facets $c \notin \{a, b\}$. By Lemma 4.4, $B'_c \subseteq A_c$ for all facets $c \neq a, b$. Then $B' \subseteq A$.

Because it is a subset, $P(B') \leq P(A)$. By Lemma 4.3, $P(B) = P(B')$, so that $P(B) \leq P(A)$. ■

4.2.3 Example results

Examples of the resulting partial order are given in Figures 4 and 5. For comparison, results of the shooting experiment are given in Tables 5 and 6. In the figures, lines connect two facets that are comparable; the higher facet has a greater shooting experiment size than the lower.

Table 5: Facets of the master packing knapsack polytope with $n = 9$

Facet	Coefficients	Shooting %
A	0 0 0 0 1 1 1 1 1	31.3
B	0 0 0 1 1 2 2 2 2	18.1
C	1 2 3 4 5 6 7 8 9	13.3
D	0 0 2 3 3 4 6 6 6	11.9
E	0 1 1 2 2 3 3 4 4	10.4
F	0 0 1 1 2 2 3 3 3	6.0
G	0 2 3 4 5 6 7 9 9	3.2
H	0 1 2 3 3 4 5 6 6	3.0
I	0 1 2 2 4 4 5 6 6	2.8

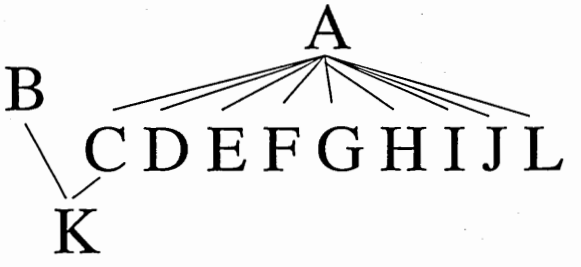

Figure 5: Partial order for the master cyclic group polyhedron with $n = 10, r = 9$

Table 6: Facets of the master cyclic group polyhedron with $n = 10, r = 9$

Facet	Coefficients	Shooting %
A	1 0 1 0 1 0 1 0 1	28.9
B	1 2 3 4 0 1 2 3 4	16.2
C	4 3 2 6 0 4 3 2 6	12.1
D	1 2 3 4 5 6 7 8 9	11.8
E	9 18 7 6 15 14 3 12 21	8.6
F	3 6 4 2 5 3 1 4 7	5.6
G	9 8 7 6 5 4 3 2 11	4.6
H	4 3 2 1 5 4 3 2 6	3.4
I	2 4 6 3 5 2 4 6 8	3.0
J	6 7 3 4 5 6 2 3 9	2.7
K	1 2 1 2 1 2 1 2 3	1.8
L	6 2 3 4 5 6 7 3 9	1.3

In Figure 4, the partial order indicates that facet A has the largest shooting experiment size, which is confirmed by the shooting experiment. The partial order also suggests that facets B and C have large shooting experiment sizes, and Table 5 reveals that they were hit the most often after facet A.

In Figure 5, the partial order suggests that facets A and B are good, which is confirmed by the shooting experiment. It also correctly suggests that facet K is not good. It doesn't give any information on the comparisons of other facets.

The partial order for each polyhedron studied is given in Appendix B along with the tables of measures.

Although it does not give as much information as performing the shooting experiment, the partial order has the advantage of being a deterministic result, unlike the Monte Carlo estimate of the shooting experiment sizes.

The partial order is also significant in that it demonstrates a way in which the shooting experiment can be used beyond simply performing the shooting experiment to get a Monte Carlo estimate.

4.3 Best-case improvement

For knapsack problems, we may consider best-case improvement as presented in Section 2.4.1. The strength of a facet-defining inequality (ρ, ρ_n) with ρ_n scaled to equal 1 is $\frac{\max\{\rho^T x : x \in P\}}{1}$, where P is the LP relaxation. Since P is defined by nonnegativity and a single inequality, the extreme points all lie on coordinate axes. Therefore the maximum is determined by a single coordinate direction. The value in the direction of coordinate i is $n\rho_i/i$, so the best-case improvement measure has value $n \max_i \frac{\rho_i}{i}$.

For cyclic group problems, best-case improvement doesn't make sense as we've defined it, because there is no standard relaxation of the polyhedron. One option is to use the entire nonnegative orthant as the relaxation, in which case the optimal extreme point is always the origin. Unfortunately, the optimal objective value is zero, so using the best-case ratio doesn't provide useful information.

We may look at the absolute improvement instead, however, based on nonnegative

objective vectors that are scaled to be unit vectors (without scaling, comparing absolute improvements would make no sense). Since the relaxation has an objective value of 0, we want an objective vector that maximizes the objective value with the constraint present. This objective vector is normal to the facet, and the change is $\rho_0/||\rho||$.

For both knapsack and cyclic group problems these values are easy to compute. Results of the correlation with other measures is given in Section 4.8, and the measures themselves are in Appendix B.

4.4 Facet volume

This section describes how we can find Monte Carlo estimates of the facet volume for both master cyclic group problems and master packing knapsack problems.

4.4.1 Sampling points in a simplex uniformly

In order to estimate the volumes, we will need to sample points uniformly from a simplex.

Definition 4.5 *The following algorithm generates coordinates $x_1, \ldots, x_n$ for a uniformly random point from the simplex defined by $\sum_{i=1}^{n} a_i x_i \leq b, x \geq 0$.*

1. *Initialize $r = b$ and $i = n$.*
2. *Generate a uniform $(0,1)$ random variable Z.*
3. *Set $x_i = (1 - \sqrt[i]{Z})\frac{r}{a_i}$.*
4. *Set $r = r - a_i x_i$.*
5. *Set $i = i - 1$.*
6. *If $i \geq 1$, return to Step 2.*

Proposition 4.6 *The algorithm of Definition 4.5 gives a uniform random point in the simplex defined by $\sum_{i=1}^{n} a_i x_i \leq b, x \geq 0$.*

Proof: Consider the intersection of the simplex with the plane $x_n = x_n^*$, where $0 \leq x_n^* \leq \frac{b}{a_n}$. This intersection is a simplex in $n-1$ dimensions, where the coordinates $x_1, \ldots, x_{n-1}$ lie

in the $(n-1)$-dimensional simplex given by nonnegativity and the inequality $\sum_{i=1}^{n-1} a_i x_i \leq b - a_n x_n^*$.

The volume of this simplex is

$$\frac{(b - a_n x_n^*)^{n-1}}{(n-1)! \Pi_{i=1}^{n-1} a_i}.$$

For a uniform distribution in the original simplex, the marginal probability density for $x_n = x_n^*$ is given by

$$f(x_n^*) = \frac{\frac{(b-a_n x_n^*)^{n-1}}{(n-1)! \Pi_{i=1}^{n-1} a_i}}{\int_0^{b/a_n} \frac{(b-a_n t)^{n-1}}{(n-1)! \Pi_{i=1}^{n-1} a_i} dt} = \frac{n a_n (b - a_n x_n^*)^{n-1}}{b^n}.$$

Therefore the cumulative distribution function is given by

$$F(x_n^*) = \int_0^{x_n^*} \frac{n a_n (b - a_n t)^{n-1}}{b^n} dt = 1 - \frac{1}{b^n}(b - a_n x_n^*)^n.$$

Inverting the function F gives

$$F^{-1}(U) = \frac{b}{a_n}(1 - \sqrt[n]{1-U}).$$

To sample x_n^*, we simply evaluate F^{-1} at a uniform $(0,1)$ value U. Since uniform random variables are symmetric about their mean, we can use $Z = 1 - U$, which is also a uniform $(0,1)$ random variable. This gives the equation used in the algorithm.

Once we have fixed a value for x_n, the remaining coordinates lie in a smaller-dimensional simplex and are uniformly distributed in it. Thus, we must change the right-hand-side, but then we may repeat the process to sample the coordinates $x_{n-1}, x_{n-2}, \ldots, x_1$. This proves the proposition. ■

4.4.2 Master cyclic group problems

This section describes how to obtain a Monte Carlo estimate of the volume of master cyclic group facets. Consider a facet defined by $\pi^T x \geq \pi_r$ in $\mathbf{R}^{n-1}$. If any coordinates of π are zero, then the volume is infinite.

Otherwise, use Proposition 4.6 to choose $x_1, \ldots, x_{n-2}$ uniformly at random from the simplex defined by $\sum_{i=1}^{n-2} \pi_i x_i \leq \pi_r$. Project this point onto the inequality's hyperplane by

computing x_{n-1} to make the inequality tight:

$$x_{n-1} = \pi_r - \sum_{i=1}^{n-2} \pi_i x_i.$$

Check whether the resulting point x is a feasible point for the polyhedron. In practice, we have done this by comparing against every other facet, though it is possible to separate in polynomial time without an explicit list of facets.

The volume of the original simplex is $\frac{1}{(n-1)!}\Pi_{i=1}^{n-1}\frac{\pi_r}{\pi_i}$. There is also a factor that results from the projection of x_{n-1}: the final space is larger by a factor of $\frac{\pi_{n-1}}{||\pi||}$. If the fraction of valid points in the sample is p, then the volume estimate is

$$p\frac{1}{(n-1)!}\left(\Pi_{i=1}^{n-1}\frac{\pi_r}{\pi_i}\right)\frac{\pi_{n-1}}{||\pi||}.$$

Estimates of cyclic group facet volumes appear along with other measures in Appendix B, while their correlations are discussed in Section 4.8. At times the difference in the volume estimates of two facets is not statistically significant. The test we used for statistical significance appears in Appendix A.

4.4.3 Master packing knapsack problems

It is possible to obtain a Monte Carlo estimate for knapsack facet volumes in a similar way.

Use Proposition 4.6 to choose $x_1, x_2, \ldots, x_{n-1}$ uniformly at random from the simplex defined by nonnegativity and $\sum_{i=1}^{n-1} ix_i \leq n$. Project onto the hyperplane defined by (ρ, ρ_n) by setting

$$x_n = \frac{\rho_n - \sum_{i=1}^{n-1} \rho_i x_i}{\rho_n}.$$

Every facet has a strictly positive coefficient in the nth coefficient (in fact, in every coefficient after $n/2$), so this value is always defined.

Check whether the resulting point is in the polytope. We currently do this by checking an explicit list of facets, though as before we could separate without such a list.

The volume of the original simplex is $\frac{n^{n-1}}{((n-1)!)^2}$. There is also a factor that results from the projection of x_n: the final space is larger by a factor of $\frac{\rho_n}{||\rho||}$. If the fraction of valid points in the sample is p, then the volume estimate is

$$p\frac{n^{n-1}}{((n-1)!)^2}\frac{\rho_n}{||\rho||}.$$

Because the same base simplex is used, we don't actually do separate tests for each facet. Each time a point is generated, the projection is checked on every facet. In at most one case, the projected point still lies in the polytope. This makes the process of estimating the volumes of all facets more efficient, similar to the way that the shooting experiment is simultaneously performed for all facets.

Estimates of facet volumes appear along with other measures in Appendix B, and correlations with other measures appear in Section 4.8.

4.5 Chvátal-Gomory rank

Chvátal-Gomory rank only applies to knapsack facets, because the cyclic group problem does not have a natural LP relaxation. For knapsack polytopes, we cannot easily determined the exact Chvátal-Gomory rank of facets, but as described in Section 1.4.1 we can computationally determine which facets have rank 1 and which do not. In addition, the defining inequality of the knapsack has rank 0, so the facets are divided into three rank groups. This provides another method for comparing facets.

The correlation of C-G rank with other measures is presented in Section 4.8 and the C-G ranks themselves are given in Appendix B.

4.6 Number of tight inequalities

We consider an additional measure that was not presented in Chapter 2 since it applies only to cyclic group and knapsack problems. The measure is the number of tight inequalities in formulation (4) or (6). All facets satisfy some of the inequalities in these formulations at equality, but due to degeneracy some facets satisfy more of them at equality. The number satisfied at equality is easily checked directly.

Evans [15] and Gomory and Johnson [22] found that this measure has a strong nonlinear correlation with shooting experiment size.

4.7 An empirical measure of usefulness

This section describes an empirical measure of the usefulness of knapsack facets in branch-and-bound, which we have added for comparison with the other measures. There is no

similar measure for cyclic group facets, since the cyclic group problem is not naturally solved by branch-and-bound.

The measure of usefulness is based on the minimum number of branch-and-bound nodes required to solve an instance, assuming that the method of selecting the branching variable is fixed. Specifically, all branch-and-bound nodes that are not fathomed by the true optimal solution are counted, but any others are not. This removes any variability based on the choice of backtracking rule, though it does still depend on the branching rule. In these tests we always branched on the most fractional variable. We will call the resulting number of nodes the *BBT size* of the tree.

For each master knapsack polytope, 1000 random objective vectors were generated. The objective coefficients came from iid positive normal values, each multiplied by its index. For example, the coefficient c_4 was 4 times a positive normal random value. Without this weighting, the knapsack constraint would tend to cause a strong preference for the lower-indexed variables, since more of them "fit" in the knapsack. In fact, we are really multiplying by the coefficient of the corresponding variable in the knapsack constraint, which happens to be the same as the index.

Each instance was solved by branch-and-bound after the addition of each facet singly as well as each pair of facets. The reason for considering pairs is that facets may interact with one another in ways that magnify or suppress any benefits. It is possible to test larger sets of facets simultaneously as well, but we chose to limit our tests to singletons and pairs for reasons of practicality.

The measure for a facet is the average of BBT sizes each time that facet was used, either alone or as one of a pair. The correlations of this measure with other measures is given in Section 4.8. The actual results of the BBT tests are given along with other measures in Appendix B. We also performed tests of statistical significance for the differences between the values. This test is described in Appendix A.

Table 7: Measures for the packing knapsack polytope with $n = 9$

Facet	Best-case Imp.	Tight Ineq	C-G Rank	Volume	Shooting Origin	Shooting Interior	BBT Size
0 0 0 0 1 1 1 1 1	1.800	14	1	5.671e-04	313	437	2.856
0 0 0 1 1 2 2 2 2	1.500	11	2+	2.977e-04	181	289	2.652
0 0 1 1 2 2 3 3 3	1.286	10	1	1.494e-04	60	67	3.141
0 0 2 3 3 4 6 6 6	1.286	9	2+	3.024e-04	119	190	2.898
0 1 1 2 2 3 3 4 4	1.125	14	1	1.080e-03	104	377	2.104
0 1 2 2 4 4 5 6 6	1.200	10	2+	1.531e-04	28	58	3.368
0 1 2 3 3 4 5 6 6	1.125	10	1	1.535e-04	30	86	3.159
0 2 3 4 5 6 7 9 9	1.125	10	2+	2.262e-04	32	70	3.607
1 2 3 4 5 6 7 8 9	1	20	0	9.279e-03	133	1104	n/a

Table 8: Measures for the cyclic group polyhedron with $n = 10, r = 9$

Facet	Best-case Adaptation	Tight Inequalities	Volume	Shooting
1 0 1 0 1 0 1 0 1	0.447	28	∞	289
1 2 1 2 1 2 1 2 3	0.557	12	1.909e-04	18
1 2 3 4 0 1 2 3 4	0.516	22	∞	162
1 2 3 4 5 6 7 8 9	0.533	20	9.142e-03	118
2 4 6 3 5 2 4 6 8	0.552	13	6.387e-04	30
3 6 4 2 5 3 1 4 7	0.545	15	2.624e-03	56
4 3 2 1 5 4 3 2 6	0.548	15	1.147e-03	34
4 3 2 6 0 4 3 2 6	0.526	18	∞	121
6 2 3 4 5 6 7 3 9	0.553	12	5.010e-04	13
6 7 3 4 5 6 2 3 9	0.553	12	5.016e-04	27
9 8 7 6 5 4 3 2 11	0.547	16	1.484e-03	46
9 18 7 6 15 14 3 12 21	0.541	14	3.958e-03	86

4.8 Comparing the measures

This section presents results of the correlations between measures. Measures were compiled for knapsack problems of size $n = 6$ to $n = 14$ and cyclic group problems with $n = 7$ to $n = 14$ and nonzero r. Complete tables of the measures are given in Appendix B.

4.8.1 Example tables of measures

Example results of the measures are given in Table 7 and Table 8.

The measures presented first are deterministic: best-case improvement (adapted in the

case of cyclic group polyhedra), number of tight inequalities, and Chvátal-Gomory rank. In these measures there are often ties between facets. The remaining measures are estimates: volume, shooting experiment sizes, and empirical tests of branch-and-bound tree size. These measures are much less likely to have exact ties, but in many cases the difference between two measures is not statistically significant. For example, in Table 7, the difference between the volume estimates for the second and fourth facets is not statistically significant. The third, sixth, and seventh facets are mutually insignificant differences as well. The tests used for statistical significance for each measure are described in Appendix A.

In Table 7, the last facet does not have a BBT size measure since it is the defining inequality of the knapsack and therefore present in the LP relaxation.

4.8.2 Correlation between measures

We are most interested in correlation between measures. Because of significant differences in the scales used by the measures, we have considered correlation non-parametrically by examining pairwise concordance and discordance. Given two measures, we consider each pair of facets. Either the two measures "agree" on which of the facets is better, they "disagree", they both indicate a tie, or one indicates a tie and the other does not. A tie occurs either because of a true tie in the measure or because of estimated values whose difference is not statistically significant at the 0.05 level.

For most measures, we consider a larger value to be better. This is true for best-case improvement, the number of tight inequalities, the volume, and shooting experiment sizes. For Chvátal-Gomory rank and BBT size, we consider a lower value to be better. Therefore, concordance may indicate positive or negative correlation, depending on the pair of measures considered.

We summarize the results by indicating the percentage of pairs of facets that are for which the measures are concordant ("agree", including both indicate ties), the percentage for which the measures are discordant ("disagree"), and the percentage for which one indicates a tie and the other does not. We call the last possibility a *weak pair* because it does not strongly indicate concordance or discordance.

Table 9: Pairwise concordance of knapsack measures

		B-C I	Ineq	Vol	Sh O	Sh I	C-G	BBT
	Concordant Pairs		38%	43%	57%	52%	20%	64%
Best-case	Discordant Pairs		43%	42%	19%	32%	32%	14%
Improvement	Weak Pairs		19%	15%	24%	16%	48%	22%
	Concordant Pairs	38%		71%	58%	70%	56%	57%
Tight	Discordant Pairs	43%		13%	15%	12%	4%	19%
Ineq	Weak Pairs	19%		16%	27%	18%	40%	24%
	Concordant Pairs	43%	71%		66%	68%	39%	60%
Volume	Discordant Pairs	42%	13%		12%	17%	12%	23%
	Weak Pairs	15%	16%		23%	15%	48%	17%
	Concordant Pairs	57%	58%	66%		65%	41%	62%
Shooting	Discordant Pairs	19%	15%	12%		10%	15%	9%
Origin	Weak Pairs	24%	27%	23%		25%	44%	29%
	Concordant Pairs	52%	70%	68%	65%		47%	66%
Shooting	Discordant Pairs	32%	12%	17%	10%		9%	14%
Interior	Weak Pairs	16%	18%	15%	25%		44%	20%
	Concordant Pairs	20%	56%	39%	41%	47%		36%
C-G	Discordant Pairs	32%	4%	12%	15%	9%		12%
Rank	Weak Pairs	48%	40%	48%	44%	44%		52%
	Concordant Pairs	64%	57%	60%	62%	66%	36%	
BBT	Discordant Pairs	14%	19%	23%	9%	14%	12%	
Size	Weak Pairs	22%	24%	17%	29%	20%	52%	

4.8.3 Summary results

By aggregating data, we may consider the pairwise correlation across all knapsack problems. These results are given in Table 9.

The labels on the top row are abbreviations for the measures and appear in the same order as the rows. By looking across a row, it is possible to see how one measure correlates with each of the others. There are a total of 906 pairs of facets. When the BBT size is considered, the defining inequality is omitted, and there are 804 pairs of facets.

Note that concordance and discordance should generally be considered together, or misleading conclusions may be drawn. For example, the volume measure is concordant with best-case improvement on 43% of pairs and concordant with C-G rank on 39% of pairs. Alone, these numbers appear similar. When we consider discordance as well, however, we see that volume and best-case improvement are discordant on 42% of pairs. This indicates

no correlation between volume and best-case improvement. In contrast, volume and C-G rank are discordant on only 12% of pairs. Therefore, there is a correlation between volume and C-G rank, albeit not an exceptionally strong one.

Looking at concordance alone, the highest value is 71%, between the number of tight inequalities and volume. With a discordance of 13%, this does indicate a relatively strong correlation.

The smallest discordance is 4%, between the number of tight inequalities and C-G rank. Their concordance is only 56%, but this still indicates a strong correlation. The high number of weak pairs is mostly due to the fact that our test for C-G rank distinguished only 3 levels, so there were many ties. Both C-G rank and the number of tight inequalities come from the interaction of systems of inequalities. Whether there is a theoretical basis in those systems for the strong correlation between the measures is an open question.

We may also consider some other measures that we expect to be correlated. For example, shooting from the origin and shooting from the interior were discordant for only 10% of pairs and were concordant for 65%. We also expect a relationship between volume and shooting experiment size, since both are geometric sizes. In fact, both shooting experiment sizes are correlated with facet volume, with 66% and 68% concordance and 12% and 17% discordance.

Finally, we consider BBT size. The most concordant measure is shooting from the interior at 66%. Next is best-case improvement with 64% and shooting from the origin with 62%. When we look at discordance, however, shooting from the origin is best, with only 9% discordance. Overall, the shooting experiment and best-case improvement appear to be the best predictors of BBT size, with neither measure clearly superior.

A similar summary of cyclic group measure correlation appears in Table 10. These are aggregate results based on the 18 master cyclic group polyhedra with $7 \leq n \leq 14$ and nonzero r. The total number of facet pairs is 9238.

Perhaps the most notable feature of these results is the high degree of correlation among all the measures. The highest discordance is only 15% and the lowest concordance 72%. This 72% is between the shooting experiment and volume, and it indicates a stronger correlation than it appears since the discordance between them is only 5%.

Table 10: Pairwise concordance of cyclic group measures

		B-C I	Ineq	Vol	Shoot
	Concordant Pairs		78%	81%	73%
Best-case	Discordant Pairs		15%	10%	5%
Improvement	Weak Pairs		7%	8%	21%
	Concordant Pairs	78%		77%	75%
Tight	Discordant Pairs	15%		12%	5%
Ineq	Weak Pairs	7%		12%	20%
	Concordant Pairs	81%	77%		72%
	Discordant Pairs	10%	12%		5%
Volume	Weak Pairs	8%	12%		23%
	Concordant Pairs	73%	75%	72%	
	Discordant Pairs	5%	5%	5%	
Shooting	Weak Pairs	21%	20%	23%	

Note that for the adaptation of best-case improvement, the results indicated that a lower value should be judged as better, since this gives the strong concordances indicated. That is, the facet that provides a smaller potential absolute difference in objective values is more likely to have a large volume and shooting experiment size. Thus the intuition of "best-case" is exactly backward in this case.

Since the number of tight inequalities and adapted best-case improvement are well correlated with volume and shooting experiment size and are much easier to compute, these results suggest that giving more attention to the two simpler measures may be worthwhile for researchers.

4.8.4 Tables of Correlations

4.8.4.1 Knapsack polytopes

Master packing knapsack polytopes of dimensions $n = 6$ through $n = 14$ were tested. For each polytope, there is a table containing correlation information.

Table 11 contains the correlation results for the knapsack polytope with $n = 6$. There are only 3 facets, and therefore 3 pairs. Because of these small values, the many 100% values should not be considered too impressive.

Table 11: Concordance of measures for knapsack polytope with $n = 6$

		B-C I	Ineq	Vol	Sh O	Sh I	C-G	BBT
	Concordant Pairs		33%	0%	67%	33%	33%	100%
Best-case	Discordant Pairs		67%	100%	33%	67%	67%	0%
Imp.	Weak Pairs		0%	0%	0%	0%	0%	0%
	Concordant Pairs	33%		67%	67%	100%	100%	100%
Tight	Discordant Pairs	67%		33%	33%	0%	0%	0%
Ineq	Weak Pairs	0%		0%	0%	0%	0%	0%
	Concordant Pairs	0%	67%		33%	67%	67%	0%
Volume	Discordant Pairs	100%	33%		67%	33%	33%	100%
	Weak Pairs	0%	0%		0%	0%	0%	0%
	Concordant Pairs	67%	67%	33%		67%	67%	100%
Shooting	Discordant Pairs	33%	33%	67%		33%	33%	0%
Origin	Weak Pairs	0%	0%	0%		0%	0%	0%
	Concordant Pairs	33%	100%	67%	67%		100%	100%
Shooting	Discordant Pairs	67%	0%	33%	33%		0%	0%
Interior	Weak Pairs	0%	0%	0%	0%		0%	0%
	Concordant Pairs	33%	100%	67%	67%	100%		100%
C-G	Discordant Pairs	67%	0%	33%	33%	0%		0%
Rank	Weak Pairs	0%	0%	0%	0%	0%		0%
	Concordant Pairs	100%	100%	0%	100%	100%	100%	
BBT	Discordant Pairs	0%	0%	100%	0%	0%	0%	
Size	Weak Pairs	0%	0%	0%	0%	0%	0%	

Table 12: Concordance of measures for knapsack polytope with $n = 7$

		B-C I	Ineq	Vol	Sh O	Sh I	C-G	BBT
	Concordant Pairs		30%	30%	70%	60%	0%	33%
Best-case	Discordant Pairs		50%	70%	20%	40%	40%	50%
Improvement	Weak Pairs		20%	0%	10%	0%	60%	17%
	Concordant Pairs	30%		80%	40%	70%	60%	33%
Tight	Discordant Pairs	50%		0%	30%	10%	0%	17%
Ineq	Weak Pairs	20%		20%	30%	20%	40%	50%
	Concordant Pairs	30%	80%		40%	70%	40%	50%
Volume	Discordant Pairs	70%	0%		50%	30%	0%	33%
	Weak Pairs	0%	20%		10%	0%	60%	17%
	Concordant Pairs	70%	40%	40%		70%	30%	17%
Shooting	Discordant Pairs	20%	30%	50%		20%	20%	50%
Origin	Weak Pairs	10%	30%	10%		10%	50%	33%
	Concordant Pairs	60%	70%	70%	70%		40%	33%
Shooting	Discordant Pairs	40%	10%	30%	20%		0%	50%
Interior	Weak Pairs	0%	20%	0%	10%		60%	17%
	Concordant Pairs	0%	60%	40%	30%	40%		17%
C-G	Discordant Pairs	40%	0%	0%	20%	0%		0%
Rank	Weak Pairs	60%	40%	60%	50%	60%		83%
	Concordant Pairs	33%	33%	50%	17%	33%	17%	
BBT	Discordant Pairs	50%	17%	33%	50%	50%	0%	
Size	Weak Pairs	17%	50%	17%	33%	17%	83%	

Table 12 contains the correlation results for the knapsack polytope with $n = 7$. This polytope has 5 facets, and therefore 10 pairs. Comparisons with BBT size only consider 4 facets and so 6 pairs. Again because of the small number of pairs, the results vary a great deal. One notable entry is between the number of tight inequalities and volume, which had 80% concordance and no discordance.

Table 13: Concordance of measures for knapsack polytope with $n = 8$

		B-C I	Ineq	Vol	Sh O	Sh I	C-G	BBT
	Concordant Pairs		40%	40%	70%	60%	20%	83%
Best-case	Discordant Pairs		50%	50%	20%	40%	60%	17%
Improvement	Weak Pairs		10%	10%	10%	0%	20%	0%
	Concordant Pairs	40%		80%	50%	80%	70%	83%
Tight	Discordant Pairs	50%		0%	30%	10%	0%	0%
Ineq	Weak Pairs	10%		20%	20%	10%	30%	17%
	Concordant Pairs	40%	80%		70%	80%	60%	83%
Volume	Discordant Pairs	50%	0%		30%	10%	10%	0%
	Weak Pairs	10%	20%		0%	10%	30%	17%
	Concordant Pairs	70%	50%	70%		70%	30%	67%
Shooting	Discordant Pairs	20%	30%	30%		20%	40%	17%
Origin	Weak Pairs	10%	20%	0%		10%	30%	17%
	Concordant Pairs	60%	80%	80%	70%		60%	83%
Shooting	Discordant Pairs	40%	10%	10%	20%		20%	17%
Interior	Weak Pairs	0%	10%	10%	10%		20%	0%
	Concordant Pairs	20%	70%	60%	30%	60%		50%
C-G	Discordant Pairs	60%	0%	10%	40%	20%		17%
Rank	Weak Pairs	20%	30%	30%	30%	20%		33%
	Concordant Pairs	83%	83%	83%	67%	83%	50%	
BBT	Discordant Pairs	17%	0%	0%	17%	17%	17%	
Size	Weak Pairs	0%	17%	17%	17%	0%	33%	

Table 13 contains the correlation results for the knapsack polytope with $n = 8$. Like the previous one, this polytope has 5 facets, and therefore 10 pairs. Comparisons with BBT size only consider 4 facets and therefore 6 pairs. Despite the small number of pairs, most measures do indicate a strong correlation with BBT size.

Table 14: Concordance of measures for knapsack polytope with $n = 9$

		B-C I	Ineq	Vol	Sh O	Sh I	C-G	BBT
	Concordant Pairs		33%	36%	61%	44%	19%	54%
Best-case	Discordant Pairs		42%	42%	17%	44%	42%	25%
Improvement	Weak Pairs		25%	22%	22%	11%	39%	21%
	Concordant Pairs	33%		75%	61%	69%	58%	57%
Tight	Discordant Pairs	42%		11%	19%	11%	6%	18%
Ineq	Weak Pairs	25%		14%	19%	19%	36%	25%
	Concordant Pairs	36%	75%		64%	83%	50%	71%
Volume	Discordant Pairs	42%	11%		14%	6%	17%	14%
	Weak Pairs	22%	14%		22%	11%	33%	14%
	Concordant Pairs	61%	61%	64%		69%	36%	68%
Shooting	Discordant Pairs	17%	19%	14%		14%	19%	11%
Origin	Weak Pairs	22%	19%	22%		17%	44%	21%
	Concordant Pairs	44%	69%	83%	69%		53%	79%
Shooting	Discordant Pairs	44%	11%	6%	14%		14%	14%
Interior	Weak Pairs	11%	19%	11%	17%		33%	7%
	Concordant Pairs	19%	58%	50%	36%	53%		39%
C-G	Discordant Pairs	42%	6%	17%	19%	14%		18%
Rank	Weak Pairs	39%	36%	33%	44%	33%		43%
	Concordant Pairs	54%	57%	71%	68%	79%	39%	
BBT	Discordant Pairs	25%	18%	14%	11%	14%	18%	
Size	Weak Pairs	21%	25%	14%	21%	7%	43%	

Table 14 contains the correlation results for the knapsack polytope with $n = 9$. This polytope has 9 facets, and therefore 36 pairs. Comparisons with BBT size only consider 8 facets and therefore 28 pairs. Shooting from the interior is particularly well correlated with BBT size on this polytope with a concordance of 79% and discordance of 14%. The relationship between the number of tight inequalities and C-G rank is also pronounced, with a discordance of only 6%.

Table 15: Concordance of measures for knapsack polytope with $n = 10$

		B-C I	Ineq	Vol	Sh O	Sh I	C-G	BBT
	Concordant Pairs		32%	29%	75%	57%	18%	57%
Best-case	Discordant Pairs		43%	57%	21%	39%	43%	5%
Improvement	Weak Pairs		25%	14%	4%	4%	39%	38%
	Concordant Pairs	32%		79%	54%	75%	64%	57%
Tight	Discordant Pairs	43%		4%	18%	4%	0%	10%
Ineq	Weak Pairs	25%		18%	29%	21%	36%	33%
	Concordant Pairs	29%	79%		50%	71%	54%	38%
Volume	Discordant Pairs	57%	4%		32%	18%	7%	24%
	Weak Pairs	14%	18%		18%	11%	39%	38%
	Concordant Pairs	75%	54%	50%		79%	36%	52%
Shooting	Discordant Pairs	21%	18%	32%		14%	21%	5%
Origin	Weak Pairs	4%	29%	18%		7%	43%	43%
	Concordant Pairs	57%	75%	71%	79%		46%	48%
Shooting	Discordant Pairs	39%	4%	18%	14%		11%	10%
Interior	Weak Pairs	4%	21%	11%	7%		43%	43%
	Concordant Pairs	18%	64%	54%	36%	46%		38%
C-G	Discordant Pairs	43%	0%	7%	21%	11%		0%
Rank	Weak Pairs	39%	36%	39%	43%	43%		62%
	Concordant Pairs	57%	57%	38%	52%	48%	38%	
BBT	Discordant Pairs	5%	10%	24%	5%	10%	0%	
Size	Weak Pairs	38%	33%	38%	43%	43%	62%	

Table 15 contains the correlation results for the knapsack polytope with $n = 10$. This polytope has 8 facets, and therefore 28 pairs. Comparisons with BBT size only consider 7 facets and therefore 21 pairs. Best-case improvement is particularly well correlated with BBT size on this instance, with 57% concordance and only 5% discordance. Even more striking, the number of tight inequalities is extremely well correlated with C-G rank, with 0% discordance, as well as volume and shooting from the interior. This group of three are all well correlated on this instance.

Table 16: Concordance of measures for knapsack polytope with $n = 11$

		B-C I	Ineq	Vol	Sh O	Sh I	C-G	BBT
	Concordant Pairs		41%	40%	57%	57%	24%	60%
Best-case	Discordant Pairs		41%	46%	16%	33%	31%	17%
Improvement	Weak Pairs		19%	14%	26%	10%	45%	23%
	Concordant Pairs	41%		81%	62%	74%	52%	59%
Tight	Discordant Pairs	41%		8%	15%	15%	9%	19%
Ineq	Weak Pairs	19%		11%	23%	11%	40%	22%
	Concordant Pairs	40%	81%		59%	80%	41%	67%
Volume	Discordant Pairs	46%	8%		15%	15%	18%	19%
	Weak Pairs	14%	11%		25%	4%	42%	14%
	Concordant Pairs	57%	62%	59%		73%	38%	69%
Shooting	Discordant Pairs	16%	15%	15%		7%	21%	9%
Origin	Weak Pairs	26%	23%	25%		21%	41%	22%
	Concordant Pairs	57%	74%	80%	73%		38%	69%
Shooting	Discordant Pairs	33%	15%	15%	7%		20%	19%
Interior	Weak Pairs	10%	11%	4%	21%		42%	12%
	Concordant Pairs	24%	52%	41%	38%	38%		41%
C-G	Discordant Pairs	31%	9%	18%	21%	20%		12%
Rank	Weak Pairs	45%	40%	42%	41%	42%		47%
	Concordant Pairs	60%	59%	67%	69%	69%	41%	
BBT	Discordant Pairs	17%	19%	19%	9%	19%	12%	
Size	Weak Pairs	23%	22%	14%	22%	12%	47%	

Table 16 contains the correlation results for the knapsack polytope with $n = 11$. This polytope has 14 facets, and therefore 91 pairs. Comparisons with BBT size only consider 13 facets and therefore 78 pairs. Shooting from the origin is very well correlated with BBT size on this instance, with 69% concordance and 9% discordance. There are also several examples of uncorrelated measures. Best-case improvement and the number of tight inequalities have 41% concordance and 41% discordance. Best-case improvement is also relatively uncorrelated with volume and C-G rank. Nevertheless, it is reasonably correlated with BBT size, with 60% concordance and 17% discordance.

Table 17: Concordance of measures for knapsack polytope with $n = 12$

		B-C I	Ineq	Vol	Sh O	Sh I	C-G	BBT
	Concordant Pairs		40%	48%	64%	55%	12%	78%
Best-case	Discordant Pairs		45%	43%	17%	37%	23%	3%
Improvement	Weak Pairs		15%	8%	19%	8%	65%	19%
	Concordant Pairs	40%		80%	62%	78%	37%	51%
Tight	Discordant Pairs	45%		10%	14%	12%	3%	26%
Ineq	Weak Pairs	15%		10%	24%	10%	60%	23%
	Concordant Pairs	48%	80%		67%	89%	32%	58%
Volume	Discordant Pairs	43%	10%		14%	8%	3%	27%
	Weak Pairs	8%	10%		19%	3%	65%	15%
	Concordant Pairs	64%	62%	67%		75%	32%	72%
Shooting	Discordant Pairs	17%	14%	14%		8%	9%	7%
Origin	Weak Pairs	19%	24%	19%		18%	59%	21%
	Concordant Pairs	55%	78%	89%	75%		28%	65%
Shooting	Discordant Pairs	37%	12%	8%	8%		7%	22%
Interior	Weak Pairs	8%	10%	3%	18%		65%	13%
	Concordant Pairs	12%	37%	32%	32%	28%		21%
C-G	Discordant Pairs	23%	3%	3%	9%	7%		9%
Rank	Weak Pairs	65%	60%	65%	59%	65%		70%
	Concordant Pairs	78%	51%	58%	72%	65%	21%	
BBT	Discordant Pairs	3%	26%	27%	7%	22%	9%	
Size	Weak Pairs	19%	23%	15%	21%	13%	70%	

Table 17 contains the correlation results for the knapsack polytope with $n = 12$. This polytope has 16 facets, and therefore 120 pairs. Comparisons with BBT size only consider 15 facets and therefore 105 pairs. The most striking result is the strong correlation between best-case improvement and BBT size: 78% concordance and only 3% discordance. As in the polytope for $n = 11$, best-case improvement appears relatively uncorrelated with the number of tight inequalities and volume.

Table 18: Concordance of measures for knapsack polytope with $n = 13$

		B-C I	Ineq	Vol	Sh O	Sh I	C-G	BBT
	Concordant Pairs		38%	47%	57%	53%	25%	55%
Best-case	Discordant Pairs		40%	36%	18%	29%	32%	21%
Improvement	Weak Pairs		21%	17%	25%	18%	42%	24%
	Concordant Pairs	38%		64%	55%	73%	64%	61%
Tight	Discordant Pairs	40%		17%	15%	7%	2%	14%
Ineq	Weak Pairs	21%		19%	30%	20%	34%	25%
	Concordant Pairs	47%	64%		69%	65%	42%	64%
Volume	Discordant Pairs	36%	17%		7%	16%	12%	17%
	Weak Pairs	17%	19%		24%	19%	46%	18%
	Concordant Pairs	57%	55%	69%		65%	44%	57%
Shooting	Discordant Pairs	18%	15%	7%		7%	11%	9%
Origin	Weak Pairs	25%	30%	24%		27%	45%	34%
	Concordant Pairs	53%	73%	65%	65%		54%	68%
Shooting	Discordant Pairs	29%	7%	16%	7%		7%	8%
Interior	Weak Pairs	18%	20%	19%	27%		39%	24%
	Concordant Pairs	25%	64%	42%	44%	54%		42%
C-G	Discordant Pairs	32%	2%	12%	11%	7%		11%
Rank	Weak Pairs	42%	34%	46%	45%	39%		47%
	Concordant Pairs	55%	61%	64%	57%	68%	42%	
BBT	Discordant Pairs	21%	14%	17%	9%	8%	11%	
Size	Weak Pairs	24%	25%	18%	34%	24%	47%	

Table 18 contains the correlation results for the knapsack polytope with $n = 13$. This polytope has 25 facets, and therefore 300 pairs. Comparisons with BBT size only consider 24 facets and therefore 276 pairs. There are more weak pairs on this polytope than on most earlier ones. Shooting from the interior provides a strong correlation with BBT size at 68% concordance and 8% discordance. The relationship between the number of tight inequalities and C-G rank is particularly strong, with 64% concordance and 2% discordance.

Table 19: Concordance of measures for knapsack polytope with $n = 14$

		B-C I	Ineq	Vol	Sh O	Sh I	C-G	BBT
	Concordant Pairs		43%	43%	58%	53%	19%	72%
Best-case	Discordant Pairs		41%	40%	15%	23%	25%	5%
Improvement	Weak Pairs		16%	17%	27%	24%	56%	23%
	Concordant Pairs	43%		78%	62%	52%	41%	60%
Tight	Discordant Pairs	41%		9%	14%	25%	8%	18%
Ineq	Weak Pairs	16%		13%	25%	23%	51%	22%
	Concordant Pairs	43%	78%		63%	54%	28%	60%
Volume	Discordant Pairs	40%	9%		11%	26%	14%	20%
	Weak Pairs	17%	13%		26%	21%	57%	20%
	Concordant Pairs	58%	62%	63%		54%	41%	67%
Shooting	Discordant Pairs	15%	14%	11%		14%	17%	4%
Origin	Weak Pairs	27%	25%	26%		32%	42%	29%
	Concordant Pairs	53%	52%	54%	54%		36%	67%
Shooting	Discordant Pairs	23%	25%	26%	14%		10%	11%
Interior	Weak Pairs	24%	23%	21%	32%		54%	22%
	Concordant Pairs	19%	41%	28%	41%	36%		29%
C-G	Discordant Pairs	25%	8%	14%	17%	10%		12%
Rank	Weak Pairs	56%	51%	57%	42%	54%		59%
	Concordant Pairs	.72%	60%	60%	67%	67%	29%	
BBT	Discordant Pairs	5%	18%	20%	4%	11%	12%	
Size	Weak Pairs	23%	22%	20%	29%	22%	59%	

Table 19 contains the correlation results for the knapsack polytope with $n = 14$. This polytope has 20 facets, and therefore 190 pairs. Comparisons with BBT size only consider 19 facets and therefore 171 pairs. Best-case improvement and shooting from the origin are both well-correlated with BBT size, with 5% and 4% discordances, respectively, compared to 72% and 67% concordances.

4.8.4.2 *Cyclic Group Polyhedra*

This section contains data on master cyclic group polyhedra. Polyhedra with $n = 7$ to $n = 14$ were tested.

Table 20: Concordance of measures for the cyclic group polyhedron with $n = 7, r = 6$

		B-C I	Ineq.	Vol	Shoot
	Concordant Pairs		67%	100%	83%
Best-case	Discordant Pairs		17%	0%	0%
Improvement	Weak Pairs		17%	0%	17%
	Concordant Pairs	67%		67%	50%
Tight	Discordant Pairs	17%		17%	17%
Ineq	Weak Pairs	17%		17%	33%
	Concordant Pairs	100%	67%		83%
	Discordant Pairs	0%	17%		0%
Volume	Weak Pairs	0%	17%		17%
	Concordant Pairs	83%	50%	83%	
	Discordant Pairs	0%	17%	0%	
Shooting	Weak Pairs	17%	33%	17%	

Table 20 contains the correlation results for the cyclic group polyhedron with $n = 7$ and $r = 6$. This polyhedron has 4 facets, and therefore 6 pairs. Despite the small number of pairs, the concordances between measures is reasonably strong.

Table 21: Concordance of measures for the cyclic group polyhedron with $n = 8, r = 7$

		B-C I	Ineq	Vol	Shoot
	Concordant Pairs		81%	95%	81%
Best-case	Discordant Pairs		10%	0%	5%
Improvement	Weak Pairs		10%	5%	14%
	Concordant Pairs	81%		76%	67%
Tight	Discordant Pairs	10%		10%	10%
Ineq	Weak Pairs	10%		14%	24%
	Concordant Pairs	95%	76%		76%
	Discordant Pairs	0%	10%		5%
Volume	Weak Pairs	5%	14%		19%
	Concordant Pairs	81%	67%	76%	
	Discordant Pairs	5%	10%	5%	
Shooting	Weak Pairs	14%	24%	19%	

Table 21 contains the correlation results for the cyclic group polyhedron with $n = 8$ and

$r = 7$. This polyhedron has 7 facets, and therefore 21 pairs. Adapted best-case improvement and volume are particularly well correlated with 95% concordance and 0% discordance.

Table 22: Concordance of measures for the cyclic group polyhedron with $n = 8, r = 2$

		B-C I	Ineq	Vol	Shoot
	Concordant Pairs		100%	67%	67%
Best-case	Discordant Pairs		0%	0%	0%
Improvement	Weak Pairs		0%	33%	33%
	Concordant Pairs	100%		67%	67%
Tight	Discordant Pairs	0%		0%	0%
Ineq	Weak Pairs	0%		33%	33%
	Concordant Pairs	67%	67%		33%
	Discordant Pairs	0%	0%		0%
Volume	Weak Pairs	33%	33%		67%
	Concordant Pairs	67%	67%	33%	
	Discordant Pairs	0%	0%	0%	
Shooting	Weak Pairs	33%	33%	67%	

Table 22 contains the correlation results for the cyclic group polyhedron with $n = 8$ and $r = 2$. This polyhedron has 3 facets, and therefore only 3 pairs.

Table 23: Concordance of measures for the cyclic group polyhedron with $n = 8, r = 4$

		B-C I	Ineq	Vol	Shoot
	Concordant Pairs		33%	33%	100%
Best-case	Discordant Pairs		0%	0%	0%
Improvement	Weak Pairs		67%	67%	0%
	Concordant Pairs	33%		17%	33%
Tight	Discordant Pairs	0%		17%	0%
Ineq	Weak Pairs	67%		67%	67%
	Concordant Pairs	33%	17%		33%
	Discordant Pairs	0%	17%		0%
Volume	Weak Pairs	67%	67%		67%
	Concordant Pairs	100%	33%	33%	
	Discordant Pairs	0%	0%	0%	
Shooting	Weak Pairs	0%	67%	67%	

Table 23 contains the correlation results for the cyclic group polyhedron with $n = 8$ and $r = 4$. This polyhedron has 4 facets, and therefore 6 pairs. Adapted best-case improvement and the shooting experiment are perfectly correlated on this polyhedron.

Table 24: Concordance of measures for the cyclic group polyhedron with $n = 9, r = 8$

		B-C I	Ineq	Vol	Shoot
	Concordant Pairs		81%	100%	81%
Best-case	Discordant Pairs		10%	0%	0%
Improvement	Weak Pairs		10%	0%	19%
	Concordant Pairs	81%		81%	67%
Tight	Discordant Pairs	10%		10%	5%
Ineq	Weak Pairs	10%		10%	29%
	Concordant Pairs	100%	81%		81%
	Discordant Pairs	0%	10%		0%
Volume	Weak Pairs	0%	10%		19%
	Concordant Pairs	81%	67%	81%	
	Discordant Pairs	0%	5%	0%	
Shooting	Weak Pairs	19%	29%	19%	

Table 24 contains the correlation results for the cyclic group polyhedron with $n = 9$ and $r = 8$. This polyhedron has 7 facets, and therefore 21 pairs. In this case, volume and adapted best-case improvement are perfectly correlated.

Table 25: Concordance of measures for the cyclic group polyhedron with $n = 9, r = 3$

		B-C I	Ineq	Vol	Shoot
	Concordant Pairs		68%	61%	64%
Best-case	Discordant Pairs		32%	18%	0%
Improvement	Weak Pairs		0%	21%	36%
	Concordant Pairs	68%		43%	43%
Tight	Discordant Pairs	32%		36%	21%
Ineq	Weak Pairs	0%		21%	36%
	Concordant Pairs	61%	43%		46%
	Discordant Pairs	18%	36%		4%
Volume	Weak Pairs	21%	21%		50%
	Concordant Pairs	64%	43%	46%	
	Discordant Pairs	0%	21%	4%	
Shooting	Weak Pairs	36%	36%	50%	

Table 25 contains the correlation results for the cyclic group polyhedron with $n = 9$ and $r = 3$. This polyhedron has 8 facets, and therefore 28 pairs. This polyhedron has more weak pairs than previous ones, so the concordance percentages are lower.

Table 26 contains the correlation results for the cyclic group polyhedron with $n = 10$

Table 26: Concordance of measures for the cyclic group polyhedron with $n = 10, r = 9$

		B-C I	Ineq	Vol	Shoot
	Concordant Pairs		88%	95%	83%
Best-case	Discordant Pairs		8%	0%	0%
Improvement	Weak Pairs		5%	5%	17%
	Concordant Pairs	88%		83%	80%
Tight	Discordant Pairs	8%		8%	5%
Ineq	Weak Pairs	5%		9%	15%
	Concordant Pairs	95%	83%		79%
	Discordant Pairs	0%	8%		0%
Volume	Weak Pairs	5%	9%		21%
	Concordant Pairs	83%	80%	79%	
	Discordant Pairs	0%	5%	0%	
Shooting	Weak Pairs	17%	15%	21%	

and $r = 9$. This polyhedron has 12 facets, and therefore 66 pairs. This polyhedron has particularly low discordances. Three of the six pairs of measures have 0% discordance, and the highest value is 8%.

Table 27: Concordance of measures for the cyclic group polyhedron with $n = 10, r = 2$

		B-C I	Ineq	Vol	Shoot
	Concordant Pairs		90%	67%	67%
Best-case	Discordant Pairs		10%	24%	0%
Improvement	Weak Pairs		0%	10%	33%
	Concordant Pairs	90%		57%	62%
Tight	Discordant Pairs	10%		33%	5%
Ineq	Weak Pairs	0%		10%	33%
	Concordant Pairs	67%	57%		48%
	Discordant Pairs	24%	33%		19%
Volume	Weak Pairs	10%	10%		33%
	Concordant Pairs	67%	62%	48%	
	Discordant Pairs	0%	5%	19%	
Shooting	Weak Pairs	33%	33%	33%	

Table 27 contains the correlation results for the cyclic group polyhedron with $n = 10$ and $r = 2$. This polyhedron has 7 facets, and therefore 21 pairs. The number of tight inequalities and adapted best-case improvement are particularly well correlated with 90% concordance and 10% discordance.

Table 28: Concordance of measures for the cyclic group polyhedron with $n = 10, r = 5$

		B-C I	Ineq	Vol	Shoot
	Concordant Pairs		75%	65%	71%
Best-case	Discordant Pairs		7%	11%	0%
Improvement	Weak Pairs		18%	24%	29%
	Concordant Pairs	75%		58%	69%
Tight	Discordant Pairs	7%		12%	5%
Ineq	Weak Pairs	18%		29%	26%
	Concordant Pairs	65%	58%		48%
	Discordant Pairs	11%	12%		10%
Volume	Weak Pairs	24%	29%		42%
	Concordant Pairs	71%	69%	48%	
	Discordant Pairs	0%	5%	10%	
Shooting	Weak Pairs	29%	26%	42%	

Table 28 contains the correlation results for the cyclic group polyhedron with $n = 10$ and $r = 5$. This polyhedron has 16 facets, and therefore 120 pairs. This polyhedron has a relatively high number of weak pairs, though correlation is strong among the other pairs.

Table 29: Concordance of measures for the cyclic group polyhedron with $n = 11, r = 10$

		B-C I	Ineq	Vol	Shoot
	Concordant Pairs		77%	94%	72%
Best-case	Discordant Pairs		14%	5%	0%
Improvement	Weak Pairs		8%	1%	28%
	Concordant Pairs	77%		77%	69%
Tight	Discordant Pairs	14%		13%	3%
Ineq	Weak Pairs	8%		10%	27%
	Concordant Pairs	94%	77%		72%
	Discordant Pairs	5%	13%		0%
Volume	Weak Pairs	1%	10%		28%
	Concordant Pairs	72%	69%	72%	
	Discordant Pairs	0%	3%	0%	
Shooting	Weak Pairs	28%	27%	28%	

Table 29 contains the correlation results for the cyclic group polyhedron with $n = 11$ and $r = 10$. This polyhedron has 18 facets, and therefore 153 pairs. Volume and best-case improvement are particularly well correlated, with 94% concordance and 5% discordance.

Table 30 contains the correlation results for the cyclic group polyhedron with $n = 12$

Table 30: Concordance of measures for the cyclic group polyhedron with $n = 12, r = 11$

		B-C I	Ineq	Vol	Shoot
	Concordant Pairs		79%	89%	69%
Best-case	Discordant Pairs		11%	3%	0%
Improvement	Weak Pairs		10%	8%	31%
	Concordant Pairs	79%		83%	65%
Tight	Discordant Pairs	11%		8%	3%
Ineq	Weak Pairs	10%		9%	31%
	Concordant Pairs	89%	83%		67%
	Discordant Pairs	3%	8%		0%
Volume	Weak Pairs	8%	9%		33%
	Concordant Pairs	69%	65%	67%	
	Discordant Pairs	0%	3%	0%	
Shooting	Weak Pairs	31%	31%	33%	

and $r = 11$. This polyhedron has 22 facets, and therefore 231 pairs. Discordance with the shooting experiment is particularly low, with values of 0%, 0%, and 3%, but there are more weak pairs: 31%, 31%, and 33%.

Table 31: Concordance of measures for the cyclic group polyhedron with $n = 12, r = 2$

		B-C I	Ineq	Vol	Shoot
	Concordant Pairs		100%	75%	83%
Best-case	Discordant Pairs		0%	11%	0%
Improvement	Weak Pairs		0%	14%	17%
	Concordant Pairs	100%		75%	83%
Tight	Discordant Pairs	0%		11%	0%
Ineq	Weak Pairs	0%		14%	17%
	Concordant Pairs	75%	75%		67%
	Discordant Pairs	11%	11%		8%
Volume	Weak Pairs	14%	14%		25%
	Concordant Pairs	83%	83%	67%	
	Discordant Pairs	0%	0%	8%	
Shooting	Weak Pairs	17%	17%	25%	

Table 31 contains the correlation results for the cyclic group polyhedron with $n = 12$ and $r = 2$. This polyhedron has 9 facets, and therefore 36 pairs. The number of tight inequalities and adapted best-case improvement are perfectly correlated on this polyhedron.

Table 32 contains the correlation results for the cyclic group polyhedron with $n = 12$

Table 32: Concordance of measures for the cyclic group polyhedron with $n = 12, r = 3$

		B-C I	Ineq	Vol	Shoot
	Concordant Pairs		83%	70%	66%
Best-case	Discordant Pairs		4%	15%	6%
Improvement	Weak Pairs		12%	15%	28%
	Concordant Pairs	83%		72%	66%
Tight	Discordant Pairs	4%		12%	5%
Ineq	Weak Pairs	12%		16%	29%
	Concordant Pairs	70%	72%		58%
	Discordant Pairs	15%	12%		9%
Volume	Weak Pairs	15%	16%		33%
	Concordant Pairs	66%	66%	58%	
	Discordant Pairs	6%	5%	9%	
Shooting	Weak Pairs	28%	29%	33%	

and $r = 3$. This polyhedron has 30 facets, and therefore 435 pairs. Concordances are weaker than average on this polyhedron, with more weak pairs.

Table 33: Concordance of measures for the cyclic group polyhedron with $n = 12, r = 4$

		B-C I	Ineq	Vol	Shoot
	Concordant Pairs		79%	60%	82%
Best-case	Discordant Pairs		10%	16%	0%
Improvement	Weak Pairs		11%	24%	18%
	Concordant Pairs	79%		65%	74%
Tight	Discordant Pairs	10%		23%	10%
Ineq	Weak Pairs	11%		12%	16%
	Concordant Pairs	60%	65%		60%
	Discordant Pairs	16%	23%		15%
Volume	Weak Pairs	24%	12%		25%
	Concordant Pairs	82%	74%	60%	
	Discordant Pairs	0%	10%	15%	
Shooting	Weak Pairs	18%	16%	25%	

Table 33 contains the correlation results for the cyclic group polyhedron with $n = 12$ and $r = 4$. This polyhedron has 15 facets, and therefore 210 pairs. These concordances are similar to the previous polyhedron, with a relatively high percentage of weak pairs.

Table 34 contains the correlation results for the cyclic group polyhedron with $n = 12$ and $r = 6$. This polyhedron also has 15 facets, and therefore 210 pairs. As with other

Table 34: Concordance of measures for the cyclic group polyhedron with $n = 12, r = 6$

		B-C I	Ineq	Vol	Shoot
	Concordant Pairs		81%	60%	78%
Best-case	Discordant Pairs		8%	20%	3%
Improvement	Weak Pairs		11%	20%	19%
	Concordant Pairs	81%		55%	71%
Tight	Discordant Pairs	8%		23%	8%
Ineq	Weak Pairs	11%		22%	21%
	Concordant Pairs	60%	55%		46%
	Discordant Pairs	20%	23%		19%
Volume	Weak Pairs	20%	22%		35%
	Concordant Pairs	78%	71%	46%	
	Discordant Pairs	3%	8%	19%	
Shooting	Weak Pairs	19%	21%	35%	

$n = 12$ polyhedra, this one has a high percentage of weak pairs.

Table 35: Concordance of measures for the cyclic group polyhedron with $n = 13, r = 12$

		B-C I	Ineq	Vol	Shoot
	Concordant Pairs		76%	86%	60%
Best-case	Discordant Pairs		17%	10%	4%
Improvement	Weak Pairs		7%	4%	37%
	Concordant Pairs	76%		81%	64%
Tight	Discordant Pairs	17%		10%	3%
Ineq	Weak Pairs	7%		9%	32%
	Concordant Pairs	86%	81%		65%
	Discordant Pairs	10%	10%		0%
Volume	Weak Pairs	4%	9%		34%
	Concordant Pairs	60%	64%	65%	
	Discordant Pairs	4%	3%	0%	
Shooting	Weak Pairs	37%	32%	34%	

Table 35 contains the correlation results for the cyclic group polyhedron with $n = 13$ and $r = 12$. This polyhedron has 40 facets, and therefore 780 pairs. These concordances are lower than many of the polyhedra with small n, as was the case with the $n = 12$ polyhedra.

Table 36 contains the correlation results for the cyclic group polyhedron with $n = 14$ and $r = 13$. This polyhedron has 65 facets, and therefore 2080 pairs. Volume is particularly well correlated with best-case improvement, with 89% concordance and 5% discordance.

Table 36: Concordance of measures for the cyclic group polyhedron with $n = 14, r = 13$

		B-C I	Ineq	Vol	Shoot
	Concordant Pairs		82%	89%	78%
Best-case	Discordant Pairs		12%	5%	4%
Improvement	Weak Pairs		7%	6%	18%
	Concordant Pairs	82%		83%	79%
Tight	Discordant Pairs	12%		8%	4%
Ineq	Weak Pairs	7%		10%	17%
	Concordant Pairs	89%	83%		84%
	Discordant Pairs	5%	8%		0%
Volume	Weak Pairs	6%	10%		16%
	Concordant Pairs	78%	79%	84%	
	Discordant Pairs	4%	4%	0%	
Shooting	Weak Pairs	18%	17%	16%	

Table 37: Concordance of measures for the cyclic group polyhedron with $n = 14, r = 2$

		B-C I	Ineq	Vol	Shoot
	Concordant Pairs		83%	80%	83%
Best-case	Discordant Pairs		12%	15%	6%
Improvement	Weak Pairs		5%	5%	11%
	Concordant Pairs	83%		81%	87%
Tight	Discordant Pairs	12%		13%	4%
Ineq	Weak Pairs	5%		6%	9%
	Concordant Pairs	80%	81%		77%
	Discordant Pairs	15%	13%		11%
Volume	Weak Pairs	5%	6%		12%
	Concordant Pairs	83%	87%	77%	
	Discordant Pairs	6%	4%	11%	
Shooting	Weak Pairs	11%	9%	12%	

Table 37 contains the correlation results for the cyclic group polyhedron with $n = 14$ and $r = 2$. This polyhedron has 31 facets, and therefore 465 pairs. The percentage of weak pairs is not as high as for recent polyhedra, and concordances are at or near 80%.

Table 38: Concordance of measures for the cyclic group polyhedron with $n = 14, r = 7$

		B-C I	Ineq	Vol	Shoot
	Concordant Pairs		69%	71%	75%
Best-case	Discordant Pairs		24%	17%	9%
Improvement	Weak Pairs		7%	12%	16%
	Concordant Pairs	69%		70%	79%
Tight	Discordant Pairs	24%		17%	7%
Ineq	Weak Pairs	7%		13%	13%
	Concordant Pairs	71%	70%		69%
	Discordant Pairs	17%	17%		10%
Volume	Weak Pairs	12%	13%		21%
	Concordant Pairs	75%	79%	69%	
	Discordant Pairs	9%	7%	10%	
Shooting	Weak Pairs	16%	13%	21%	

Table 38 contains the correlation results for the cyclic group polyhedron with $n = 14$ and $r = 7$. This polyhedron has 68 facets, and therefore 2278 pairs. This is the most of any polyhedron studied in this dissertation. There are quite a few weak pairs, however, leaving concordances between 69% and 79%.

CHAPTER V

MATCHING POLYTOPES

The maximum matching problem on a graph $G = (V, E)$ is

$$\begin{array}{lrcll} \max & c^T x & & & \\ s.t. & \sum_{e \in \delta(v)} x_e & \leq & 1 & \forall v \in V \\ & x_e & \in & \{0,1\} & \forall e \in E, \end{array}$$

where $\delta(v)$ denotes all edges incident with v. The standard LP relaxation replaces the final constraints above with $x_e \geq 0$.

Edmonds [14] proved that the following system describes the matching polytope:

$$\begin{array}{rcll} \sum_{e \in \delta(v)} x_e & \leq & 1 & \forall v \in V \\ \sum_{e \in \gamma(S)} x_e & \leq & \frac{|S|-1}{2} & \forall S \subset V, |S| \text{odd} \\ x & \geq & 0, & \end{array}$$

where $\gamma(S)$ is the set of edges with both ends in S. We will call the first set of constraints *node constraints* since there is one for each node. Together with nonnegativity, the node constraints define the LP relaxation. The constraints in the second line are called *odd-set constraints*, many of which denote facets.

The matching problem can be solved by a relatively efficient combinatorial algorithm, so we are not motivated by a desire to improve computation on this problem. Since we have full knowledge of the facets of the matching polytope, however, matching provides a good opportunity to test facet measures.

The only facets that are not included in the LP relaxation are defined by the odd-set constraints. We consider the case of a complete graph, so the polytope is fixed for a particular graph size $|V| = n$, and all odd-set constraints of a given size k are equivalent by symmetry. The question of interest, therefore, is how the facets defined by odd sets of different sizes compare.

Section 5.1 shows that larger-odd-set constraints are almost always intersected before smaller-odd-set constraints by the shooting experiment. Section 5.2 shows that in contrast, smaller-odd-set constraints provide better best-case improvement. Section 5.3 shows that Chvátal-Gomory rank does not distinguish among odd-set constraints. Section 5.4 discusses the possibility of performing the shooting experiment. Section 5.5 explains the difficulty of performing computational experiments, and computational results appear in Section 5.6. They offer insight into the conflicting predictions of the shooting experiment and best-case improvement: it turns out that both predictions are correct in their own way.

5.1 Analysis of the shooting experiment

In this section, we show that when considering only two sizes of odd-set constraints, the shooting experiment sizes of the larger-odd-set constraints are much larger than the shooting experiment sizes of the smaller-odd-set constraints. In fact, we show that the smaller-odd-set constraints will almost always not be hit by the shooting experiment.

To perform an analysis of shooting, it is necessary to decide on a shooting point. One natural choice for matching is the origin. This is a feasible point and all directions in the nonnegative orthant will hit facets defined by odd-set constraints. A consequence of using the origin is that it is not possible to hit the nonnegativity facets, however. If we wish to consider the nonnegativity facets as well, we must use an interior point. By symmetry of the formulation, it is only reasonable to consider points of the form $(z, z, \ldots, z)$ for some positive z. To handle both the origin and interior points, we will analyze shots from such a point $\bar{z} = (z, z, \ldots, z)$, where $z \geq 0$ and the point $\bar{z}$ is in the polytope.

Theorem 5.1 *For maximum matching on complete graphs and for $k = o(n/\log n)$, facets corresponding to odd sets of size less than k will almost always not be hit by the shooting experiment with shooting point $\bar{z} = (z, z, \ldots, z)$, where $z \geq 0$ and $\bar{z}$ is in the polytope.*

Theorem 5.1 says that as a group, larger-odd-set facets have a much larger shooting experiment size than smaller-odd-set facets, at least when only two sets are considered at a time. The rest of this section presents its proof.

Using Proposition 2.6, a facet given by the inequality (α, r) has a scaled shooting distance $t = \frac{r - z\sum \alpha_i}{\sum \alpha_i d_i}$, if that value is nonnegative.

Theorem 5.2 *For $k = o(n/\log n)$, a random shot from a point $\bar{z}$ will almost always intersect an odd-set constraint of size $k+2$ before any of size k. In particular, if $k \geq 7$, then the probability of intersecting a k-set constraint before a $k+2$-set constraint is no more than $n^k \left(\frac{3}{4}\right)^{\lfloor \frac{n-k}{2} \rfloor}$.*

An odd-set constraint of size k has the form

$$\sum_{e \in \gamma(S)} x_e \leq \frac{k-1}{2}.$$

In terms of the (α, r) notation above, we have $\alpha_e = 1$ for $e \in \gamma(S)$ and $\alpha_e = 0$ otherwise. Using Proposition 2.6, the scaled shooting distance is

$$t = \frac{\frac{|S|-1}{2} - z|\gamma(S)|}{\sum_{e \in \gamma(S)} d_e} = \frac{\frac{k-1}{2} - z\frac{k(k-1)}{2}}{\sum_{e \in \gamma(S)} d_e}.$$

We may assume the numerator is nonnegative; otherwise, the point $\bar{z}$ is not inside the polytope. If the denominator is negative or zero, then the shot never intersects that inequality, so we may restrict our attention to cases where the denominator is positive. Since the numerator is constant, we can determine which of the odd-set constraints of size k is intersected first by maximizing the denominator, since this minimizes t. This minimum value is

$$t_{\min} = \frac{\frac{k-1}{2} - z\frac{k(k-1)}{2}}{\max_{|S|=k} \sum_{e \in \gamma(S)} d_e}. \tag{12}$$

For a set S' with $|S'| = k+2$, the scaled shooting distance is

$$t' = \frac{\frac{k+1}{2} - z\frac{(k+2)(k+1)}{2}}{\sum_{e \in \gamma(S')} d_e}.$$

We wish to show that almost always, there exists a set S' such that $0 < t' < t_{\min}$. That is, we wish to show that such a set exists with probability converging to 1 as the size of the graph increases.

Let $\bar{S} \subset E$ be such that $|\bar{S}| = k$ and $\bar{S} = \arg\max_{|S|=k} \sum_{e \in \gamma(S)} d_e$. It will be enough to restrict our search to sets S' that satisfy $S' \supset \bar{S}$.

Given an arbitrary set S such that $|S| = k$, let $d_S = \frac{1}{|\gamma(S)|}\sum_{e\in\gamma(S)} d_e$ be the average weight of the edges in $\gamma(S)$. If $d_S \leq 0$, then this constraint is never intersected by shot d, so we may restrict our attention to the case that $d_S > 0$. For $S' \supset S, |S'| = k+2$, consider the $2k+1$ edges of $\gamma(S') \setminus \gamma(S)$.

Definition 5.3 *Given set S such that $|S| = k$, we say that S is* undominated *if the average edge weight of the set $\gamma(S') \setminus \gamma(S)$ is less than $d_S/2$ for every set $S' \supset S, |S'| = k+2$. Otherwise we say that set S is* dominated.

Lemma 5.4 *If S is dominated by the set S', then the facet corresponding to S' is intersected prior to the facet corresponding to S by a shot in direction d.*

Proof: Let $|S| = k$ and $|S'| = k+2$. Then by the definition of dominated, the average edge weight of $\gamma(S') \setminus \gamma(S)$ is at least $d_S/2$. Then we have

$$t_S = \frac{\frac{k-1}{2} - z\frac{k(k-1)}{2}}{\sum_{e\in\gamma(S)} d_e} = \frac{\frac{k-1}{2}(1-zk)}{\frac{k(k-1)}{2}d_S} = \frac{1-zk}{kd_S},$$

and

$$\begin{aligned} t_{S'} &= \frac{\frac{k+1}{2} - z\frac{(k+1)k}{2}}{\sum_{e\in\gamma(S')} d_e} = \frac{\frac{k+1}{2}(1-z(k+2))}{\sum_{e\in\gamma(S)} d_e + \sum_{e\in\gamma(S')\setminus\gamma(S)} d_e} \\ &\leq \frac{\frac{k+1}{2}(1-z(k+2))}{\frac{k(k-1)}{2}d_S + (2k+1)\frac{d_S}{2}} = \frac{\frac{k+1}{2}(1-z(k+2))}{\frac{k(k+1)}{2}d_S + \frac{d_S}{2}} \\ &< \frac{\frac{k+1}{2}(1-z(k+2))}{\frac{k(k+1)}{2}d_S} \\ &= \frac{1-z(k+2)}{kd_S}. \end{aligned}$$

Using the fact that $z \geq 0$ and $d_S > 0$, we have

$$t_{S'} < \frac{1-z(k+2)}{kd_S} \leq \frac{1-zk}{kd_S} = t_S.$$

Therefore the odd-set constraint corresponding to S' prevents the odd-set constraint corresponding to S from being hit by the shot. ■

Lemma 5.5 *For $k = o(n/\log n)$, there is almost always no undominated set of size k. In particular, for $k \geq 7$, the probability that there exists an undominated set S of size k is no more than $n^k \left(\frac{3}{4}\right)^{\lfloor \frac{n-k}{2} \rfloor}$.*

Proof: Let X be the number of undominated sets of size k and let X_S be an indicator variable that is 1 if S is undominated and 0 otherwise, so that $X = \sum_{|S|=k} X_S$. Then

$$E[X] = E[\sum_{|S|=k} X_S] = \sum_{|S|=k} E[X_S] = \binom{n}{k} E[X_S] \leq n^k P(X_S = 1). \tag{13}$$

We can get an upper bound on $P(X_S = 1)$ by considering possible supersets $S' \supset S$. Each S' is formed by choosing 2 of the $n-k$ nodes not in S. To preserve independence, we partition these nodes arbitrarily, so that we have $\lfloor \frac{n-k}{2} \rfloor$ independent possibilities. Let $1-p_k$ be the probability that $2k+1$ iid edge weights have average weight at least $d_S/2$. This is the probability that a particular S' dominates S. Then we have $P(X_S = 1) \leq p_k^{\lfloor \frac{n-k}{2} \rfloor}$. Using (13), we have

$$P(X \geq 1) \leq E[X] \leq n^k p_k^{\lfloor \frac{n-k}{2} \rfloor}. \tag{14}$$

For any constant value of k, it is clear that $p_k < 1$ and constant, so the exponential term in (14) causes the probability to go to zero as n increases. In particular, this is true for p_3 and p_5.

If $k \geq 7$, we claim that $p_k < 3/4$. Let $Y_1 = \frac{1}{m_1} \sum_{i=1}^{m_1} d_i$ and $Y_2 = \frac{1}{m_2} \sum_{j=1}^{m_2} d'_j$, where d_i and d'_j are iid standard normal variables. Then Y_1 and Y_2 are normally distributed with mean 0 and variances $\frac{1}{m_1}$ and $\frac{1}{m_2}$, respectively.

For an arbitrary set S, the edge weights of $\gamma(S)$ are iid standard normal, so p_k satisfies $1 - p_k = P\left(Y_1 > \frac{1}{2} Y_2 | Y_2 > 0\right)$, where $m_1 = 2k+1$ and $m_2 = \frac{k(k-1)}{2}$. That is, we are comparing the averages of two sets of iid standard normal random variables, conditioned on the fact that one of the averages, d_S, is positive. Since $k \geq 7$, we have $m_1 < m_2$. Then, $P(|Y_1| > |Y_2|) > \frac{1}{2}$, since both Y_1 and Y_2 are normal with mean 0, and Y_1 has a greater variance. Using this, we have

$$\begin{aligned} P\left(Y_1 > \frac{1}{2} Y_2 | Y_2 > 0\right) &\geq P(Y_1 > Y_2 | Y_2 > 0) = P(Y_1 > Y_2 | Y_2 > 0, Y_1 > 0) P(Y_1 > 0) \\ &= P(|Y_1| > |Y_2|) P(Y_1 > 0) > \frac{1}{2} \cdot \frac{1}{2} = \frac{1}{4}. \end{aligned}$$

We conclude that $p_k < \frac{3}{4}$.

The logarithm of the right-hand-side of (14) is $k \log n + \lfloor \frac{n-k}{2} \rfloor \log p_k$. We know that $k = o(n/\log n)$, so the first term is $o(n)$. The second term is negative since $\log p_k < 0$, and its opposite, $-\lfloor \frac{n-k}{2} \rfloor \log p_k$ is $\Theta(n)$. Thus the second term dominates, which means $p_k^{\lfloor \frac{n-k}{2} \rfloor}$ dominates (14), and $P(X \geq 1)$ goes to zero exponentially as n increases. In the case that $k \geq 7$, we can replace p_k by $\frac{3}{4}$ to get the bound in the statement of the lemma. ■

Proof of Theorem 5.2: Combining Lemmas 5.5 and 5.4, there are almost always no undominated sets of size k, so no corresponding odd-set constraint will be hit. In particular, the probability that a set of size k is hit is no more than the probability that it is undominated. Therefore, the bound in Lemma 5.5 applies. ■

We have shown that as a group, the facets corresponding to odd sets of size $k+2$ almost always are intersected prior to facets corresponding to sets of size k. In fact, we have the following corollary:

Corollary 5.6 *Consider the polytope defined by the LP relaxation of matching with the addition of k-set constraints and $(k+2)$-set constraints, where k is odd. Let s_i represent the shooting experiment size of a single facet corresponding to an odd set of size i. Then $\frac{s_k}{s_{k+2}} \to 0$ as n increases for $k = o(n/\log n)$.*

Proof: By symmetry, all facets corresponding to sets of size k have the same shooting experiment size, so s_k and s_{k+2} are well-defined.

The number of k-set constraints is $\binom{n}{k} = \frac{n!}{k!(n-k)!}$. Thus, Theorem 5.2 states that

$$\begin{aligned}
\frac{s_k \frac{n!}{k!(n-k)!}}{s_{k+2} \frac{n!}{(k+2)!(n-k-2)!}} &\leq n^k \left(\frac{3}{4}\right)^{\lfloor \frac{n-k}{2} \rfloor} \\
\frac{s_k (k+2)(k+1)}{s_{k+2}(n-k)(n-k-1)} &\leq n^k \left(\frac{3}{4}\right)^{\lfloor \frac{n-k}{2} \rfloor} \\
\frac{s_k}{s_{k+2}} &\leq \frac{n^k (n-k)(n-k-1)}{(k+2)(k+1)} \left(\frac{3}{4}\right)^{\lfloor \frac{n-k}{2} \rfloor}.
\end{aligned}$$

Since $k = o(n/\log n)$, the exponential expression dominates and the right-hand-side goes to 0 as n increases. ■

We've shown that smaller-odd-set constraints are "blocked" by larger-odd-set constraints. This allows us to prove Theorem 5.1.

Proof of Theorem 5.1: The probability that the facet corresponding to an odd set of size less than k is hit is no more than the sum of the probabilities that a facet corresponding to an odd set of size i is hit for $i < k$. Let p_k be defined as in the proof of Lemma 5.5. Let $p = \max\{p_3, p_5, \frac{3}{4}\}$. Then $p < 1$, and Theorem 5.2 shows that the probability of hitting a facet corresponding to an odd set of size i is bounded by $n^k p^{\lfloor \frac{n-k}{2} \rfloor}$.

The probability that a facet corresponding to an odd set of size less than k is hit is therefore bounded by

$$\sum_{i=1}^{(k-1)/2} n^{2i+1} p^{\lfloor \frac{n-(2i+1)}{2} \rfloor}.$$

Since $k = o(n/\log n)$, the number of terms is no more than linear, and each one is exponentially small, so the overall probability goes to 0 as n increases. ■

If shooting experiment size is indicative of usefulness, Theorem 5.1 suggests that larger-odd-set constraints are more useful than smaller-odd-set constraints for sizes that are $o(n/\log n)$.

5.2 *Best-case improvement*

This section shows that the best-case improvement ratios of smaller-odd-set constraints are better than those of larger-odd-set constraints, in contrast with the results of the previous section on the shooting experiment.

Theorem 5.7 *The strength of the odd-set constraint corresponding to set S is $\frac{|S|}{|S|-1}$.*

Proof: The matching polytope is of anti-blocking type, so Theorem 2.4 applies. Recall that the strength of a facet $\sum_{i=1}^{n} a_i x_i \leq b$ relative to relaxation P is defined as

$$\frac{\max\{a^T x : x \in P\}}{b}.$$

We are considering complete graphs and the standard LP relaxation P. For an odd-set constraint based on set S, the strength is

$$\frac{\max\{\sum_{e\in\gamma(S)} x_e : x \in P\}}{\frac{|S|-1}{2}}.$$

For complete graphs, $\max\{\sum_{e\in\gamma(S)} x_e : x \in P\}$ can be no more than $\frac{|S|}{2}$. This bound comes from summing all the node constraints for nodes in S and dividing by 2, since each edge variable appears twice. In fact, this bound can be achieved by setting $x_e = 1$ for a cycle that includes every node in S and $x_e = 0$ otherwise.

Therefore, the strength of the inequality is

$$\frac{\frac{|S|}{2}}{\frac{|S|-1}{2}} = \frac{|S|}{|S|-1}.$$

■

For example, $|S| = 3$ gives a strength of $\frac{3}{2}$. Larger odd sets have strengths of $\frac{5}{4}, \frac{7}{6}, \frac{9}{8}$, and so on.

Thus, the strength of inequalities corresponding to smaller odd sets is greater than the strength of those corresponding to larger odd sets. If best-case improvement strength correlates with the usefulness, then these results suggest that smaller-odd-set constraints are more useful than larger-odd-set constraints. This contrasts with our analysis of the shooting experiment in the previous chapter.

5.3 Chvátal-Gomory rank

For complete graphs, Chvátal-Gomory rank provides no differentiation among the odd-set constraints:

Proposition 5.8 *For the matching problem on a complete graph, all odd-set inequalities have Chvátal-Gomory rank 1.*

Proof: We will use the notation of Section 1.4.1. To see that odd-set constraints are not rank 0, note that any weighted sum of edge constraints that dominates an odd-set constraint of size k must have weights that total at least $k/2$. This is because each constraint

contributes only twice its weight in left-hand-side coefficients. Then the right-hand-side of the weighted sum is at least $k/2$. Since this is greater than $\frac{k-1}{2}$, the weighted sum does not dominate the constraint.

Now let $u_i = 1$ for all constraints of the form

$$\sum_{e \in \delta(v)} x_e \leq 1, \ v \in S$$

and let $u_i = 0$ for all other constraints. The resulting weighted sum is

$$\sum_{v \in S} \sum_{e \in \delta(v)} x_e \leq |S|.$$

Edges in $\gamma(S)$ appear twice, once for each endpoint, while edges in $\delta(S)$ appear only once, so we have

$$2 \sum_{e \in \gamma(S)} x_e + \sum_{e \in \delta(S)} x_e \leq |S|.$$

We can remove terms from the left-hand-side because of nonnegativity, which gives

$$\begin{aligned} 2 \sum_{e \in \gamma(S)} x_e &\leq |S| \\ \sum_{e \in \gamma(S)} x_e &\leq \frac{|S|}{2}. \end{aligned}$$

Finally we round down the right-hand-side to an integer. Since $|S|$ is odd, we have

$$\sum_{e \in \gamma(S)} x_e \leq \frac{|S| - 1}{2}.$$

■

For matching, therefore, Chvátal-Gomory rank does not help differentiate among constraints corresponding to odd sets of different sizes.

5.4 *Performing the shooting experiment*

Since matching can be solved in polynomial time, Theorem 3.5 indicates that there must be a polynomial-time algorithm to perform the shooting experiment on the matching polytope. Given a direction vector d, performing the shooting experiment would solve the following problem:

$$\min_{S \subset V, |S| \text{ odd}} \frac{\frac{|S|-1}{2}}{\sum_{e \in \gamma(S)} d_e}.$$

In fact, the proof of Theorem 3.5 leads to a polynomial-time algorithm using the ellipsoid algorithm, but such an algorithm would not be efficient. Whether there is a combinatorial algorithm for this problem is an open question.

5.5 *Complexity of odd-set constraints*

In Section 5.6 we present computational results on the usefulness of odd-set inequalities on test instances. Unfortunately, we are limited to instances of small size, and this section presents two results that help explain why testing with odd-set constraints is difficult. In each case, we prove the result for the more restricted case of maximum perfect matching and then show that it applies to maximum matching as well.

The maximum perfect matching problem on $G = (V, E)$ is

$$\begin{array}{lrcll} \max & c^T x & & & \\ s.t. & \sum_{e \in \delta(v)} x_e & = & 1 & \forall v \in V \\ & x_e & \in & \{0,1\} & \forall e \in E. \end{array}$$

The only difference is that the node constraints must be satisfied at equality. For ease of notation, we will abbreviate the set of node constraints as $Ax = 1$, where A represents the node-edge incidence matrix of the graph, and the right-hand-side is a vector of all 1's. The corresponding abbreviation for maximum matching is $Ax \leq 1$.

Because of the equality node constraints, odd-set constraints for perfect matching may be written as

$$\sum_{e \in \delta(S)} x_e \geq 1$$

for each odd set $S \subset V$. We will use this form for odd-set constraints in this section.

Section 5.5.1 shows that the problem of separating k-set constraints is NP-hard when $k = \Omega(n)$. Section 5.5.2 shows that in most cases, the polytope defined by the LP relaxation and a collection of k-set constraints has very fractional extreme points. Together, these results suggest that there is not a combinatorial algorithm for solving the optimization problem with k-set constraints or for separating k-set constraints, which would have made the testing of Section 5.6 easier.

5.5.1 Complexity

In this section, we consider the separation problem for sets of odd-set constraints and the corresponding optimization problems. Padberg and Rao [36] gave a polynomial-time separation algorithm over all odd-set constraints. For the case that only 3-set constraints are added, Cornuéjols and Pulleyblank [10] gave a polynomial-time algorithm for the optimization problem. We show that for many other subsets of odd-set constraints, the separation problem is NP-hard.

5.5.1.1 Including only odd sets of size $n/2$ is NP-hard

Consider the case that the only odd-set constraints that we wish to enforce are those of size $n/2$ (we are assuming $n/2$ is odd). Note that there are $\binom{n}{n/2} = \Omega(2^{n/2})$ such sets, so enumeration is not possible in polynomial time.

The separation problem is then a search problem as follows:

Definition 5.9 *Given a vector $x \in \mathbf{R}^{|E|}$, determine that x satisfies $x \geq 0, Ax = 1$, and all $(n/2)$-set constraints, or demonstrate a constraint that x violates.*

Since $x \geq 0$ and $Ax = 1$ comprise a polynomial number of constraints, these can be checked directly, and the separation problem is no easier than the following recognition problem:

Definition 5.10 *BISECTION $< 1, Ax = 1, x \geq 0, n/2$ odd: Given $x \in \mathbf{R}^{|E|}$ such that $x \geq 0, Ax = 1$, and $n/2$ is odd, determine that x satisfies all $n/2$-cuts (so all are ≥ 1) or determine that one is violated.*

Theorem 5.11 *The problem BISECTION $< 1, Ax = 1, x \geq 0, n/2$ odd is NP-complete.*

Corollary 5.12 *Optimizing over the polytope formed from the perfect matching LP relaxation with the addition of constraints for odd sets of size $n/2$ is NP-hard.*

Corollary 5.12 will follow from Theorem 5.11 by the equivalence of separation and optimization [24]. To prove Theorem 5.11, we will reduce from MAXCUT. The next five subsections show steps in the reduction. Note that the nonnegativity constraint already applies to MAXCUT, and we maintain it throughout the reduction.

MAXCUT to MAXCUT, $Ax = T$, n odd.

If n is even, add an isolated vertex to the instance of MAXCUT to get an equivalent instance with n odd.

Let $T \geq \max_{v \in V} \sum_{e \ni v} x_e$. Add two new nodes v', v'' for each vertex v to form a triangle. Let $T' = \sum_{e \ni v} x_e$. Let edges $\{v, v'\}$ and $\{v, v''\}$ have weight $(T - T')/2$ and let edge $\{v', v''\}$ have weight $(T + T')/2$. Then the new graph satisfies $Ax = T$, and $3n$ is odd.

We are looking for a max cut (S, S'). Assume that $v \in S$. Then it will always be to the best advantage to have v' and v'' in opposite sets for a cut contribution of T. Putting both in S' is not as good since the contribution is $T - T'$. Thus, the max cut in the new graph will have weight $nT +$ (max cut in old graph).

MAXCUT, $Ax = T$, n odd to MAX BISECTION, $Ax = T'$, $n/2$ odd.

Let the current graph be $G = (V, E)$ with $|V| = n$. Form a new graph G' by adding n additional vertices with edges of weight $T/(n-1)$ between each pair and edges of weight $T/(2(n-1))$ between each original vertex and each new vertex. Then G' satisfies $Ax = T'$, where $T' = T + Tn/(2(n-1))$, and the number of vertices in G' is twice an odd number.

Any bisection of G' has edges within G and other edges involving the new vertices. The contribution from these "other" edges will always be $n^2T/(2(n-1))$. Therefore, the max bisection of G' will be determined by the max cut in G and vice-versa.

MAX BISECTION, $Ax = T$, $n/2$ odd to MIN BISECTION, $Ax = T'$, $n/2$ odd.

Let the current graph be $G = (V, E)$ with $|V| = n$. Let $M \geq \max_e x_e$. Form a new graph G' by replacing each edge weight x_e with $x'_e = M - x_e$. (Treat the graph G as a complete graph, where non-existent edges have weight 0.) Since every bisection has the same number of edges, the contribution due to M is constant, and the min bisection in G' will be determined by the max bisection in G and vice versa. Also, G' will satisfy $Ax = (n-1)M - T$.

MIN BISECTION, $Ax = T$, $n/2$ odd to BISECTION $< k''$, $Ax = T$, $k'' \geq 2T$, $n/2$ odd.

Note that MIN BISECTION is really BISECTION $\leq k$, where threshold k is an unrestricted parameter. First, if $k < 2T$, add weights $T/(n-1)$ to every edge in G (treating G as a complete graph as in the previous step). Then $Ax = T + T = 2T$ for the new vector x, and the value of every bisection increases by $\frac{n}{2}\left(\frac{n}{2}\right)\left(\frac{T}{n-1}\right) > 2T$. Setting $k' = k + \frac{n}{2}\left(\frac{n}{2}\right)\left(\frac{T}{n-1}\right)$ gives an instance with threshold $k' \geq 2T$. Second, scale T, all edge weights, and k' by integer M to make all values integers. Set $k'' = Mk' + 1/2$.

BISECTION $< k$, $Ax = T$, $k \geq 2T$, $n/2$ odd to Separation.

In this step we show that being able to choose any $k \geq 2T$ doesn't help us more than having only the choice T. Then we can simply scale all edges by a factor of $1/T$ to get the separation problem.

For each vertex v, add two new nodes v', v'' as in Section 5.5.1.1, now with edge weights $(k-T)/2$ and $(k+T)/2$, such that every node has incident edges totaling weight k (where $k \geq 2T$).

If there is a bisection of weight $\leq k$ in the original graph, then we can use that same bisection (this time putting both v' and v'' on the same side of the cut as v) to get a bisection of weight $\leq k$ in the new graph. Conversely, if there is a bisection of weight $\leq k$ in the new graph then we need to show a bisection in the original graph.

Note that the bisection in the new graph cannot split up two or more triplets, since such a split has weight at least $2(k-T)$, which is at least k by the assumption $k \geq 2T$. The bisection also cannot split only one triplet, or it isn't really a bisection. Therefore, the bisection does not split any triplets and so determines a bisection in the original graph with weight $\leq k$.

We have now reduced to the problem BISECTION $< k$, $Ax = k$, $n/2$ odd. By scaling every edge, we have the separation problem: BISECTION < 1, $Ax = 1$, $n/2$ odd.

5.5.1.2 Other size odd sets

We have shown that the separation problem is NP-hard when only $n/2$-sets are included. In this section we prove that we can reduce to the separation problem for odd sets of size $2\lceil \frac{\alpha n}{2} \rceil - 1$, where $0 < \alpha < 1/2$ is a constant. Note that the expression simply gives the

greatest odd number less than or equal to αn.

Theorem 5.13 *For any $0 < \alpha < 1/2$, the separation problem for a cut of size $2\lceil \frac{\alpha n}{2} \rceil - 1$ with weight < 1 in a graph that satisfies $Ax = 1$ is NP-hard.*

Proof: We will reduce to this problem from BISECTION < 1, $Ax = 1$, $n/2$ odd. Choose nonnegative even integers m_1 and m_2 such that

$$\begin{aligned} m_1 &> \frac{n}{2} \\ m_2 &> \frac{\alpha}{2-4\alpha} n \\ m_1 &= 2\left\lceil \frac{\alpha(n+m_1+m_2)}{2} \right\rceil - 1 - \frac{n}{2} \end{aligned}$$

To see that such a choice is possible, first choose even integers m_1 and m_2 large enough to satisfy the inequalities. Then consider the equality constraint. If the right hand side is less than the left hand side, fix m_1 and increase the value of m_2 to

$$m_2 = 2\left\lfloor \frac{(\frac{1}{2}-\alpha)n + (1-\alpha)m_1 + 1}{2\alpha} \right\rfloor$$

This is an even integer that satisfies the equality constraint.

If the right hand side of the equation is greater than the left hand side, fix m_2 and increase m_1 to

$$m_1 = 2\left\lceil \frac{\alpha m_2 - (\frac{1}{2}-\alpha)n - 1}{2(1-\alpha)} \right\rceil$$

Again, this is an even integer that satisfies the equality constraint.

Now, we are given a graph on n vertices where $n/2$ is odd and the graph satisfies $Ax = 1$. Add $m_1 + m_2$ new vertices. Add new edges to form two cliques from the new vertices: one of size m_1 and one of size m_2. Make the edge weights be $1/(m_1 - 1)$ in the first clique and $1/(m_2 - 1)$ in the second clique. Then the new graph satisfies $Ax = 1$.

Note that the size of the "small" side of the cut is $2\lceil \alpha(n+m_1+m_2)/2 \rceil - 1 = m_1 + n/2$, which is odd. In any cut of size $m_1 + n/2$, if either of the cliques is split by the cut, the clique edges in the cut will have total weight at least 1. Therefore in any cut of weight less than 1, neither clique will be split. The numbers m_1 and m_2 were chosen such that $m_2 > m_1 + n/2$ and $m_1 + m_2 > m_2 + n/2$. Thus, the m_2 clique is too large to go on

the "small" side of the cut and both cliques together are too "large" to go on either side. Therefore in any cut of weight less than 1 (and size $m_1 + n/2$), the m_1 clique will go on the small side along with $n/2$ original nodes and the m_2 clique will go on the large side (also with $n/2$ original nodes).

Therefore, if there exists a cut of weight strictly less than 1 in the new graph, it must be formed entirely of edges among the original vertices, and it gives a bisection of weight less than 1 in the original graph. The converse is easy.

Note that we can choose m_1 and m_2 to be polynomial in n, so constructing the graph can be done in polynomial time. This completes the proof. ■

Again, we get a corollary from the equivalence of separation and optimization [24].

Corollary 5.14 *For any $0 < \alpha < 1/2$, the optimization problem over the polytope formed from the perfect matching LP relaxation with the addition of constraints for odd sets of size $2\lceil \frac{\alpha n}{2} \rceil - 1$ is NP-hard.*

5.5.1.3 Ranges of cuts

In this section, we extend the previous result to ranges of odd-set sizes. If the lower end of the range is of the form $2\lceil \frac{\alpha n}{2} \rceil - 1$ as above, then the separation problem is NP-hard regardless of which other values are allowed.

Theorem 5.15 *Given $0 < \alpha < 1/2$ and a function $S(n)$ mapping n to a subset of odd integers between $2\lceil \frac{\alpha n}{2} \rceil - 1$ and $n/2$, where $2\lceil \frac{\alpha n}{2} \rceil - 1 \in S(n)$, the separation problem for cuts of sizes in $S(n)$ with weight < 1 in a graph that satisfies $Ax = 1$ is NP-hard.*

Proof: We can reduce from the separation problem for sets of size $k(n) := 2\lceil \frac{\alpha n}{2} \rceil - 1$, which we proved is NP-hard in the previous section. We are given a graph satisfying $Ax = 1$. Add 1 to the weight of every edge in the graph (treating it as a complete graph), so that the graph now satisfies $Ax = n$. There exists a cut in the new graph with size in the desired range and weight $< 1 + k(n)(n - k(n))$ if and only if there exists a cut in the original graph with size $k(n)$ and weight < 1.

To see this, note that any cut in the new graph of size greater than $k(n)$ will have at least $1+k(n)(n-k(n))$ edges and so will have weight at least $1+k(n)(n-k(n))$. Therefore, a cut of lower weight must be of size $k(n)$, and so it has weight < 1 in the original graph. The converse is easy.

To complete the reduction, we need to account for the fact that $Ax = n$, but we are looking for a cut of weight $< 1+k(n)(n-k(n))$. For sufficiently high n, $1+k(n)(n-k(n))$ is greater than $2n$, so we are almost in the situation that is covered in Section 5.5.1.1. As in that section, we add two new nodes v', v'' for each node v, to increase the incident edge weights on each node to $1 + k(n)(n - k(n))$.

We must argue that if there is a cut in the new graph with weight $< 1+k(n)(n-k(n))$, then there is such a cut that does not split up a triplet. Note that no such cut can split two triplets, since then the weight of the cut would be too high. It is also not possible to split exactly one triplet, since then there couldn't be exactly $k(3n)$ vertices on one side. By scaling, we have reduced to the case that $Ax = 1$ and we wish to find a cut of weight < 1, which proves that the problem with ranges is NP-hard. ∎

Corollary 5.16 *Given $0 < \alpha < 1/2$ and a function $S(n)$ mapping n to a subset of odd integers between $2\lceil \frac{\alpha n}{2} \rceil - 1$ and $n/2$, where $2\lceil \frac{\alpha n}{2} \rceil - 1 \in S(n)$, the optimization problem for the polytope formed from the perfect matching LP relaxation with the addition of constraints for odd sets of sizes in $S(n)$ is NP-hard.*

5.5.1.4 Extension to maximum matching

These complexity results apply to maximum matching as well. The analogs of Definition 5.9 and 5.10 for maximum matching are the following:

Definition 5.17 *Given a vector $x \in \mathbf{R}^{|E|}$, determine that x satisfies $x \geq 0, Ax \leq 1$, and all $(n/2)$-set constraints, or demonstrate a constraint that x violates.*

Definition 5.18 *BISECTION $< 1, Ax \leq 1, x \geq 0, n/2$ odd: Given $x \in \mathbf{R}^{|E|}$ such that $x \geq 0, Ax \leq 1$, and $n/2$ is odd, determine that x satisfies all $n/2$-cuts (so all are ≥ 1) or determine that one is violated.*

Each of the theorems also has a corollary for maximum matching.

Corollary 5.19 *The problem BISECTION* $< 1, Ax \leq 1, x \geq 0, n/2$ *odd is NP-complete.*

Proof: The reductions that prove Theorem 5.11 work in this case as well. The resulting problem satisfies $Ax = 1$, so it also satisfies $Ax \leq 1$ and a polynomial-time algorithm for BISECTION $< 1, Ax \leq 1, x \geq 0, n/2$ odd would solve it. ■

By the equivalence of separation and optimization, we have a corollary for optimization:

Corollary 5.20 *Optimizing over the polytope formed from the maximum matching LP relaxation with the addition of constraints for odd sets of size* $n/2$ *is NP-hard.*

The same argument as in the proof of Corollary 5.19 proves corollaries to Theorems 5.13 and 5.15.

Corollary 5.21 *For any* $0 < \alpha < 1/2$, *the separation problem for a cut of size* $2\lceil \frac{\alpha n}{2} \rceil - 1$ *with weight* < 1 *in a graph that satisfies* $Ax \leq 1$ *is NP-hard.*

Corollary 5.22 *Given* $0 < \alpha < 1/2$ *and a function* $S(n)$ *mapping* n *to a subset of odd integers between* $2\lceil \frac{\alpha n}{2} \rceil - 1$ *and* $n/2$, *where* $2\lceil \frac{\alpha n}{2} \rceil - 1 \in S(n)$, *the separation problem for cuts of sizes in* $S(n)$ *with weight* < 1 *in a graph that satisfies* $Ax \leq 1$ *is NP-hard.*

Finally, we have the following optimization corollaries:

Corollary 5.23 *For any* $0 < \alpha < 1/2$, *the optimization problem over the polytope formed from the maximum matching LP relaxation with the addition of constraints for odd sets of size* $2\lceil \frac{\alpha n}{2} \rceil - 1$ *is NP-hard.*

Corollary 5.24 *Given* $0 < \alpha < 1/2$ *and a function* $S(n)$ *mapping* n *to a subset of odd integers between* $2\lceil \frac{\alpha n}{2} \rceil - 1$ *and* $n/2$, *where* $2\lceil \frac{\alpha n}{2} \rceil - 1 \in S(n)$, *the optimization problem for the polytope formed from the maximum matching LP relaxation with the addition of constraints for odd sets of sizes in* $S(n)$ *is NP-hard.*

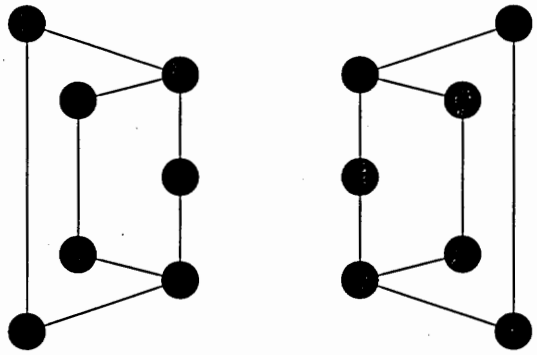

Figure 6: Edges with weight zero

5.5.2 Fractionality

Cornuéjols and Pulleyblank [10] showed that when only 3-set constraints are added to the LP relaxation of matching, the resulting polytope is $\frac{1}{2}$-integral. When any other combination of odd-set constraints is added to the perfect matching LP relaxation, however, the guarantee of $\frac{1}{2}$-integrality is lost.

In this section, we prove the following theorem:

Theorem 5.25 *For any positive integer m and any odd integer $k > 3$, the perfect matching polytope for the complete graph on $6 + 2m(k-3)$ nodes with constraints for all odd sets of size less than or equal to k is not $\frac{1}{q}$-integral for any integer $q < 2m - 1$.*

The rest of this section is devoted to proving Theorem 5.25 by demonstrating a family of complete graphs with $6 + 2m(k-3)$ nodes, edge weights is $\{0, 1\}$, and minimum perfect matching of value $1/(2m-1)$. Section 5.5.2.1 gives a small counterexample to demonstrate the idea, while Section 5.5.2.2 presents the entire family along with the proof that the optimal solution in each case has value $1/(2m-1)$. Section 5.5.2.4 extends the result to maximum matching polytopes.

5.5.2.1 A small counterexample

First, consider the case that $k = 5$ and $m = 2$, so we have a complete graph on 14 vertices. We set the weight of each of the edges to either zero or one. In particular, the edge weights we set to zero are shown in Figure 6.

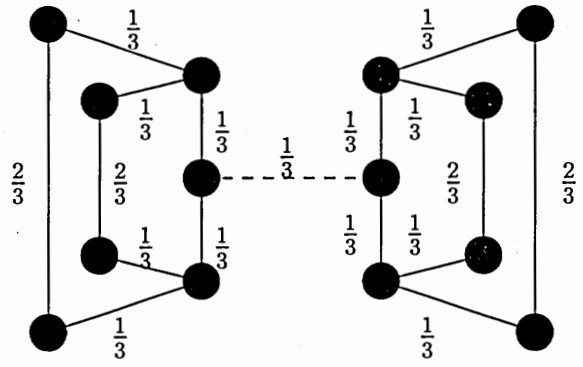

Figure 7: Optimal Solution

Then the minimum perfect matching with 3-set and 5-set inequalities enforced has total weight 1/3. Each edge in the optimal solution is matched with a value of $0, 1/3$, or $2/3$, as shown in Figure 7.

To prove that this solution is optimal, we would need to demonstrate a dual feasible solution that satisfies complementary slackness and also has an objective value of 1/3. Rather than do that for this small problem, we will now present the general family of counterexamples.

5.5.2.2 A family of counterexamples

Consider minimum perfect matching with odd-set constraints up to size k. The primal problem is

$$\begin{aligned} \text{minimize} \quad & \sum_{e \in E} w_e x_e \\ \text{subject to} \quad & x(\delta(v)) = 1 \quad \forall v \in V \\ & x(\delta(S)) \geq 1 \quad \forall S \subseteq V, |S| \text{ odd}, |S| \leq k \\ & x_e \geq 0 \quad \forall e \in E \end{aligned}$$

where $\delta(v)$ denotes the set of edges incident with v, $\delta(S)$ denotes the set of edges that cross out of set S, and $x(A)$ means the sum of x variables for edges in the set A (where A is $\delta(v)$ or $\delta(S)$).

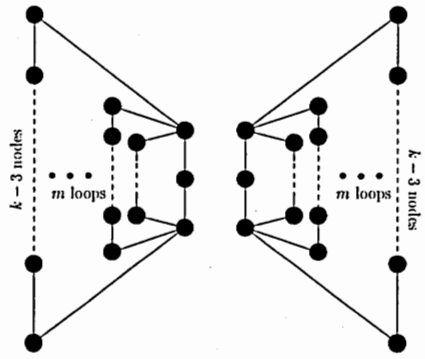

Figure 8: Edges with weight zero in the general graph

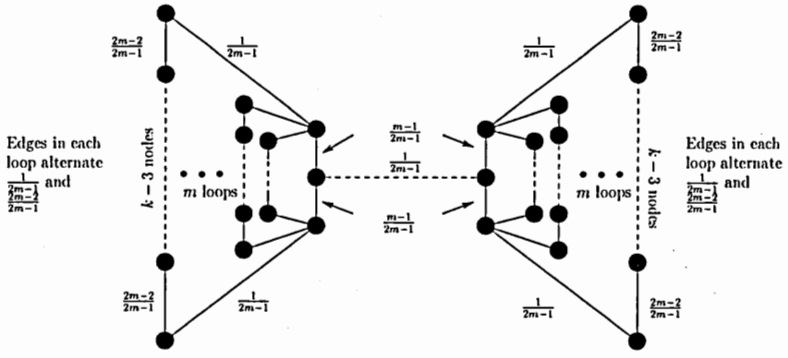

Figure 9: Primal Solution

The dual is

$$\begin{aligned}
\text{maximize} \quad & \sum_{v \in V} y_v + \sum_{S \subseteq V, |S| \text{ odd}, |S| \leq k} y_S \\
\text{subject to} \quad & \sum_{S: e \in \delta(S)} y_S + y_u + y_v \leq w_e \quad \forall e = \{u, v\} \in E \\
& y_v \quad \text{free} \\
& y_S \geq 0
\end{aligned}$$

Our counterexample graph is a complete graph with $6 + 2m(k-3)$ nodes, and we again make most of the edge weights equal to one. Those edges with weight zero are shown in Figure 8. The primal solution is shown in Figure 9. The dual node values are shown in Figure 10. The complete dual solution also includes a number of k-set dual values, which are not shown on the diagram. In particular, each loop of k nodes has a dual value of $\frac{1}{2(2m-1)}$.

We must show that these solutions each have an objective value of $1/(2m-1)$, satisfy complementary slackness, and are feasible.

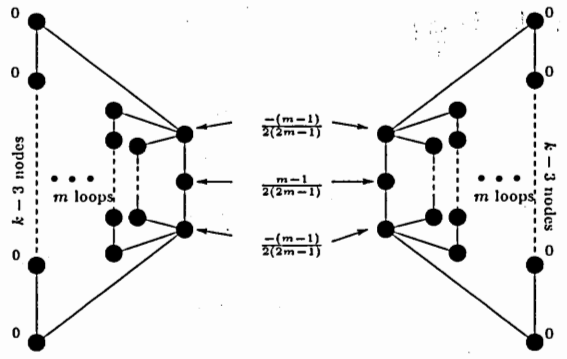

Each loop of k nodes also has a dual value of $\frac{1}{2(2m-1)}$.

Figure 10: Dual Solution

For ease of discussion, we will refer to the three types of nodes as follows:

center nodes: These are the two nodes (one in each half) of degree 2 in Figure 8 that are contained in every loop.

branching nodes: These are the four nodes with degree greater than 2 in Figure 8.

corner nodes: These are the remaining nodes, each of which has degree 2 in Figure 8 and is contained in exactly one loop.

Objective Values. In the primal solution, note that the only edge with weight 1 that is used is the dashed edge between the two center nodes. This has value $\frac{1}{2m-1}$ in the solution, so the objective value is also that value.

In the dual solution, each half of the graph has node duals totaling $-\frac{m-1}{2(2m-1)}$, so the total of node duals is $-\frac{m-1}{2m-1}$. In addition, there are $2m$ loops (m on each half), each with a k-set dual value of $\frac{1}{2(2m-1)}$. The sum of k-set duals is therefore $\frac{m}{2m-1}$, for a total objective value of $\frac{m}{2m-1} - \frac{m-1}{2m-1} = \frac{1}{2m-1}$. This shows that the primal and dual solutions have the same objective value.

Complementary Slackness. We must show that edges with positive values in the primal solution correspond to dual constraints that are satisfied at equality and that non-zero dual values correspond to primal constraints that are satisfied at equality.

First examine primal edges. All of the zero weight edges have positive values, as does the "bridge" edge between the two center nodes. There are three types of zero weight edges: edges from a center node to a branching node (of which there are 4), edges from a branching node to a corner node (of which there are $4m$), and edges between two corner nodes (of which there are $2m(k-4)$).

The dual constraint that must be satisfied at equality for each edge is

$$\sum_{S:e\in\delta(S)} y_S + y_u + y_v \leq w_e.$$

Edges from a center node to a branching node do not cross any of the k-sets with positive dual values, and their node duals are opposite, so their LHS sums to zero, which equals their weight.

Similarly, edges between corner nodes do not cross any 5-sets with positive dual values, and their endpoints have duals of zero, so they trivially satisfy the constraint at equality.

Edges from branching nodes to corner nodes each cross $m-1$ of the k-set constraints, all of them except the one they are contained in. This is a dual contribution of $\frac{m-1}{2(2m-1)}$. However, the branching node has a dual value of $-\frac{m-1}{2(2m-1)}$, which makes the total sum zero, as required.

Finally, the bridge edge crosses every one of the $2m$ k-set constraints, for a dual contribution of $\frac{2m}{2(2m-1)}$. The contribution from its two endpoints is $\frac{2(m-1)}{2(2m-1)}$, for a total dual sum of $\frac{2m+2(m-1)}{2(2m-1)} = \frac{2(2m-1)}{2(2m-1)} = 1$. Since the weight of this edge is also one, the complementary slackness condition is met.

Now consider the nonzero dual values. The nodes are not a concern, since the primal constraints on nodes are equality constraints anyway. We must simply confirm that the primal constraints corresponding to the positive 5-set duals are satisfied at equality. Those constraints are

$$x(\delta(S)) \geq 1.$$

Each k-set constraint contains the k nodes in a single loop, so the (positive) edges passing out of the set include two branching-corner edges for each of the $m-1$ other loops in the same half of the graph, as well as the bridge edge to the other half of the graph. The

sum of these primal values is

$$2(m-1)\frac{1}{2m-1}+\frac{1}{2m-1}=\frac{2m-2+1}{2m-1}=1.$$

So the primal constraint is satisfied at equality, and all complementary slackness conditions are satisfied.

Primal Feasibility. It is easy to confirm that the equality constraints on nodes are all satisfied. Keep in mind that each branching node has one edge to a center node and m edges to corner nodes.

For odd sets, the constraints we must satisfy are

$$x(\delta(S)) \geq 1 \; \forall S \subseteq V, |S| \text{ odd}, |S| \leq k.$$

We will prove that all odd-set constraints except k-set constraints are satisfied by an inductive argument. The base case is the individual node constraints, which we already mentioned.

Now assume we have that all odd sets of size less than or equal to k' are satisfied. We now consider odd sets of size $k'+2$, assuming $k'+2 < k$. Note that any such set which is not connected in the graph in Figure 9 will have at least one odd connected component. Since that odd component has size at most k', it satisfies an odd-set constraint, which means that the sum of primal edge variables leaving the component is at least 1. Thus, the $(k'+2)$-set constraint we are considering is also satisfied. Therefore, we need only consider odd sets that are connected in Figure 9.

We consider the case that all of the nodes in the odd set are corner nodes. Since the set is connected, these must all belong to the same loop. Therefore there are only two primal edges leaving the set. It is easy to verify that given an odd path of nodes, one of these edges will have primal value $1/(2m-1)$ while the other will have primal value $(2m-2)/(2m-1)$. The sum is 1, so the constraint is satisfied.

Next, note that the highest primal values are $(2m-2)/(2m-1)$, which occur alternatingly between corner nodes in a loop. If any one of these edges crosses out of the set we are considering, then the odd-set constraint is almost satisfied. Any other edge crossing out

of the set will bring the total to 1 or higher. Since there must be at least one such edge, any set with a $(2m-2)/(2m-1)$ crossing out is satisfied. This means we may restrict our attention to sets in which corner nodes always appear in pairs so that no $(2m-2)/(2m-1)$ edge leaves the set.

We are now considering $(k'+2)$-sets in which the nodes are connected (in Figure 9), in which at least one branching or center node appears, and in which corner nodes appear in adjacent pairs as described above. Since $k'+2 < k$, we cannot include an entire loop, so if any corner nodes are included, they must form a terminating path of pairs from one of the branching nodes. Note that the edge leaving this set in the loop has value $1/(2m-1)$, which is the same as if the corner pairs were not in the set at all (then the edge leaving the set would be the $1/(2m-1)$ edge that is incident with the branching node). Thus, this odd-set constraint is satisfied if the corresponding smaller odd-set constraint without the corner nodes is satisfied. Since we are assuming by induction that this is so, we no longer need to consider sets which contain any corner nodes.

The sets that remain contain only center and/or branching nodes. There are two types of such 3-sets, and one type of 5-set. One 3-set possibility is a center node and its two adjacent branching nodes. The outgoing edges are the bridge edge and $2m$ branching-corner edges. The sum of primal values is $1/(2m-1)+(2m)/(2m-1) > 1$, so the constraint is satisfied. The other 3-set possibility is both center nodes and one branching nodes. In this case, three center-branching edges leave the set, which is already enough to satisfy the constraint. The only 5-set possibility is both center nodes and all but one branching nodes. The edges leaving this set are one center-branching edge and $3m$ branching-corner edges, which easily satisfies the constraint.

Thus, we have shown that all odd-set constraints are satisfied except k-set constraints. Note that most k-set constraints can be inductively handled in the same manner. The only new possibility is that an entire loop is the set. The edges that leave such a set are the bridge edge and $2(m-1)$ branching-corner edges (2 for each of the other loops). The sum of primal values is $1/(2m-1)+(2m-2)/(2m-1) = 1$, so the constraint is satisfied. Actually, we already mentioned that earlier when dealing with complementary slackness.

Thus, we have shown that all odd-set constraints are satisfied, which proves primal feasibility.

Dual Feasibility. For dual feasibility we must check the constraint

$$\sum_{S:e\in\delta(S)} y_S + y_u + y_v \leq w_e$$

for each edge. Note that in the complementary slackness section, we already did this for all edges with positive values in the primal solution. Thus, we must only check the remaining edges, which are those edges that do not appear in Figure 8 (except the bridge edge, which was already handled).

All of the unused edges have weight 1, so we just need to show that the dual sum for any edge is no more than one. Note that since edges with endpoints in different halves of the graph cross every one of the k-set duals, checking these edges is enough (for example, if a corner-center edge in one half violated the constraint, than a corner-center edge that crosses halves would certainly violate it as well).

The effective dual values for the three types of nodes when crossing halves are as follows:

center: $\frac{m-1}{2(2m-1)} + \frac{m}{2(2m-1)} = \frac{1}{2}$.

branching: $-\frac{m-1}{2(2m-1)} + \frac{m}{2(2m-1)} = \frac{1}{2(2m-1)}$.

corner: $0 + \frac{1}{2(2m-1)} = \frac{1}{2(2m-1)}$.

Since none of these effective duals is more than $1/2$, there is no chance that a dual sum can be more than one.

This proves dual feasibility.

5.5.2.3 Summary

We have presented a graph with $6+2m(k-3)$ nodes, edge weights in $\{0,1\}$, and a minimum perfect matching of weight $\frac{1}{2m-1}$. This completes the proof of Theorem 5.25.

In fact, only the k-set dual values were used. When we checked primal feasibility we showed that all smaller odd-set constraints are satisfied, but since none of their dual values

were used, excluding them does not affect the proof. Therefore, we have proved the following slightly stronger theorem:

Theorem 5.26 *For any positive integer m and any odd integer $k > 3$, the perfect matching polytope for the complete graph on $6 + 2m(k-3)$ nodes with constraints for odd sets of size k and any subset of smaller odd sets is not $\frac{1}{q}$-integral for any integer $q < 2m - 1$.*

5.5.2.4 Extension to maximum matching

The fractional vertices found in the preceding sections are present when odd-set constraints are added to the maximum matching LP relaxation as well.

Corollary 5.27 *For any positive integer m and any odd integer $k > 3$, the maximum matching polytope for the complete graph on $6 + 2m(k-3)$ nodes with constraints for odd sets of size k and any subset of smaller odd sets is not $\frac{1}{q}$-integral for any integer $q < 2m-1$.*

Proof: Let P be the perfect matching LP relaxation polytope with some odd-set constraints present, and let Q be the maximum matching LP relaxation polytope with the same odd-set constraints. The only difference between P and Q is that P satisfies all node constraints at equality. Since node constraints are valid inequalities for Q, P is a face of Q.

An extreme point of P is a face of dimension zero, and every face of P is a face of Q because P is a face of Q (see Schrijver [37], for example). Thus the extreme points of P are also faces of Q with dimension zero, so they are extreme points of Q.

The corollary now follows from Theorem 5.26. ■

5.6 Computational results

We performed several computational tests of the facets. The measure used is the minimum size of the branch-and-bound tree, assuming that branching is done on variables and the most fractional variable is chosen for branching. This measure is described in more detail in Section 4.7, where it was used for knapsack problems.

Graphs of even sizes from $|V| = 14$ to $|V| = 24$ were tested. In each size, tests were performed with all the 3-set constraints present and with all the 5-set constraints present.

Table 39: Branch-and-bound performance of matching instances

	Number of nodes					
Facets included	14	16	18	20	22	24
All 3-sets	1.0380	1.0720	1.0700	1.0820	1.1100	1.1040
All 5-sets	1.0140	1.0180	1.0120	1.0080	1.0140	1.0100
100 3-sets	1.2580	1.3688	1.4040	1.5170	1.5344	1.6744
100 5-sets	1.2920	1.4126	1.4476	1.5502	1.5640	1.6972
100 7-sets	1.3050	1.4290	1.4508	1.5614	1.5688	1.7052
100 9-sets			1.4562	1.5612	1.5708	1.7046
100 11-sets					1.5746	1.7056

In addition, tests were done using only 100 randomly selected odd-set constraints of each size. In each case 1000 trials were performed, with objective coefficients taken iid from the positive normal distribution. For the random sets of facets, the test was performed with 10 different random sets and the results were averaged. Note that since k-sets are equivalent to $(n-k)$-sets, odd sets were only tested up to size $|V|/2$.

Table 39 gives the average minimum tree size for each test. Because of the small sizes of the graphs, in many cases the instances were solved at the root node. For this reason the averages are all near 1.

The trends are consistent. Adding all the five-set constraints is clearly better than all the three-set constraints. On the other hand, when a constant number of constraints is added, the 3-sets perform the best and smaller-odd-set constraints perform better than larger-odd-set constraints in general.

The data may explain the apparent contradiction between the shooting experiment analysis of Section 5.1 and best-case improvement analysis of Section 5.2.

The shooting experiment analysis considered the constraints in groups, and suggested that the larger-odd-set constraints would be more useful. When used as a group, this analysis is consistent with the data, since adding all 5-set constraints was always significantly better than all 3-set constraints. This analysis apparently does not carry over to small groups of facets. Note that Corollary 5.6 does not contradict this statement. It is true that when considering only k-sets and $(k+2)$-sets, each $(k+2)$-set facet has a much larger

shooting experiment size than each k-set facet, but these sizes are caused by the interactions of all the k-set and $(k+2)$-set facets. Therefore, despite its appearance Corollary 5.6 is also a statement comparing the groups of facets.

On the other hand, best-case improvement is found by considering individual facets. The analysis of Section 5.2 suggests that smaller-odd-set constraints are better, and the data supports this prediction on a facet-for-facet comparison. Best-case improvement can also be applied to groups of facets, however, and the data does not support its predictions in that case.

Thus, the data suggest that best-case improvement is best considered on the facet level, and that shooting experiment size should be considered in the context in which it is analyzed, in this case with all of the facets in the same class.

5.7 Summary

The shooting experiment, best-case improvement, and Chvátal-Gomory rank make different predictions of usefulness for the facets of the matching polytope. The shooting experiment suggests that larger-odd-set constraints are more useful, while best-case improvement suggests that smaller-odd-set constraints are more useful. Chvátal-Gomory rank does not differentiate between them.

Empirical tests seem to support both the shooting experiment and best-case improvement predictions when considered in the context of the analyses. That is, when all facets of a given size are present, as in the shooting experiment analysis, the shooting experiment analysis agrees with the data: larger-odd-set constraints are more useful. When only a small number of facets are present, however, the data agrees with the best-case improvement prediction: smaller-odd-set constraints are better.

For best-case improvement, this highlights the fact that the measure is at heart a measure of individual facets and casts doubt on its usefulness as a measure of polyhedra with many facets. For the shooting experiment, the results point to the importance of making predictions in the same context as the analysis that produced them.

CHAPTER VI

NODE-PACKING POLYTOPES

Given a graph $G = (V, E)$, *unweighted node packing* is the problem

$$\begin{array}{lrcll} \max & \sum_{v \in V} x_v & & & \\ s.t. & x_u + x_v & \leq & 1 & \forall \{u, v\} \in E \\ & x_v & \in & \{0, 1\} & \forall v \in V. \end{array}$$

This problem is also known as the maximum independent set problem or the maximum stable set problem. We will call the inequalities *edge inequalities*, since there is one for each edge in the graph.

In this chapter we consider several measures applied to the node-packing problem. Section 6.2 discusses an empirical study by Nemhauser and Sigismondi of clique and odd-hole inequalities, which motivates our analysis. Section 6.3 shows that the shooting experiment will almost always hit clique inequalities rather than odd-hole inequalities. Section 6.4 shows a similar result for best-case improvement. In contrast, Section 6.5 shows that odd-hole inequalities have a much lower Chvátal-Gomory rank than clique inequalities. In Section 6.6, we consider lifted odd-hole inequalities. Section 6.7 summarizes the results of the chapter.

6.1 Facets and valid inequalities for node packing

Not all the facets of the node-packing polytope are known, but inequalities that are commonly used as cutting planes include clique inequalities and odd-hole inequalities.

Clique inequalities are of the form

$$\sum_{v \in C} x_v \leq 1,$$

where C is the node set of a clique in the graph. Padberg [35] showed that clique inequalities are facet-defining for node packing if the clique is maximal.

An odd hole is a set H of vertices such that $|H|$ is odd and the induced subgraph on H is a chordless cycle containing all the nodes of H. Given such a set H, the corresponding odd-hole inequality is

$$\sum_{v \in H} x_v \leq \frac{|H|-1}{2}.$$

Note that odd holes of size 3 are cliques, so we assume that $|H| \geq 5$. An odd-hole inequality is facet-defining on the node-packing polytope of the induced subgraph. Odd-hole inequalities are generally not facet-defining on the larger graph, though they can always be used to generate facet-defining inequalities through a process called *lifting*.

A *lifted odd-hole inequality* has the form

$$\sum_{v \in H} x_v + \sum_{v \notin H} \alpha_v x_v \leq \frac{|H|-1}{2}.$$

The coefficients α_v are called lifted coefficients. One approach to lifting that ensures that the resulting lifted inequality is facet-defining is *sequential maximal lifting*. This is done by determining each lifted coefficient in turn, selecting the greatest possible value for which the intermediate inequality remains valid.

That is, let $\sum_{v \in H} x_v + \sum_{v \in L} \alpha_v x_v \leq \frac{|H|-1}{2}$ be the inequality so far, and let $i \notin H \cup L$. Let S be the set of integer feasible node-packing solutions for the graph under consideration. For a maximal lifting of α_i, set

$$\alpha_i = \frac{|H|-1}{2} - \max\left\{ \sum_{v \in H} x_v + \sum_{v \in L} \alpha_v x_v : x \in S, x_i = 1 \right\}.$$

Padberg [35] proved that the resulting inequality is facet-defining. It may be possible to generate more than one facet-defining lifted inequality from a single odd-hole inequality by lifting the coefficients in different orders.

6.2 Computational study by Nemhauser and Sigismondi

Nemhauser and Sigismondi did empirical tests on node-packing instances using a cut-and-branch algorithm with clique inequalities and odd-hole inequalities [33]. They added a large number of clique inequalities before solving at the root node and separated additional clique inequalities heuristically. Odd-hole inequalities were separated exactly and then

lifted to form facet-defining inequalities. Since separation was done over unlifted odd-hole inequalities, it is possible that violated lifted odd-hole inequalities existed but were not found by the algorithm.

Their test instances were random graphs of various densities. The sizes of the graphs ranged from $|V| = 30$ to $|V| = 120$. They found that performance and usefulness of the facets varied with the density of the graph. Overall, they found that clique inequalities were much more useful than odd-hole inequalities. For medium density graphs ($0.4 \leq p \leq 0.6$) they found that violated odd-hole inequalities were almost never present once clique inequalities had been added. For lower densities ($0.1 \leq p \leq 0.2$) odd-hole inequalities did help in solving the instances, though to a lesser extent than clique inequalities.

In the remainder of this chapter, we consider several facet measures in light of the empirical results of Nemhauser and Sigismondi.

6.3 Shooting experiment

In this section we show that in a comparison of clique inequalities and odd-hole inequalities, the shooting experiment sizes of clique inequalities are in general much larger than the shooting experiment sizes of odd-hole inequalities. Recall that although Nemhauser and Sigismondi lifted odd-hole inequalities before applying them to the instance, they separated only over unlifted odd-hole inequalities.

Definition 6.1 *The* clique and hole relaxation of node-packing *is the polytope defined by the LP relaxation of the node-packing problem with the addition of all clique and odd-hole inequalities.*

Theorem 6.2 *For random graphs with constant density parameter p, the shooting experiment on the clique and hole relaxation of the node-packing polytope with the origin as shooting point will almost always not hit a facet defined by an odd-hole inequality.*

In the theorem, the implied probability space takes into account both the random graph of the instance and the random direction of the shot.

Proof: Let d be a spherically symmetric random vector in the nonnegative orthant. Using Proposition 2.6, the scaled shooting distance to a clique inequality is

$$t_C = \frac{1}{\sum_{v \in C} d_v},$$

and to an odd-hole inequality is

$$t_H = \frac{\frac{|H|-1}{2}}{\sum_{v \in H} d_v}.$$

We will show that t_H for all odd-hole inequalities is almost always greater than the minimum value of t_C, so that a clique inequality is almost always hit by the shooting experiment.

Let $d_{\max} = \max_{v \in V} d_v$ be the value of the greatest coordinate in the random direction d. Then an odd hole of size $|H|$ satisfies

$$t_H \geq \frac{\frac{|H|-1}{2}}{\sum_{v \in H} d_{\max}} = \frac{1}{2d_{\max}} \cdot \frac{|H|-1}{|H|}.$$

Since $|H| \geq 5$, we have in particular that

$$t_H \geq \frac{2}{5d_{\max}}. \tag{15}$$

Next we consider the probability that $d_{\max}$ is a large value. Let $k > 0$ be arbitrary. Recall that the spherically symmetric distribution of d comes from iid positive normal coordinates. For a given coordinate d_v, we have

$$P(d_v > k) = \int_k^\infty \frac{2}{\sqrt{2\pi}} e^{-z^2/2} dz.$$

Since $k > 0$ we know that $e^{-z^2/2} < e^{-z^2/2} + \frac{1}{z^2} e^{-z^2/2}$ for all $z \geq k$. Thus,

$$P(d_v > k) < \int_k^\infty \frac{2}{\sqrt{2\pi}} (e^{-z^2/2} + \frac{1}{z^2} e^{-z^2/2}) dz = -\sqrt{\frac{2}{\pi}} \frac{1}{z} e^{-z^2/2} \Big|_k^\infty = \sqrt{\frac{2}{\pi}} \frac{1}{k} e^{-k^2/2}.$$

Since there are $n = |V|$ coordinates, we have

$$P(d_{\max} > k) \leq \sum_{v \in V} P(d_v > k) < \sqrt{\frac{2}{\pi}} \frac{n}{k} e^{-k^2/2}.$$

In particular,

$$P\left(d_{\max} > \sqrt{2 \log n}\right) < \sqrt{\frac{2}{\pi}} \frac{n}{\sqrt{2 \log n}} \frac{1}{n} = \sqrt{\frac{1}{\pi}} \frac{1}{\sqrt{\log n}}.$$

This value goes to zero as n increases. Using the last expression with (15), we have that almost always, for all odd-hole inequalities, t_H is no less than $\frac{2}{5\sqrt{2\log n}}$.

To show that there exists a clique with $t_C < \frac{2}{5\sqrt{2\log n}}$, consider only the $n/2$ nodes with the greatest d_v values. Let $c > 0$ be any constant smaller than the median of the positive normal distribution. Then almost always, all of these values d_v are greater than c.

Using Proposition 1.3 from Section 1.4.4, among these nodes there is almost always a clique C' of size $2\log_{1/p}(n/2) - 2\log_{1/p}\log_{1/p}(n/2)$. Then almost always,

$$t_{C'} \leq \frac{1}{2c\log_{1/p}(n/2) - 2c\log_{1/p}\log_{1/p}(n/2)}.$$

There exists n_0 such that

$$\forall n \geq n_0, \quad 2c\log_{1/p}(n/2) - 2c\log_{1/p}\log_{1/p}(n/2) \geq \frac{5}{2}\sqrt{2\log n}.$$

Therefore, almost always $t_{C'} \leq \frac{2}{5\sqrt{2\log n}}$ and almost always $t_H \geq \frac{2}{5\sqrt{2\log n}}$ for all odd-holes H. This proves that almost always, no odd-hole inequality will be hit by the shooting experiment. ■

In their computational experiments, Nemhauser and Sigismondi found that once clique inequalities were added, no violated odd-hole inequalities were found for medium density graphs ($0.4 \leq p \leq 0.6$) that they tested. Violated odd-hole inequalities were found for lower density graphs ($0.1 \leq p \leq 0.2$), however.

Notice that for smaller values of p, the expected size of the largest clique is smaller, so from our analysis above we would expect odd-hole inequalities to be more competitive in terms of the shooting experiment as well.

If there is a correlation between the shooting experiment size and the usefulness of the facets, then Theorem 6.2 suggests that as n increases, violated odd-hole inequalities would become rare once clique inequalities are added, even for low density random graphs. Testing this hypothesis is one possible area for future research.

6.4 Best-case improvement

We show in this section that the best-case improvement value for clique inequalities is much larger than for odd-hole inequalities. The node-packing polytope is an anti-blocking

polytope, so we can use Theorem 2.4 from Section 2.4.1.

Theorem 6.3 *The strength of an odd-hole constraint defined by vertex set H relative to the standard node-packing relaxation is $\frac{|H|-1}{|H|}$. The strength of a clique constraint defined by clique C relative to the standard node-packing relaxation is $\frac{|C|}{2}$.*

Proof: The strength of an odd-hole constraint with respect to the standard LP relaxation P is

$$\frac{\max\{\sum_{v\in H} x_v : x \in P\}}{\frac{|H|-1}{2}}.$$

An upper bound for the numerator comes from summing the edge inequalities for edges in the hole. There are $|H|$ such edges and each node is adjacent to two of them, so we have $2\sum_{v\in H} x_v \leq |H|$ or $\sum_{v\in H} x_v \leq \frac{|H|}{2}$. In fact we can achieve this upper bound by setting $x_v = 1/2$ for $v \in H$. Therefore, $\max\{\sum_{v\in H} x_v : x \in P\} = \frac{|H|}{2}$, and the strength of the inequality is

$$\frac{\frac{|H|}{2}}{\frac{|H|-1}{2}} = \frac{|H|}{|H|-1}.$$

Clique inequalities have a strength of

$$\frac{\max\{\sum_{v\in C} x_v : x \in P\}}{1}.$$

Summing all the edge inequalities in the clique gives an upper bound on the strength of $(|C|-1)\sum_{v\in C} x_v \leq \frac{|C|(|C|-1)}{2}$ or $\sum_{v\in C} x_v \leq \frac{|C|}{2}$. Again, setting $x_v = 1/2$ for $v \in C$ gives the upper bound, so the strength of the inequality is $\frac{|C|}{2}$. ■

Among odd-hole inequalities, 5-holes (the smallest odd holes) are the strongest, with a strength of $\frac{5}{4}$. Larger odd-hole inequalities have strengths of $\frac{7}{6}, \frac{9}{8}, \frac{11}{10}$, and so on. If we allowed odd holes of size 3, then the strength would start at $\frac{3}{2}$ and decrease as the size of the hole increases.

Clique inequalities, on the other hand, start with a strength of $\frac{3}{2}$ when $|C| = 3$ and then increase in strength as the size of the clique increases.

If best-case improvement correlates with usefulness, then these strengths suggest that clique inequalities are much more valuable than odd-hole inequalities. This conclusion

agrees with the shooting experiment analysis from the last section as well as the empirical findings of Nemhauser and Sigismondi.

6.5 *Chvátal-Gomory rank*

In this section, we show that clique inequalities have much higher Chvátal-Gomory ranks than odd-hole inequalities.

Proposition 6.4 *Odd-hole constraints have Chvátal-Gomory rank 1.*

Proof: Let H be the set of odd-hole vertices. If the odd-hole constraint corresponding to H were rank 0, it would be dominated by a nonnegative sum of edge constraints. Since there are $|H|$ edges in the hole and each constraint cannot contribute more than 2, the weights in the sum must total at least $|H|/2$. Thus the right-hand-side of the weighted sum is at least $|H|/2$. Since this is greater than $\frac{|H|-1}{2}$, odd-hole constraints are not rank 0.

Using the notation of Section 1.4.1, set $u_i = 1$ for all inequalities of the form

$$x_v + x_w \leq 1, \quad \forall \{v, w\} \in E, \quad v, w \in H,$$

and $u_i = 0$ otherwise. There are $|H|$ such edges, and each vertex in H is adjacent to two of the edges, so the weighted sum of inequalities is

$$2 \sum_{v \in H} x_v \leq |H|.$$

Dividing by 2 and rounding down gives

$$\sum_{v \in H} x_v \leq \frac{|H| - 1}{2}.$$

This shows that the odd-hole constraint has rank 1. ■

In contrast, Chvátal [7] stated without proof that the clique inequality based on clique C has rank $\Theta(\log |C|)$.

Based on the results of Nemhauser and Sigismondi, then, larger Chvátal-Gomory rank is indicative of greater usefulness. This makes some intuitive sense, since inequalities of higher C-G rank are in a sense more powerful by construction. However, these results contradict

the perception that the lower ranked cuts provide most of the benefits. Recall that the knapsack tests in Chapter 4 supported this perception with a mild correlation between low C-G rank and usefulness in branch-and-bound tests. The conflicting conclusions of the two chapters suggest that C-G rank may not be a good general indicator of facet usefulness.

6.6 Lifted odd-hole inequalities

Nemhauser and Sigismondi separated over unlifted odd-hole inequalities, but they lifted the inequalities before applying them to the problem. Therefore, their results on the usefulness of odd-hole inequalities relate in part to lifted inequalities, though their results on the presence of violated odd-hole inequalities reflect only unlifted inequalities.

They acknowledged that the performance of their implementation might improve if efforts were made to identify violated lifted odd-hole inequalities, although these efforts would have to be heuristic in nature. In this section we consider what the facet measures suggest about the potential usefulness of lifted odd-hole inequalities.

6.6.1 Shooting experiment

Using the notation from the proof of Theorem 6.2, a lifted odd-hole inequality has a scaled shooting distance of

$$t_{LH} = \frac{\frac{|H|-1}{2}}{\sum_{v \in H} d_v + \sum_{v \notin H} \alpha_v d_v}.$$

As long as some α_v are greater than zero, this scaled shooting distance is better than that of the unlifted odd-hole inequality. Intuitively this makes sense, since the lifted odd-hole inequality is facet-defining, while the unlifted inequality is not facet-defining unless the two are the same.

Determining the minimum possible value of t_{LH} is difficult, however, primarily due to the complexity of lifting. We will consider only a subset of lifted odd-hole inequalities. Given H, the lifted inequality will have a low value of t_{LH} if $\sum_{v \notin H} \alpha_v d_v$ is high. With this motivation, we consider those liftings in which $\alpha_v \in \left\{0, \frac{|H|-1}{2}\right\}$, since $\frac{|H|-1}{2}$ is the highest possible lifted coefficient.

If $\alpha_v = \frac{|H|-1}{2}$, then it must be the case that v is adjacent to every node in H and every

other node with positive lifted coefficient. Thus, the nodes with $\alpha_v = \frac{|H|-1}{2}$ form a clique, and each is also adjacent to every node in H.

Definition 6.5 *A* clique-lifted odd-hole inequality *is an inequality of the form*

$$\sum_{v \in H} x_v + \sum_{v \in C'} \frac{|H|-1}{2} x_v \leq \frac{|H|-1}{2},$$

where $C' \cap H = \emptyset$.

Due to the restriction on the allowable values of the lifting coefficients, it is possible that a clique-lifted odd-hole inequality is not facet-defining even if no other coefficients can be lifted into the clique.

We will consider the expected values of shooting distance, and prove the following result:

Theorem 6.6 *Let* $t_{C_{\max}}$ *be the scaled shooting distance to the inequality defined by the largest clique in the graph. Given an odd-hole* H*, let* $t_{LH_{\max}}$ *be the scaled shooting distance to the clique-lifted odd-hole inequality based on* H *and the largest clique* C' *such that all nodes in* C' *are adjacent to every node in* H*. Then* $E[t_{C_{\max}}] \geq E[t_{LH_{\max}}]$*, almost always, where the expectation is over the space of directions, and the "almost always" is over the space of random graphs with density* p.

Proof: In the case of a clique, we have

$$E[t_C] = \frac{1}{E[\sum_{v \in C} d_v]} = \frac{1}{|C|} \cdot \frac{1}{E[d_v]}.$$

In the case of a clique-lifted odd-hole, we have

$$E[t_{LH}] = \frac{\frac{|H|-1}{2}}{E[\sum_{v \in H} d_v + \sum_{v \in C'} \frac{|H|-1}{2} d_v]} = \frac{1}{\frac{2|H|}{|H|-1} + |C'|} \cdot \frac{1}{E[d_v]}.$$

Since $|H| \geq 5$,

$$E[t_{LH}] \leq \frac{1}{(|C'| + \frac{5}{2}) E[d_v]}.$$

Therefore, we only need to show that $|C| \geq |C'| + \frac{5}{2}$, almost always.

Let $\epsilon > 0$ be a constant. From Proposition 1.3, the largest clique C in the graph almost always satisfies $|C| \geq d(n,p) - \epsilon$, where

$$d(n,p) = 2\log_{\frac{1}{p}} n - 2\log_{\frac{1}{p}} \log_{\frac{1}{p}} n + 1 + \log_{\frac{1}{p}}(\frac{e}{2}). \tag{16}$$

In contrast C' is a clique such that every node in C' is adjacent to every node in H. Then C' is a clique in the subgraph defined by nodes adjacent to every node of H.

Let X_v be an indicator variable such that $X_v = 1$ if v is adjacent to every node in H and $X_v = 0$ otherwise. Then $X = \sum_{v \in V \setminus H} X_v$ is the size of the set of candidate nodes for C'. X is a binomial random variable with parameters $n - |H|$ and $p^{|H|}$. Note that decreasing the value of $|H|$ makes both parameters larger, so that if X' corresponds to odd-hole H' and $|H'| < |H|$, then

$$P(X > a) < P(X' > a) \tag{17}$$

for any positive constant a. Therefore, we can get an upper bound on $P(X > a)$ for any odd-hole by considering a smaller odd-hole.

With this in mind, let X' be the value for the case $|H'| = 5$. Then X' has expectation $(n-5)E[X'_v] = (n-5)P(X'_v = 1) = (n-5)p^5$. Using a Hoeffding bound, we know that for any $\delta > 0$,

$$P\left(X' > (n-5)p^5(1+\delta)\right) \leq e^{-\frac{\delta^2(n-5)p^5}{2(1+\delta/3)}}.$$

The right-hand-side is exponentially small in n, so $X' \leq (n-5)p^5(1+\delta)$ almost always. Using (17), for any odd-hole H with corresponding random variable X, we have

$$P\left(X > (n-5)p^5(1+\delta)\right) < P\left(X' > (n-5)p^5(1+\delta)\right) \leq e^{-\frac{\delta^2(n-5)p^5}{2(1+\delta/3)}},$$

so $X \leq (n-5)p^5(1+\delta)$ almost always.

To determine a bound on the size of C', we can plug our upper bound on X into (16). For ease of notation, let $\log x = \log_{1/p} x$ in the following equations. The size of C' almost

always satisfies

$$\begin{aligned}
|C'| + \frac{5}{2} &\leq d((n-5)p^5(1+\delta), p) + \epsilon + \frac{5}{2} \\
&\leq d(np^5(1+\delta), p) + \epsilon + \frac{5}{2} \\
&= 2\log(np^5(1+\delta)) - 2\log\log(np^5(1+\delta)) + 1 + \log(e/2) + \epsilon + \frac{5}{2} \\
&= 2\log n - 2\log\log n + 1 + \log(e/2) - \epsilon \\
&\quad + 2\log(p^5) + 2\log(1+\delta) - 2\log\log(np^5(1+\delta)) + 2\log\log n + 2\epsilon + \frac{5}{2} \\
&= d(n,p) - \epsilon - 10 + 2\log(1+\delta) - 2\log\log(np^5(1+\delta)) + 2\log\log n + 2\epsilon + \frac{5}{2} \\
&\leq |C| - 10 + 2\log(1+\delta) - 2\log\log(np^5(1+\delta)) + 2\log\log n + 2\epsilon + \frac{5}{2} \\
&= |C| - \frac{15}{2} + 2\log(1+\delta) - 2\log\log(np^5(1+\delta)) + 2\log\log n + 2\epsilon. \qquad (18)
\end{aligned}$$

Finally, we will have $|C'| + \frac{5}{2} \leq |C|$ if we confirm that the sum of the terms of (18) other than $|C|$ is nonpositive. We wish to show

$$\begin{aligned}
\frac{15}{2} + 2\log\log(np^5(1+\delta)) &\geq 2\log\log n + 2\log(1+\delta) + 2\epsilon \\
\frac{15}{4} + \log\log(np^5(1+\delta)) &\geq \log\log n + \log(1+\delta) + \epsilon \\
\log p^{-15/4} + \log\log(np^5(1+\delta)) &\geq \log\log n + \log(1+\delta) + \log p^{-\epsilon} \\
\log\left(p^{-15/4}\log(np^5(1+\delta))\right) &\geq \log\left(\log n(1+\delta)p^{-\epsilon}\right) \\
p^{-15/4}\log(np^5(1+\delta)) &\geq \log n(1+\delta)p^{-\epsilon} \\
(p^{-15/4} - (1+\delta)p^{-\epsilon})\log n &\geq -p^{-15/4}\log(p^5(1+\delta)).
\end{aligned}$$

We can choose δ and ϵ such that the coefficient of $\log n$ is positive, so that the expression is almost always satisfied. This means that $|C'| + \frac{5}{2} \leq |C|$ almost always, which completes the proof. ■

Theorem 6.6 indicates that we expect a clique-lifted odd-hole inequality based on the largest clique possible to have a smaller scaled shooting distance than the facet defined by the largest clique in the graph. This is not as strong as the earlier result on unlifted odd-hole inequalities, however, for two reasons. First, it is only a result on expected scaled distances, when it is the minimum scaled distance that determines which facet is hit. In

addition, the cliques C and C' that minimize t_C and t_{LH} may not be the largest cliques, since a smaller clique with particularly high direction coordinates would be better.

Nevertheless, this result suggests that the shooting experiment sizes of clique inequalities are larger than even lifted odd-hole inequalities.

6.6.2 Best-case improvement

Using Definition 2.3, the strength of a lifted odd-hole inequality is

$$\frac{\max\{\sum_{v\in H} x_v + \sum_{v\notin H} \alpha_v x_v : x \in P\}}{\frac{|H|-1}{2}},$$

where P is the LP relaxation of node-packing.

By setting $x_v = \frac{1}{2}$ for all v, we get a lower bound on strength:

$$\frac{\frac{1}{2}|H| + \frac{1}{2}\sum_{v\notin H} \alpha_v}{\frac{|H|-1}{2}} = \frac{|H| + \sum_{v\notin H} \alpha_v}{|H|-1}.$$

The strongest lower bound on a lifted inequality is therefore the one that maximizes $\sum_{v\notin H} \alpha_v$.

Thus, best-case improvement indicates that lifted odd-hole inequalities are significantly stronger than unlifted odd-hole inequalities, and the difference depends on the sum $\sum_{v\notin H} \alpha_v$.

6.7 Summary

For node packing, the shooting experiment and best-case improvement suggest that clique inequalities are much more useful than odd-hole inequalities. This agrees with the empirical tests of Nemhauser and Sigismondi. The analysis of the shooting experiment suggests that for lower densities, odd-hole inequalities will be more competitive with cliques, which may explain why Nemhauser and Sigismondi found odd-hole inequalities more useful on instances with low densities. This hypothesis could be confirmed by testing larger graphs with the low densities to see whether the usefulness of odd-hole inequalities diminishes with size, as the shooting experiment predicts.

For both measures, lifted odd-hole inequalities appear much better than unlifted odd-hole inequalities, though we do not know exactly how much. This suggests that efforts to separate lifted odd-hole inequalities directly may be worthwhile.

The clique inequalities have a much higher Chvátal-Gomory rank than odd-hole inequalities. This contradicts the notion that inequalities with lower rank provide most of the benefit. The results of Chapter 4, on the other hand, indicate that inequalities with lower Chvátal-Gomory rank are more useful. These conflicting results suggest the Chvátal-Gomory rank is not a good general predictor of facet usefulness.

CHAPTER VII

EXPONENTIAL SIZE BRANCH-AND-BOUND TREES

The previous three chapters used the facet measures of Chapter 2 to compare the facets of several combinatorial optimization problems. This chapter instead presents an example of the limits of facet usefulness.

In Sections 4.8 and 5.6 we used the size of the branch-and-bound tree as an empirical measure of the usefulness of facets. In this chapter, we consider the size of the branch-and-bound tree again, demonstrating a collection of instances for which a large class of facets has limited usefulness in reducing the branch-and-bound tree size.

Previous work showing lower bounds on the size of a branch-and-bound tree has been done by Jeroslow [28]; Chvátal [8]; Gu, Nemhauser, and Savelsbergh [26]; and Dash [12]. In most of these cases, the goal was to demonstrate particular instances in which branch-and-bound would perform badly, thereby proving complexity results about worst-case performance. More details on these results are given in Section 1.3.

We are more concerned with average-case performance, so Chvátal's analysis stands out. He gives a class of random instances for which an exponential number of branch-and-bound nodes are required with probability converging to 1 as the size of the instance increases.

Building on Chvátal's results, we consider the case in which simple lifted cover inequalities are added to his formulation.

7.1 Statement of the result

Following Chvátal [8], we consider knapsack instances of the following form:

$$\begin{array}{lrcll} \max & \sum_{i=1}^{n} a_i x_i & & & \\ s.t. & \sum_{i=1}^{n} a_i x_i & \leq & \lfloor \frac{\sum_{i=1}^{n} a_i}{2} \rfloor & \\ & x_i & \in & \{0,1\} \qquad & i = 1, \ldots, n, \end{array} \tag{19}$$

where the coefficients a_i are integers selected independently and uniformly such that $1 \leq a_i \leq 10^{n/2}$.

For ease of discussion, we denote the right-hand-side of the inequality by $r \equiv \lfloor \frac{\sum_{i=1}^{n} a_i}{2} \rfloor$ and the upper bound on coefficients by $B \equiv 10^{n/2}$.

Rather than a standard branch-and-bound framework, Chvátal considered a slight generalization, a class of algorithms that he called *recursive algorithms.* These have the capabilities of branching, fathoming, dominance, and improving the current solution. Branching, fathoming, and improving the current solution all match the description of branch-and-bound in Section 1.1. In particular, branching is performed on a single variable, though the selection of branching variable and the process of exploring nodes may be arbitrary. In terms of branch-and-bound, dominance allows the removal of a node if there is another node with the same set of fixed variables that has—considering only the fixed variables—at least as much slack in the constraint and at least as good an objective value. For a precise definition of this class of algorithms, see [8].

We will present our results using the language of branch-and-bound, though the results of this chapter do apply to Chvátal's class of recursive algorithms.

Theorem 7.1 (Chvátal) *With probability converging to 1 as $n \to \infty$, every recursive algorithm (as described in the previous paragraph) operating on an instance of (19) will create at least $2^{n/10}$ nodes in the process of solving.*

For a knapsack problem with constraint $\sum_{i=1}^{n} a_i x_i \leq b$, a *cover* is a set $C \subseteq \{1, \ldots, n\}$ such that $\sum_{i \in C} a_i > b$. A *minimal cover* is a cover C such that no subsets of C are covers. A minimal cover C defines the following *cover inequality*, which is a valid inequality for the knapsack problem:

$$\sum_{i \in C} x_i \leq |C| - 1.$$

Although cover inequalities are not facet-defining in general, they can be strengthened to form facet-defining inequalities through a process called *lifting.* We will consider a special case of a lifted cover inequality called a *simple lifted cover.* Given a cover C, a simple lifted

cover inequality has the form

$$\sum_{i \in C} x_i + \sum_{i \notin C} \alpha_i x_i \leq |C| - 1,$$

The values α_i are called *lifted coefficients* and are determined through a process called *sequential lifting.* See Gu et al.[25] or Wolsey [38] for discussions of lifted cover inequalities. Here we describe the process briefly for simple lifted cover inequalities.

Definition 7.2 *The sequential lifting process for simple cover inequalities is as follows. Let C be the cover. Let the indices not in C be ordered arbitrarily $i_1, i_2, \ldots, i_m$.*

1. *Initialize $K = \emptyset$, $a = 1$.*

2. *Let $j = i_a$.*

3. *Determine lifted coefficient α_j as follows:*

$$\alpha_j = |C| - 1 - \max \left\{ \sum_{i \in C} x_i + \sum_{k \in K} \alpha_k x_k : x \in S, x_j = 1 \right\}, \tag{20}$$

   where S is the set of feasible integer solutions to the original knapsack problem.

4. *Set $K = K \cup \{j\}$, and $a = a + 1$.*

5. *If $a \leq m$, return to Step 2.*

Note that $\alpha_j \leq |C| - 1$. Also note that by induction, (20) shows that α_j is integer for all j.

Gu et al. [26] considered the use of simple lifted cover inequalities on knapsack problems. They showed that branch-and-cut using simple lifted cover inequalities requires an exponential number of nodes for the following class of knapsack instances, parametrized by scalar n and vectors δ and ξ:

$$\begin{array}{lrcl} \max & \sum_{j=1}^{12n} (2\theta - \xi_j) x_j + \sum_{12n+1}^{20n} (3\theta - \xi_j) x_j & & \\ s.t. & \sum_{j=1}^{12n} (2 \cdot 2^n - \delta_j) x_j + \sum_{j=12n+1}^{20n} (3 \cdot 2^n - \delta_j) x_j & \leq & 6n \cdot 2^n \\ & x & \in & \{0,1\}^{20n}, \end{array} \tag{21}$$

where $n \geq 10$, $\theta = (60n \cdot 2^n)^{20n+1}$, $\delta_j \in \{1, \ldots, \lfloor 2^{n-1}/3n \rfloor\}$ for all $1 \leq j \leq 20n$, and $\xi_j \in \{1, \ldots, 2^n\}$ for all $1 \leq j \leq 20n$.

Like system (19), system (21) requires large coefficients. Note that (21) can be viewed as perturbations of the underlying instance given when $\delta_j = \xi_j = 0$ for all j.

In this chapter, we consider the same random instances as Chvátal but with the presence of simple lifted cover inequalities. We assume that all simple lifted cover inequalities are present, so our results represent the best possible performance of a branch-and-cut algorithm.

Recall from Section 1.4.3 that an event parametrized by n occurs *almost always* if the probability of the event converges to 1 as the value n goes to infinity. Note that the intersection of a finite number of events that occur almost always also occurs almost always.

The central result of this chapter is the following:

Theorem 7.3 *With probability converging to 1 as $n \to \infty$, every branch-and-bound algorithm that branches on variables operating on an instance of (19) with the addition of all simple lifted cover inequalities will create at least $2^{n/30}$ branch-and-bound nodes in the process of solving.*

Section 7.2 presents several properties that an instance of (19) possesses with probability converging to 1 as n increases. The fact that they occur with this probability is proven in Section 7.3. Section 7.4 proves that any instance possessing the properties will require an exponential number of branch-and-bound nodes, which leads to the proof of Theorem 7.3. A summary of the chapter appears in Section 7.5.

7.2 Properties of the random instances

For convenience in later discussion, let the knapsack coefficients be labeled so that $a_1 \leq a_2 \leq \cdots \leq a_n$. We denote the upper bound of the distribution of coefficients by $B \equiv 10^{n/2}$ and the right-hand-side of the knapsack inequality by $r \equiv \lfloor \frac{1}{2} \sum a_i \rfloor$.

Let $\delta > 0$ be a constant that will be chosen later. We consider instances that possess the following properties:

1. For every q such that $\frac{n}{100} \leq q \leq \frac{99n}{100}$, the qth largest coefficient, a_{n-q+1}, satisfies $a_{n-q+1} < \left(\frac{n-q}{n}B + 1\right)(1+\delta)$.

2. The right-hand-side of the knapsack constraint, $r \equiv \lfloor \frac{1}{2} \sum a_i \rfloor$, satisfies

$$\frac{n(B+1)}{4}(1-\delta) < r < \frac{n(B+1)}{4}(1+\delta).$$

3. All covers include at least 7 variables with coefficients larger than $\frac{3}{5}B$.

We will refer to these as Properties 1, 2, and 3, respectively.

7.3 *Instances almost always possess the properties*

In this section we show that Properties 1, 2, and 3 are satisfied by an instance of (19) with probability going to 1 as n increases without bound.

Lemma 7.4 *Property 1: Let $\delta > 0$ be an arbitrary constant. Almost always, for every q such that $\frac{n}{100} \leq q \leq \frac{99n}{100}$, the qth largest coefficient, a_{n-q+1}, satisfies $a_{n-q+1} < \left(\frac{n-q}{n}B + 1\right)(1+\delta)$.*

Proof: For each q such that $\frac{n}{100} \leq q \leq \frac{99n}{100}$, let m_q be the number of coefficients greater than $\left(\frac{n-q}{n}B + 1\right)(1+\delta)$. Then m_q is a binomial random variable, with expected value

$$\begin{aligned} E[m_q] &= n\frac{B - \left\lfloor \left(\frac{n-q}{n}B + 1\right)(1+\delta) \right\rfloor}{B} \\ &\leq n\frac{B - \frac{n-q}{n}B(1+\delta)}{B} \\ &= n(1 - \frac{n-q}{n}(1+\delta)) = q - \delta(n-q). \end{aligned}$$

Note that $E[m_q] = \Theta(n)$, since $\frac{n}{100} \leq q \leq \frac{99n}{100}$.

Using a Chernoff bound, we have that for constant δ',

$$m_q \geq (q - \delta(n-q))(1+\delta') = q - \delta(n-q) + \delta' q - \delta\delta'(n-q),$$

with probability at most

$$\left(\frac{e^{\delta'}}{(1+\delta')^{(1+\delta')}}\right)^{\mu}, \tag{22}$$

where $\mu = E[m_q] = \Theta(n)$.

By choosing $\delta' < \frac{\delta(n-q)}{q}$, (22) gives a bound on $P(m_q \geq q)$. The probability that there exists a coefficient that exceeds its bound is no more than the sum of the $\frac{98n}{100}$ probability bounds. Since it is a linear sum of exponentially small terms, this sum is also exponentially small, so the lemma is proven. ■

Lemma 7.5 *Property 2: For any constant $\delta > 0$, the right-hand-side of the knapsack constraint, $r \equiv \lfloor \frac{1}{2} \sum a_i \rfloor$, satisfies*

$$\frac{n(B+1)}{4}(1-\delta) < r < \frac{n(B+1)}{4}(1+\delta),$$

almost always.

Proof: The right-hand-side of the knapsack constraint, $\lfloor \frac{1}{2} \sum a_i \rfloor$, has expected value at least $\frac{1}{4}n(B+1) - 1$ and no more than $\frac{1}{4}n(B+1)$.

Given δ and sufficiently high n, we can choose $\delta' > 0$ such that $\left(\frac{1}{4}n(B+1) - 1\right)(1-\delta') > \frac{n(B+1)}{4}(1-\delta)$. Then, using a Hoeffding bound as described in Section 1.4.3, we have

$$\begin{aligned} P\left(r < \frac{n(B+1)}{4}(1-\delta)\right) &< P\left(r < (\frac{1}{4}n(B+1) - 1)(1-\delta')\right) \\ &\leq e^{-\frac{1}{2B}(\delta')^2 E[r]} \leq e^{-\frac{1}{2B}(\delta')^2(\frac{1}{4}n(B+1)-1)}. \end{aligned}$$

Similarly,

$$P\left(\frac{1}{2}\sum a_i > \frac{1}{4}n(B+1)(1+\delta)\right) \leq e^{-\frac{\delta^2 E[r]}{2B(1+\delta/3)}} \leq e^{-\frac{\delta^2(\frac{1}{4}n(B+1)-1)}{2B(1+\delta/3)}}$$

Together these two bounds prove the lemma. ■

The next lemma states that the sum of all the coefficients less than $\frac{3}{5}B$ is almost always not enough to form a cover. This is used in Lemma 7.7 to show that there are some large coefficients in any cover.

Lemma 7.6 *There exists constant $\delta_1 > 0$ such that for all $0 < \delta < \delta_1$, the following relation holds almost always:*

$$\sum_{\{i:a_i \leq \frac{3}{5}B\}} a_i < \frac{n(B+1)}{4}(1-\delta).$$

Proof: Note that B is evenly divisible by 5, and divide the range of coefficients into five "bins": $(0, \frac{1}{5}B], (\frac{1}{5}B, \frac{2}{5}B], (\frac{2}{5}B, \frac{3}{5}B], (\frac{3}{5}B, \frac{4}{5}B], (\frac{4}{5}B, B]$. Let b_i be the number of knapsack coefficients that fall into bin $(\frac{i-1}{5}B, \frac{i}{5}B]$, for $i = 1, \ldots, 5$. Then the sum of the coefficients in the first three bins is no more than $\frac{1}{5}Bb_1 + \frac{2}{5}Bb_2 + \frac{3}{5}Bb_3$.

Note that b_i is a binomial random variable with expected value $\frac{1}{5}n$. Using a Chernoff bound as described in Section 1.4.3, we have that for all $\delta > 0$,

$$P\left(b_i > \frac{n}{5}(1+\delta)\right) < \left(\frac{e^\delta}{(1+\delta)^{1+\delta}}\right)^{n/5}.$$

The right hand side is exponentially small in n if δ is constant.

We can sum the three probabilities for b_1, b_2, and b_3 to get an exponentially small probability that any of them is more than $\frac{n}{5}(1+\delta)$. So with probability converging to 1 as n increases, the sum of all coefficients less than 3/5 is no more than

$$\frac{1}{5}Bb_1 + \frac{2}{5}Bb_2 + \frac{3}{5}Bb_3 \leq \frac{6}{5}B \max_{i\in\{1,2,3\}} b_i \leq \frac{6}{5}\frac{nB}{5}(1+\delta) = \frac{6nB}{25}(1+\delta).$$

For any $\delta < \frac{1}{25}$, we have

$$\frac{n(B+1)}{4}(1-\delta) > \frac{n(B+1)}{4}(\frac{24}{25}) = \frac{6n(B+1)}{25} > \frac{6nB}{25}.$$

Therefore we can choose $0 < \delta < \frac{1}{25}$ such that

$$\frac{n(B+1)}{4}(1-\delta) > \frac{6nB}{25}(1+\delta).$$

Thus, we have proven the lemma with $\delta_1 = \frac{1}{25}$. ■

Lemma 7.6 has given the first requirement on δ, specifically that $\delta < \frac{1}{25}$.

Lemma 7.7 *Property 3: All covers have at least 7 coefficients greater than* 3/5, *almost always.*

Proof: Using Lemma 7.6, we see that there must be at least one coefficient greater than 3/5. In fact, by considering the proof of Lemma 7.6, we see that the gap between the two quantities is almost always

$$\frac{nB}{4}(1-\delta) - \frac{6nB}{25}(1+\delta) = \Omega(nB),$$

if $0 < \delta < \frac{1}{25}$ is constant.

Since coefficients are bounded by B, this proves that almost always $\Omega(n)$ coefficients greater than 3/5 are needed in order to form a cover. In particular, we almost always have at least 7 such coefficients. ■

Theorem 7.8 *Let $0 < \delta < \delta_1$ be constant, where δ_1 is a constant satisfying Lemma 7.5. Then with probability converging to 1 as $n \to \infty$, an instance of (19) has Properties 1, 2, and 3.*

Proof: By Lemmas 7.4, 7.5, and 7.6, each of the three properties holds almost always. The intersection of this finite number of events also holds almost always. ■

7.4 *Instances that satisfy the properties require exponential trees*

In this section, we show that instances possessing properties 1, 2, and 3 will require an exponential number of branch-and-bound nodes to solve. Together with Theorem 7.8, this will prove Theorem 7.3.

This section is split into three stages. Section 7.4.1 presents results on the lifted coefficients in any cover. Section 7.4.2 uses these results to prove a central lemma about the form of lifted cover inequalities. Section 7.4.3 uses the lemmas to prove Theorem 7.3.

7.4.1 Lifted coefficients are small

In this section we prove that lifted coefficients have value 0, 1, or 2, with at most a small number of coefficients with value 2. For the first lemma, recall from (19) that a_j is the knapsack coefficient of variable x_j, which corresponds to lifted coefficient α_j.

Lemma 7.9 *Consider the lifting process of Definition 7.2. In step 3 of the process, if the lifted coefficient is α_j, then the corresponding knapsack coefficient a_j must be at least as large as the optimal objective value of the following IP.*

C is the cover set, and K is as defined in Definition 7.2. There are binary variables x_i and y_i for each $i \in C \cup K$ and a single continuous variable Δ. We continue to use

$r \equiv \lfloor \frac{1}{2} \sum_{i=1}^{n} a_i \rfloor$.

$$
\begin{array}{rrcll}
\max & \sum_{i \in C \cup K} a_i y_i + \Delta & & & \\
s.t. & \sum_{i \in C} x_i + \sum_{k \in K} \alpha_k x_k & = & |C| - 1 & \\
 & \Delta & = & r - \sum_{i \in C \cup K} a_i x_i & \\
 & \Delta & \geq & 0 & \\
 & \sum_{i \in C} y_i + \sum_{k \in K} \alpha_k y_k & = & \alpha_j - 1 & \\
 & y_i & \leq & x_i & \forall i \in C \cup K \\
 & x_i, y_i & \in & \{0,1\} & \forall i \in C \cup K
\end{array}
\tag{23}
$$

Note that Δ is in fact constrained to be integer since all coefficients and variables are integer.

Proof: We will think of the binary variable vectors x and y as representing subsets of the original variables. For example, to represent the cover set C with x, we would set $x_i = 1$ for $i \in C$ and $x_i = 0$ otherwise.

First note that the IP is always feasible. To see this, let x represent the cover set C less any one element, so that the first equality of (23) is satisfied. Such a set x cannot violate the original knapsack constraint, so Δ as defined in the second equality must be nonnegative, satisfying the third constraint. Let y represent any subset of x of size $\alpha_j - 1$. Since $\alpha_j \leq |C| - 1$ by Definition 7.2, such subsets exist. This value for y satisfies the fourth and fifth constraints in (23), so the solution is feasible.

Assume the lemma is not true, so that a_j is smaller than the optimal objective value to (23). Let (x^*, y^*, Δ^*) be an optimal solution to (23) and let $z^* = x^* - y^*$. Note that $z^* \in \{0,1\}^n$, since $y_i^* = 1$ implies $x_i^* = 1$.

Define $\tilde{z}$ by $\tilde{z}_j = 1$, $\tilde{z}_i = z_i^*$ for all $i \in C \cup K$, and $\tilde{z}_i = 0$ otherwise.

Consider $\tilde{z}$ in light of the maximization in (20). We have

$$\sum_{i=1}^{n} a_i \tilde{z}_i = a_j + \sum_{i \in C \cup K} a_i z_i^* = a_j + \sum_{i \in C \cup K} a_i x_i^* - \sum_{i \in C \cup K} a_i y_i^* = a_j + r - \Delta^* - \sum_{i \in C \cup K} a_i y_i^*.$$

Since $a_j < \sum_{i \in C \cup K} a_i y_i^* + \Delta^*$ by assumption, this gives $\sum_{i=1}^{n} a_i \tilde{z}_i < r$. Therefore, $\tilde{z}$ satisfies the knapsack constraint and $\tilde{z} \in S$.

The value of the maximization in (20) is given by

$$\begin{aligned}\sum_{i\in C}\tilde{z}_i + \sum_{k\in K}\alpha_k\tilde{z}_k &= \sum_{i\in C}z_i^* + \sum_{k\in K}\alpha_k z_k^* = \sum_{i\in C}x_i^* + \sum_{k\in K}\alpha_k x_k^* - \sum_{i\in C}y_i^* - \sum_{k\in K}\alpha_k y_k^* \\ &= |C| - 1 - (\alpha_j - 1) = |C| - \alpha_j.\end{aligned}$$

This proves that $\alpha_j \leq |C| - 1 - (|C| - \alpha_j) = \alpha_j - 1$. This contradiction proves the lemma.

■

Lemma 7.10 *For instances that possess Property 3, all simple lifted cover inequalities will have $\alpha_i \leq 2$ for all i.*

Proof: Assume that $\alpha_j \geq 3$. Let x be defined by the original cover, and let y represent the set containing the two largest coefficients from the cover. Let these two coefficients be a_k and a_l. These values of x and y satisfy (23), so the objective value $a_k + a_l + \Delta$ gives a lower bound on the optimum. By Property 3 we know that a_k and a_l are greater than $\frac{3}{5}B$, so we conclude that $a_j > \frac{6}{5}B + \Delta > \frac{6}{5}B$. But this is impossible, so the lemma is proved by contradiction. ■

Lemma 7.11 *For instances that possess Property 3, the number of indices for which $\alpha_i = 2$ in any simple lifted cover inequality is no more than 3.*

Proof: Consider IP (23) of Lemma 7.9. We will consider lower bounds on the objective value. In this case the α_j value is 2, so y represents a set containing a single variable, either from the cover set or one with a lifted coefficient of 1.

Assume for a contradiction that there are at least four lifted coefficients with value 2 and that the first four are $\alpha_{i_1}, \alpha_{i_2}, \alpha_{i_3}$, and α_{i_4}.

For α_{i_1}, let $x^{(1)}$ be given by the variables in the cover C with the $|C| - 1$ largest coefficients a_i. Clearly this leads to a feasible solution $(x^{(1)}, y^{(1)}, \Delta^{(1)})$ to (23). Let the 7 largest coefficients in C be $k_1, k_2, \ldots, k_7$. These must exist by Property 3.

Consider α_{i_2}. We construct a feasible solution $x^{(2)}$ by "trading" indices k_1 and k_2 for i_1. Specifically, construct $x^{(2)}$ by setting $x_{i_1}^{(2)} = 1, x_{k_1}^{(2)} = 0, x_{k_2}^{(2)} = 0$, and $x_i^{(2)} = x_i^{(1)}$ for all other indices i. To see that $x^{(2)}$ satisfies the first equality in (23), note that we have

replaced two variables from the cover with $\alpha_{i_1} = 2$. Any choice of a single variable for y from $x^{(2)}$ other than i_1 leads to a feasible system. The value for Δ is given by

$$\Delta^{(2)} = r - \sum a_i x_i^{(2)} = r - \sum a_i x_i^{(1)} + a_{k_1} + a_{k_2} - a_{i_1} = \Delta^{(1)} + a_{k_1} + a_{k_2} - a_{i_1}.$$

By Property 3, the two coefficients a_{k_1} and a_{k_2} are each over $\frac{3}{5}B$ while a_{i_1} is most B, so $\Delta^{(2)} > \Delta^{(1)} + \frac{3}{5}B + \frac{3}{5}B - B = \Delta^{(1)} + \frac{1}{5}B$.

For α_{i_3}, we construct a solution $x^{(3)}$ by "trading" the next two largest coefficients, k_3 and k_4, for α_{i_2}. That is, let $x_{i_2}^{(3)} = 1, x_{k_3}^{(3)} = 0, x_{k_4}^{(3)} = 0$, and $x_i^{(3)} = x_i^{(2)}$ for all other i. This leads to a feasible solution as before, and by Property 3, $\Delta^{(3)} > \Delta^{(2)} + \frac{1}{5}B > \Delta^{(1)} + \frac{2}{5}B$.

Finally, for α_{i_4}, we construct $x^{(4)}$ by removing k_5 and k_6 and adding i_3. By Property 3, $\Delta^{(4)} > \Delta^{(1)} + \frac{3}{5}B$. In the objective of (23), y represents a single variable in the set represented by x. We can choose x_{k_7}, which is at least $\frac{3}{5}B$ by Property 3. Therefore we have shown that $a_{i_4} > \Delta^{(1)} + \frac{3}{5} + \frac{3}{5} > \frac{6}{5}$. This is impossible, which proves that we cannot have four lifted coefficients with value 2. ■

7.4.2 The ratio of cover size to sum of coefficients

In this section, we present the key lemma leading to the proof of Theorem 7.3.

Lemma 7.12 *There exists $\delta_2 > 0$ such that for every instance that satisfies Properties 1, 2, and 3 with $0 < \delta < \delta_2$, every simple lifted cover inequality satisfies $\frac{|C|-1}{|C|+\sum_{i \notin C} \alpha_i} > \frac{3}{5}$.*

Proof: Based on Property 2 and the upper bound of B on coefficients, we need at least $\frac{n}{4}(1-\delta) > \frac{n}{5}$ variables to form a cover. Consider a simple lifted cover constraint and let T be the set of variables with non-zero coefficients. Let $t = |T|$, so we know $\frac{n}{5} \leq t \leq n$.

For a given t, we wish to consider the minimum value of $\frac{|C|-1}{|C|+\sum \alpha_i}$. The denominator is between t and $t+3$, since at most 3 variables have $\alpha_i = 2$ and no values of α_i are higher. For the numerator, we would like to know how small the cover itself can be.

Since the lifted cover inequality is a valid inequality, it must be the case that no feasible solution to the knapsack problem has more than $|C| - 1$ variables from T, so any set $U \subset T, |U| \geq |C|$ must satisfy $\sum_{i \in U} a_i > r$. We get a lower bound on the size of $|C|$ by considering the variables in T with the smallest coefficients and determining the number of

them that it takes to exceed r. For fixed t, we want the lowest of these lower bounds. This occurs when T contains the variables with the t highest coefficients overall.

We will show that even in this case, at least 3/5 of the coefficients are needed in the cover. Assume that the coefficients are indexed so that $a_1 \leq a_2 \leq \cdots \leq a_n$. Then we are considering the coefficients $a_{n-t+1}, a_{n-t+2}, \ldots, a_{n-\lceil \frac{2}{5}t \rceil}$, and their sum,

$$X \equiv \sum_{i=n-t+1}^{n-\lceil \frac{2}{5}t \rceil} a_i = \sum_{q=t}^{\lceil \frac{2}{5}t \rceil - 1} a_{n-q-1}. \tag{24}$$

By Property 1, the qth largest coefficient is no more than $\left(\frac{n-q}{n}B + 1\right)(1+\delta)$, for $\frac{n}{100} \leq q \leq \frac{99n}{100}$. Let Y be the contribution to the sum from values of q outside this range. The contribution to Y from values of $q < \frac{n}{100}$ is at most $\frac{n}{100}B$, while the contribution from the values of $q > \frac{99n}{100}$ is at most $\frac{n}{100}\left(\frac{B}{100} + 1\right)(1+\delta)$. Thus,

$$Y < \frac{n}{100}B + \frac{n}{100}\left(\frac{B}{100} + 1\right)(1+\delta) < \frac{n}{100}\left(\frac{101B}{100} + 1\right)(1+\delta).$$

Using the bounds on a_{n-q-1}, we have

$$\begin{aligned}
X &\leq Y + \sum_{q=t}^{\lceil \frac{2}{5}t \rceil - 1} \left(\frac{n-q}{n}B + 1\right)(1+\delta) \\
&= Y + (1+\delta) \sum_{q=t}^{\lceil \frac{2}{5}t \rceil - 1} (B + 1 - \frac{q}{n}B) \\
&= Y + (1+\delta) \sum_{q=t}^{\lceil \frac{2}{5}t \rceil - 1} (B+1) - (1+\delta) \sum_{q=t}^{\lceil \frac{2}{5}t \rceil - 1} \frac{q}{n}B \\
&\leq Y + (1+\delta)\frac{3}{5}t(B+1) - (1+\delta)\frac{B}{n} \sum_{q=t}^{\lceil \frac{2}{5}t \rceil - 1} q \\
&\leq Y + (1+\delta)\frac{3}{5}t(B+1) - (1+\delta)\frac{B}{n}\frac{(\frac{7}{5}t)(\frac{3}{5}t)}{2} \\
&= Y + (1+\delta)\frac{3}{5}t\left(B + 1 - \frac{7Bt}{10n}\right)
\end{aligned}$$

By taking the derivative with respect to t, we find that this value is maximized when $t = \frac{5(B+1)}{7B}n$, at which point we have

$$X \leq Y + \frac{3}{14}n\frac{(B+1)^2}{B}(1+\delta) \leq \frac{n}{100}\left(\frac{101B}{100} + 1\right)(1+\delta) + \frac{3}{14}n\frac{(B+1)^2}{B}(1+\delta).$$

We need to show that $X < r$. By Property 2, that is equivalent to

$$\frac{n}{100}\left(\frac{101B}{100}+1\right)(1+\delta)+\frac{3}{14}n\frac{(B+1)^2}{B}(1+\delta) < \frac{n(B+1)}{4}(1-\delta). \tag{25}$$

Since $\frac{n}{100}\left(\frac{101B}{100}+1\right)+\frac{3}{14}n\frac{(B+1)^2}{B} < \frac{n(B+1)}{4}$, we can choose $\delta' > 0$ such that (25) holds for all $0 < \delta < \delta'$.

The one other requirement on δ is that it be less than δ_1 from Theorem 7.8. Therefore, we choose $\delta_2 < \min\{\delta', \delta_1\}$ and have proven the lemma. ■

Lemma 7.12 has given the final condition on the choice of δ for Properties 1, 2, and 3 from Section 7.2. Specifically, we choose $0 < \delta < \delta_2$ so that all the previous lemmas will hold.

7.4.3 Chvátal's class of problems requires an exponential tree even in the presence of simple lifted cover inequalities

We are now ready to prove Theorem 7.3. In part this is based on Chvátal's proof. The key additional idea comes from Lemma 7.12.

Proof of Theorem 7.3: We claim that if no more than $n/30$ variables are fixed by branching, then the LP solution of the resulting node cannot be fathomed.

Chvátal [8] proved that almost always the following properties hold:

4. $\sum_{i\in I} a_i \leq r$ whenever $|I| \leq n/10$.

5. There is no set $I \subset \{1, 2, \ldots, n\}$ such that $\sum_{i\in I} a_i = r$.

By Theorem 7.8, Properties 1, 2, and 3 also hold almost always.

By Property 4, fixing at most $n/30 < n/10$ variables leaves the LP relaxation feasible. We claim that the LP relaxation almost always has optimal objective value r. Then by Property 5, the node cannot be fathomed.

We claim that by setting all unfixed variables to $\frac{11}{20}$, the left-hand-side sum of the knapsack constraint will exceed r and no simple lifted cover constraints will be violated. Reducing the value of some of the unfixed variables will then give a feasible fractional solution with left-hand-side sum—and therefore objective value—of r exactly.

First we check that we can exceed r in the objective. Let F be the set of fixed variables, so we are interested in $\sum_{i \notin F} \frac{11}{20} a_i = \frac{11}{20} \sum_{i \notin F} a_i$. Since the maximum coefficient value is B, we have

$$\begin{aligned}
\sum_{i=1}^{n} a_i &\geq 2r \\
\sum_{i \notin F} a_i &\geq 2r - \sum_{i \in F} a_i \\
\sum_{i \notin F} a_i &\geq 2r - \frac{n}{30} B \\
\sum_{i \notin F} a_i &\geq 2r - \frac{n}{30}(B+1).
\end{aligned}$$

Using the lower bound for r from Property 2 gives that for any constant $\delta_1 > 0$, the following holds almost always:

$$\frac{11}{20} \sum_{i \notin F} a_i \geq \frac{11}{20} \left(\frac{n(B+1)}{2}(1-\delta_1) - \frac{n(B+1)}{30} \right) = \frac{n(B+1)}{4} \left(\frac{11}{10}(1-\delta_1) - \frac{11}{150} \right).$$

Choose $\delta_1 > 0$ and $\delta_2 > 0$ such that $\frac{11}{10}\delta_1 + \delta_2 < \frac{4}{150}$. Then $\delta_1 < \frac{10}{11} \cdot \frac{4}{150} - \frac{10}{11}\delta_2$, and

$$\begin{aligned}
\frac{11}{20} \sum_{i \notin F} a_i &\geq \frac{n(B+1)}{4} \left(\frac{11}{10}(1-\delta_1) - \frac{11}{150} \right) \\
&> \frac{n(B+1)}{4} \left(\frac{11}{10} - (\frac{4}{150} - \delta_2) - \frac{11}{150} \right) \\
&= \frac{n(B+1)}{4}(1-\delta_2) > r.
\end{aligned}$$

This shows that almost always, our fractional solution has objective value r.

Next we check that no simple lifted cover inequalities are violated. Let an inequality be specified by the sets C and K. From Lemma 7.11, we know that almost always at most 3 lifted coefficients have value 2. Then we need to verify that

$$\sum_{i \in C} x_i + \sum_{i \in K} \alpha_i x_i \leq |C| - 1. \tag{26}$$

A worst-case assumption is that all fixed variables are fixed to 1 and that all of them appear in an inequality, so we have

$$\sum_{i \in C} x_i + \sum_{i \in K} \alpha_i x_i \leq \sum_{i \in C \cup K} x_i + 3 \leq \frac{n}{30} + 3 + (|C| + |K| - \frac{n}{30})\frac{11}{20}.$$

Lemma 7.12 showed that $\frac{|C|-1}{|C|+\sum_{k\in K}\alpha_k} > 3/5$ almost always for all simple lifted cover inequalities, from which we will use $|K| < \frac{2|C|}{3} - \frac{5}{3}$. Using this in the previous equation, we wish to confirm

$$\begin{aligned} \frac{n}{30} + 3 + (\frac{5}{3}|C| - \frac{5}{3} - \frac{n}{30})\frac{11}{20} &\leq |C| - 1 \\ \frac{n}{30} \cdot \frac{9}{20} + 4 - \frac{11}{12} &\leq \frac{|C|}{12}. \end{aligned}$$

Finally, we use the fact that $|C| > \frac{n}{4}(1-\delta) > \frac{n}{5}$, almost always. This gives

$$\begin{aligned} \frac{n}{30} \cdot \frac{9}{20} + 4 - \frac{11}{12} &\leq \frac{n}{60} \\ 4 - \frac{11}{12} &\leq \frac{n}{600}. \end{aligned}$$

This verifies that the original inequality (26) holds almost always. Therefore, almost always there are no violated inequalities.

Note that the conclusion applies to all simple lifted cover inequalities simultaneously. That is, we relied on Lemma 7.12, which applies to every simple lifted cover inequality.

We have shown that with at most $n/30$ variables fixed, the LP relaxation has optimal objective value r. Therefore, no such node can be fathomed. Since we are branching on variables, there are at least $2^{n/30}$ such nodes in the branch-and-bound tree, almost always.

■

The main idea of the proof is that as long as not too many variables are fixed, the simple lifted cover inequalities do not prevent us from having all fractional variables set to values strictly greater than 1/2.

7.5 Summary

We have shown that for a particular family of random knapsack instances, even the presence of every simple lifted cover inequality will not prevent the branch-and-bound tree from almost always having an exponential number of nodes.

It is not surprising that there are some knapsack instances for which the branch-and-bound tree has exponential size, since the knapsack problem is NP-hard. The fact that almost every random instance as considered in this chapter requires an exponential number of nodes even with a large number of cuts present is more significant.

It is possible that the result is specific to the type of instance being considered and that branch-and-cut algorithms will perform better on other knapsack instances and other problems. The fact that almost always no integer solution satisfies the knapsack constraint at equality is one indication that these instances are special.

If this result is indicative of general branch-and-cut performance, however, than it suggests that while cutting planes may help reduce the number of nodes, the number is still exponential most of the time. Whether similar results apply to other instances and problems is an important open question.

CHAPTER VIII

CONTRIBUTIONS AND FUTURE RESEARCH

This chapter summarizes the results and contributions of the dissertation, discusses conclusions about measure performance overall, and presents future research possibilities.

8.1 Summary of contributions

In Chapter 2, we presented several measures of facets or cutting planes and discussed some inherent similarities and differences among them.

We presented polar properties of the shooting experiment in Chapter 3. In particular, we showed that the shooting experiment on a polyhedron is equivalent to optimization on its polar polyhedron. A consequence is that optimizing over a polyhedron and performing the shooting experiment are polynomial-time equivalent, as long as a shooting point in the polyhedron is known. These results were extended to blockers of blocking polyhedra and anti-blockers of anti-blocking polyhedra as well.

Chapter 4 considered master cyclic group polyhedra and master knapsack polytopes. We developed a deterministic partial order on the shooting experiment sizes to complement previous research on performing the shooting experiment. We also developed Monte Carlo methods for estimating facet volume for both types of polyhedra and a linear program to determine whether the Chvátal-Gomory rank is 1 or higher for knapsack polyhedra. We discussed an empirical measure of the usefulness of cutting planes: the minimum size of the branch-and-bound tree when branching on variables with a specified branching rule.

We computed or estimated each measure for 9 master knapsack polyhedra and 19 master cyclic group polyhedra. For master knapsack polytopes, we found that best-case improvement and the shooting experiment provided the best correlation with our measure of branch-and-bound tree size, with neither measure clearly superior. A low Chvátal-Gomory rank was positively but less strongly correlated with better branch-and-bound performance.

Other notable relationships were strong correlations between volume and shooting experiment size and between low Chvátal-Gomory rank and a high number of tight inequalities in the facet formulation. For master cyclic group polyhedra, we found that all four measures considered were well correlated. In particular, the straightforward computations of the number of tight inequalities and best-case improvement were relatively well correlated with the more expensive estimates of shooting experiment size and facet volume.

In Chapter 5, we considered matching polyhedra for complete graphs. We focused on the odd-set constraints, which provide all the non-trivial facets. An analysis of the shooting experiment to compare two sizes of odd-set constraints showed that as a group, larger-odd-set constraints will almost always be hit by the shooting experiment rather than smaller-odd-set constraints. In contrast, the best-case improvement strength of a facet corresponding to an odd set of size k is $\frac{k}{k-1}$, suggesting that smaller-odd-set constraints are better than larger-odd-set constraints. Chvátal-Gomory rank does not distinguish among the sizes: all odd-set constraints have a Chvátal-Gomory rank of 1. We performed computational tests to check these contradictory predictions and found that with a constant number of random constraints of a given size present, smaller-odd-set constraints reduced the branch-and-bound tree size more than larger-odd-set constraints. When all constraints of a given size were present, however, larger-odd-set constraints reduced the branch-and-bound tree size more. Thus, both the best-case improvement and shooting experiment predictions were correct in the appropriate context. This demonstrates the importance of differentiating between isolated facets and large sets of facets.

We considered node-packing polytopes in Chapter 6 in light of an empirical study by Nemhauser and Sigismondi, which tested clique inequalities and odd-hole inequalities. We determined that on the clique-and-hole relaxation of node-packing, clique inequalities are almost always hit by the shooting experiment. We showed that the best-case improvement ratio of the constraint defined by a clique C is $\frac{|C|}{2}$, while the best-case improvement ratio of an odd-hole constraint based on an odd hole H is $\frac{|H|-1}{|H|}$. Thus, both measures predict that clique inequalities are significantly stronger than odd-hole inequalities, in agreement with the results of Nemhauser and Sigismondi.

In Chapter 7 we considered the limits of facet usefulness. We extended a result of Chvátal by demonstrating that the class of random knapsack instances he studied will almost always require an exponential number of branch-and-bound nodes even when all simple lifted cover inequalities are added to the relaxation.

Perhaps the most significant contribution of this dissertation is the evidence we found supporting the use of the shooting experiment and best-case improvement ratio. These measures were generally tractable to analyze and the results were generally well correlated with the size of the branch-and-bound trees in our empirical tests. This adds more credibility to the study and use of these two measures to examine cutting planes.

8.2 Conclusions

Among the measures considered, the shooting experiment and best-case improvement offer the best correlation with usefulness across the four problems studied. In most cases, analyses of both of these measures were tractable. Both measures provided results that agreed with the empirical tests of knapsack problems in Chapter 4 and node-packing problems in Chapter 6.

For the matching problem, however, the two measures disagreed. The computational results of that chapter offer a possible explanation: it is necessary to treat isolated facets and large sets of facets differently. Since best-case improvement is based on consideration of individual facets, we should be cautious when trying to apply best-case improvement to relaxations with many facets present. For the shooting experiment, our analyses have tended to consider large groups of facets, and the results of the analysis seem to apply best to that case. Therefore, a possible area of future work is to analyze the shooting experiment in a way that better considers individual facets. Note that performing the shooting experiment does exactly that.

Chvátal-Gomory rank presented conflicting predictions. For the knapsack problems, a low Chvátal-Gomory rank was weakly correlated with good empirical performance. This supports the intuition that low-rank facets provide most of the benefit of cuts. For node packing, on the other hand, high Chvátal-Gomory rank was a good predictor of usefulness.

This supports the idea that as the rank increases, the value of the cuts becomes greater and greater. On matching, Chvátal-Gomory rank did not distinguish among the facets. Taken together, these results suggest that Chvátal-Gomory rank is not a reliable predictor of facet usefulness in general. Perhaps it can be effectively considered for specific problem classes, but it is not consistent across problems.

8.3 Possible future research

8.3.1 Specific questions

In performing empirical tests on matching polytopes in Chapter 5, we considered the polytope with all odd-set constraints of a given size present and with 100 randomly chosen constraints present. It may be that different results are obtained if a fixed number of *violated* constraints of a given size are added. This could be tested by adding cuts through a call-back routine, though the complexity results of Section 5.5 suggest that the constraints may have to be separated through enumeration or another inefficient manner. Nevertheless, the results may aid in better understanding the conflicting predictions of shooting and best-case improvement.

In Chapter 6, our analysis of lifted odd-hole inequalities suggested that they are considerably stronger than unlifted odd-holes. An empirical comparison of the two groups' usefulness could confirm or disprove this hypothesis. In particular, it might help indicate whether it is worthwhile to try to find violated lifted odd-hole constraints for which the underlying odd-hole constraints are not violated. This was a possibility that Nemhauser and Sigismondi mentioned but did not test.

The result of Chapter 7 on exponential branch-and-bound trees brings up an important question: Is the result telling us something about inherent limits in branch-and-cut algorithms, or about the difficulty of the particular instances considered? Trying to extend this analysis to knapsack problems with a much lower right-hand-side would be a first step towards answering this question.

An incidental problem that arose was computation of Chvátal-Gomory ranks for facets of the master knapsack polyhedra. Our computational approach could only distinguish

between rank 1 and higher ranks. Theoretically, it should be possible to distinguish rank 2 facets as well, though this proved to be a challenge computationally. Overcoming these obstacles and extending this approach further would provide a tool for consideration of facets on other problems.

8.3.2 Theoretical relationships between measures

Chapter 3 presented a polar relationship between the shooting experiment and the probability of integrality. This suggests a way that theoretical results on one of the measures can be translated to theoretical results on the other. Since the polar changes as cuts are added to a polyhedron, however, the exact nature of this relationship is unclear.

Another pair of measures that merits additional theoretical consideration is the Chvátal-Gomory rank of knapsack facets and the number of tight inequalities in the formulation for knapsack facets from Chapter 4. The empirical tests showed a strong correlation between low Chvátal-Gomory rank and high number of tight inequalities. It may be that there is a theoretical explanation for this correlation.

8.3.3 General extensions

The problems considered in this dissertation are classical IP problems. Although they can play important roles in real-world formulations, it is almost never in the pure form analyzed here. One important question is whether the best-case improvement and shooting experiment predictions carry over to more complicated IPs used in real-world applications. A next step in that direction might be consideration of problems such as capacitated facility location, which has aspects of the problems studied in this dissertation but is more widely used in practice.

Investigation of other facet measures also seems warranted. In particular, none of the measures considered in this dissertation take a known objective vector into account, even though this information is known to branch-and-cut algorithms. For that reason, none of these measures are strong candidates for use in actual computation, especially for general IPs. An example of a measure that does take the objective vector into account is the angle between the objective and the hyperplane defined by the facet. An attempt at analyzing

this or a related measure would provide another step toward improving the performance of branch-and-cut in practice.

APPENDIX A

TESTS OF STATISTICAL SIGNIFICANCE FOR MEASURES USED ON KNAPSACK AND CYCLIC GROUP POLYHEDRA

This appendix presents the methodology used to test for statistical significance of pairwise differences in three measures used in Chapter 4: the shooting experiment, volume estimate, and empirical tests of branch-and-bound tree sizes.

A.1 Shooting experiment

We are considering the shooting experiment sizes of two facets, A and B. Recall that shooting experiment sizes are probabilities, and let p_A and p_B represent the true shooting experiment sizes of the facets.

Performing N trials of the shooting experiment gives random variables X_A and X_B such that $E[X_A/N] = p_A$ and $E[X_B/N] = p_B$. Together X_A and X_B come from a multinomial distribution. Given X_A, X_B, and N, we wish to consider the null hypothesis that $p_A = p_B$ with alternative hypothesis $p_A \neq p_B$. Since we calculate X_A and X_B in the same set of trials, the values are dependent, and we cannot use a traditional t-test for this hypothesis.

Instead, we consider the random variable $Z = \frac{X_A - X_B}{N}$, which has expected value $\mu_Z = (p_A - p_B)$. The null hypothesis is now $\mu_Z = 0$.

Since X_A and X_B come from a multinomial distribution, their covariance is $-Np_Ap_B$. Therefore, we have

$$\mathrm{Var}(Z) = \frac{p_A(1-p_A) + p_B(1-p_B) + 2p_Ap_B}{N}.$$

Approximating $p_A \approx \frac{X_A}{N}, p_B \approx \frac{X_B}{N}$ gives an estimated variance, which we denote $\widehat{\mathrm{Var}}(Z)$. Since we have a large sample, we use the central-limit theorem and form an approximate

95%-confidence interval of

$$\left(\frac{X_A - X_B}{N} - 1.96\sqrt{\widehat{\mathrm{Var}Z}}, \frac{X_A - X_B}{N} + 1.96\sqrt{\widehat{\mathrm{Var}Z}}\right).$$

We reject the null hypothesis at the 0.05 level if this interval does not contain 0.

These tests were performed with code written by the author in Perl.

A.2 Volume estimates

Volume estimates were obtained using a Monte Carlo estimation. The underlying random variable is therefore a binomial random variable, which is scaled based on the number of trials, the volume of the sample set, and the facet being tested.

Let X_A and X_B be the binomial random variables for two facets. If there are N trials, then the volume estimates are aX_A/N and bX_B/N for some constants a and b.

To test whether the difference is significant, we consider the random variable defined by $Z = \frac{aX_A - bX_B}{N}$. If p_A and p_B are the true parameters of X_A and X_B, then

$$E[Z] = \frac{aE[X_A] - bE[X_B]}{N} = ap_A - bp_B \tag{27}$$

$$Var(Z) = (\frac{a}{N})^2 Var(X_A) + (\frac{b}{N})^2 Var(X_B) - 2\frac{ab}{N^2} Cov(X_A, X_B) \tag{28}$$

A.2.1 Cyclic group tests

The cyclic group tests were performed independently, so the covariance is zero, and

$$Var(X_A) = Np_A(1 - p_A), \quad Var(X_B) = Np_B(1 - p_B).$$

Then $Var(Z) = \frac{a^2}{N} p_A(1 - p_A) + \frac{b^2}{N} p_B(1 - p_B)$.

Since we have a large sample, we approximate the variance by substituting our sample proportions X_A/N and X_B/N for p_A and p_B. Then, using the central-limit theorem, we compute an approximate 95% confidence interval for $E[Z]$. If this interval does not contain 0, then we reject the null hypothesis that $ap_A = bp_B$.

A.2.2 Knapsack tests

The knapsack tests were not done independently. A given Monte Carlo trial could only register a valid point for at most one facet. Therefore, the values X_A and X_B come from a

multinomial distribution, and their covariance is given by $Cov(X_A, X_B) = -Np_Ap_B$. Using this in (28) gives $Var(Z) = \frac{a^2}{N}p_A(1-p_A) + \frac{b^2}{N}p_B(1-p_B) + \frac{2ab}{N}p_Ap_B$.

Again, since we have a large sample, we approximate the variance by substituting our sample proportions X_A/N and X_B/N for p_A and p_B. Then, using the central-limit theorem, we compute an approximate 95% confidence interval for $E[Z]$. If this interval does not contain 0, then we reject the null hypothesis that $ap_A = bp_B$.

These tests were performed using code written by the author in Perl.

A.3 Branch-and-bound tree sizes

Let X_{ii} be a random variable corresponding to the minimum size of a branch-and-bound tree when only facet i is added to the relaxation. Similarly, let X_{ij} be random variables corresponding to the minimum size of the tree when facets i and j are added. If there are m facets total, let $X_j = \frac{1}{m}\sum_{i=1}^{m} x_{ji})$. Then X_j is the random variable we estimated.

One trial to estimate X_j is done by performing one test each of X_{ji} for $i = 1, \ldots, m$. We performed 1000 such trials for each facet and averaged the result to get our sample mean for X_j. To determine whether two facet means are different, we performed a paired t-test on the 1000 trials for each facet, and tested at the 0.05 level. The values X_j and X_k are not independent, since both depend on X_{jk}, but the paired t-test does not require independence.

The t-tests were done using the software R or S-plus.

APPENDIX B

MEASUREMENTS OF CYCLIC GROUP AND KNAPSACK POLYHEDRA

This section presents data from the tests of Chapter 4. All tests were performed by the author with the exceptions of the shooting experiment for cyclic group polyhedra and shooting from the origin for knapsack polyhedra. These shooting results were supplied by Lisa Evans.

B.1 Knapsack polytopes

Master packing knapsack polytopes of dimensions $n = 6$ through $n = 14$ were tested. For each polytope, there is a table containing the measure results and a diagram of the partial order In the partial order, numbers represent facets in the order they appear in the table of measures. If a number is not present, that facet is not comparable to any other in the partial order.

Table 40: Measures for the packing knapsack polytope with $n = 6$

Facet	Best-case Imp.	Tight Ineq	C-G Rank	Volume	Shooting Origin	Shooting Interior	BBT Size
0 0 1 2 2 2	1.500	5	1	2.722e-02	446	748	1.101
0 2 3 4 6 6	1.200	4	2+	2.977e-02	240	289	1.237
1 2 3 4 5 6	1	9	0	2.523e-01	314	1972	n/a

Figure 11: Partial order for the packing knapsack polytope with $n = 6$

Table 41: Measures for the packing knapsack polytope with $n = 7$

Facet	Best-case Imp.	Tight Ineq	C-G Rank	Volume	Shooting Origin	Shooting Interior	BBT Size
0 0 0 1 1 1 1	1.750	8	1	7.537e-03	384	576	2.300
0 0 1 1 2 2 2	1.400	7	1	5.993e-03	218	401	2.168
0 1 1 2 2 3 3	1.167	8	1	1.185e-02	112	167	1.910
0 1 2 2 3 4 4	1.167	7	1	6.387e-03	108	141	2.285
1 2 3 4 5 6 7	1	12	0	8.045e-02	178	1568	n/a

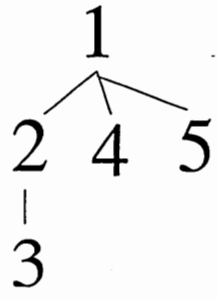

Figure 12: Partial order for the packing knapsack polytope with $n = 7$

Table 42: Measures for the packing knapsack polytope with $n = 8$

Facet	Best-case Imp.	Tight Ineq	C-G Rank	Volume	Shooting Origin	Shooting Interior	BBT Size
0 0 0 1 2 2 2 2	1.600	9	2+	2.136e-03	387	490	1.613
0 0 1 1 1 2 2 2	1.333	11	1	3.295e-03	268	319	1.464
0 1 1 2 3 3 4 4	1.200	9	1	1.739e-03	88	217	1.894
0 2 3 4 5 6 8 8	1.143	8	2+	1.699e-03	70	157	2.117
1 2 3 4 5 6 7 8	1	16	0	3.190e-02	187	1635	n/a

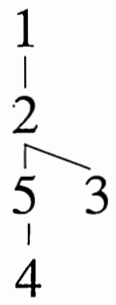

Figure 13: Partial order for the packing knapsack polytope with $n = 8$

Table 43: Measures for the packing knapsack polytope with $n = 9$

Facet	Best-case Imp.	Tight Ineq	C-G Rank	Volume	Shooting Origin	Shooting Interior	BBT Size
0 0 0 0 1 1 1 1 1	1.800	14	1	5.671e-04	313	437	2.856
0 0 0 1 1 2 2 2 2	1.500	11	2+	2.977e-04	181	289	2.652
0 0 1 1 2 2 3 3 3	1.286	10	1	1.494e-04	60	67	3.141
0 0 2 3 3 4 6 6 6	1.286	9	2+	3.024e-04	119	190	2.898
0 1 1 2 2 3 3 4 4	1.125	14	1	1.080e-03	104	377	2.104
0 1 2 2 4 4 5 6 6	1.200	10	2+	1.531e-04	28	58	3.368
0 1 2 3 3 4 5 6 6	1.125	10	1	1.535e-04	30	86	3.159
0 2 3 4 5 6 7 9 9	1.125	10	2+	2.262e-04	32	70	3.607
1 2 3 4 5 6 7 8 9	1	20	0	9.279e-03	133	1104	n/a

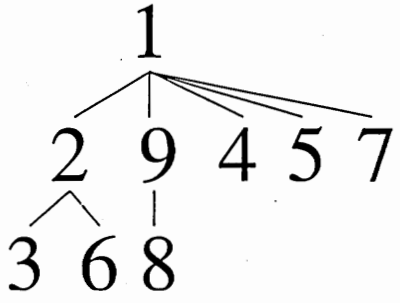

Figure 14: Partial order for the packing knapsack polytope with $n = 9$

Table 44: Measures for the packing knapsack polytope with $n = 10$

Facet	Best-case Imp.	Tight Ineq	C-G Rank	Volume	Shooting Origin	Shooting Interior	BBT Size
0 0 0 0 1 2 2 2 2 2	1.667	15	2+	1.223e-04	307	475	2.542
0 0 0 1 1 1 2 2 2 2	1.429	15	1	9.551e-05	194	298	2.530
0 0 1 2 2 2 3 4 4 4	1.250	14	2+	8.674e-05	109	118	2.819
0 0 2 2 3 4 4 6 6 6	1.250	12	2+	7.044e-05	98	96	2.643
0 1 2 2 3 4 4 5 6 6	1.111	15	1	1.188e-04	46	113	2.623
0 2 2 4 5 6 8 8 10 10	1.143	12	2+	8.217e-05	33	83	3.021
0 2 3 4 5 6 7 8 10 10	1.111	14	2+	1.100e-04	62	113	3.429
1 2 3 4 5 6 7 8 9 10	1	25	0	2.805e-03	151	1165	n/a

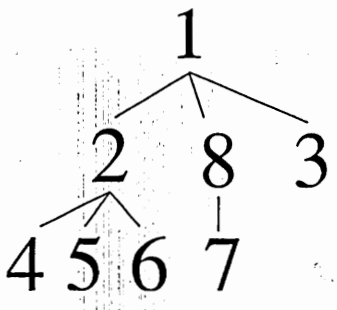

Figure 15: Partial order for the packing knapsack polytope with $n = 10$

Table 45: Measures for the packing knapsack polytope with $n = 11$

Facet	Best Case	Tight Ineq	C-G Rank	Volume	Shooting Orig.	Shooting Int.	BBT Size
0 0 0 0 0 1 1 1 1 1 1	1.833	21	1	2.625e-05	302	403	4.401
0 0 0 0 1 1 2 2 2 2 2	1.571	17	2+	1.330e-05	166	167	4.647
0 0 0 1 1 1 1 2 2 2 2	1.375	20	1	3.106e-05	188	245	3.908
0 0 1 1 1 2 2 2 3 3 3	1.222	20	1	3.180e-05	98	168	4.223
0 0 1 1 2 2 3 3 4 4 4	1.222	14	1	2.395e-06	20	26	4.775
0 0 2 3 4 4 5 6 8 8 8	1.222	13	2+	4.044e-06	28	42	4.986
0 1 1 2 2 3 3 4 4 5 5	1.100	21	1	4.898e-05	50	121	3.776
0 1 1 2 3 3 4 5 5 6 6	1.146	15	1	4.448e-06	10	14	5.004
0 1 2 2 3 4 5 5 6 7 7	1.122	15	1	3.605e-06	7	21	5.510
0 1 2 2 4 4 6 6 7 8 8	1.179	14	2+	3.035e-06	19	17	5.039
0 1 2 3 4 4 5 6 7 8 8	1.100	14	1	2.094e-06	6	12	5.256
0 2 3 4 5 6 7 8 9 11 11	1.100	17	2+	1.459e-05	19	53	5.667
0 2 3 4 6 6 8 9 10 12 12	1.100	14	2+	6.130e-06	17	24	5.085
1 2 3 4 5 6 7 8 9 10 11	1	30	0	6.422e-04	70	1064	n/a

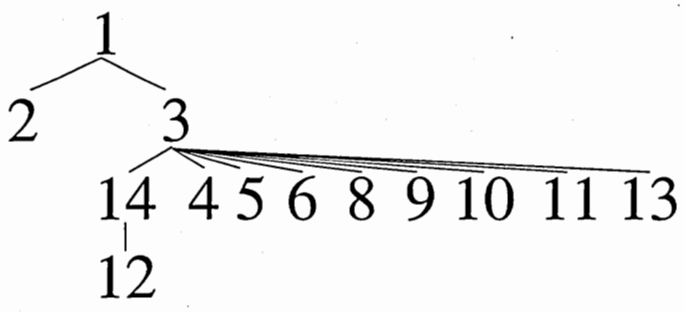

Figure 16: Partial order for the packing knapsack polytope with $n = 11$

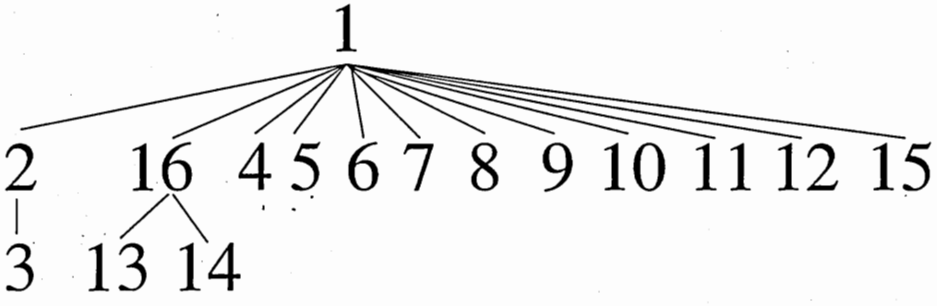

Figure 17: Partial order for the packing knapsack polytope with $n = 12$

Table 46: Measures for the packing knapsack polytope with $n = 12$

Facet	Best Case	Tight Ineq	C-G Rank	Volume	Shooting Orig.	Shooting Int.	BBT Size
0 0 0 0 0 1 2 2 2 2 2 2	1.714	22	2+	4.799e-06	295	388	2.361
0 0 0 0 1 1 1 2 2 2 2 2	1.500	21	2+	3.067e-06	178	138	2.251
0 0 0 2 2 3 4 4 6 6 6 6	1.333	15	2+	8.257e-07	56	37	2.744
0 0 0 2 3 3 3 4 6 6 6 6	1.333	17	2+	2.482e-06	101	107	2.511
0 0 1 1 1 2 3 3 3 4 4 4	1.286	19	2+	1.710e-06	45	43	2.945
0 0 1 1 2 2 2 3 3 4 4 4	1.200	21	1	3.151e-06	56	75	2.858
0 0 1 2 3 3 3 4 5 6 6 6	1.200	17	2+	1.081e-06	28	17	2.867
0 0 3 4 4 6 8 8 9 12 12 12	1.200	14	2+	1.036e-06	21	24	3.184
0 0 3 4 5 6 7 8 9 12 12 12	1.200	14	2+	8.514e-07	19	20	3.417
0 1 1 2 2 3 4 4 5 5 6 6	1.143	21	1	3.661e-06	27	85	3.137
0 1 2 2 3 4 5 6 6 7 8 8	1.125	16	2+	3.550e-07	6	13	3.496
0 1 3 4 4 6 8 8 9 11 12 12	1.143	15	2+	5.366e-07	9	13	3.291
0 2 2 4 5 6 7 8 10 10 12 12	1.111	17	2+	2.154e-06	10	41	3.340
0 2 3 4 5 6 7 8 9 10 12 12	1.091	22	2+	7.035e-06	47	109	3.621
0 2 4 4 7 8 9 12 12 14 16 16	1.125	15	2+	6.989e-07	9	16	3.574
1 2 3 4 5 6 7 8 9 10 11 12	1	36	0	1.683e-04	93	1124	n/a

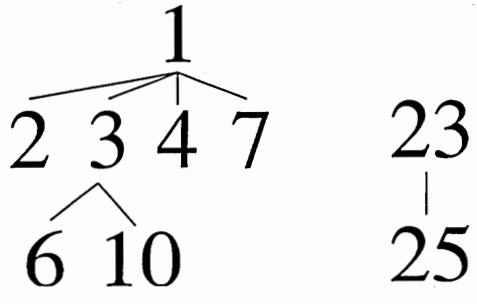

Figure 18: Partial order for the packing knapsack polytope with $n = 13$

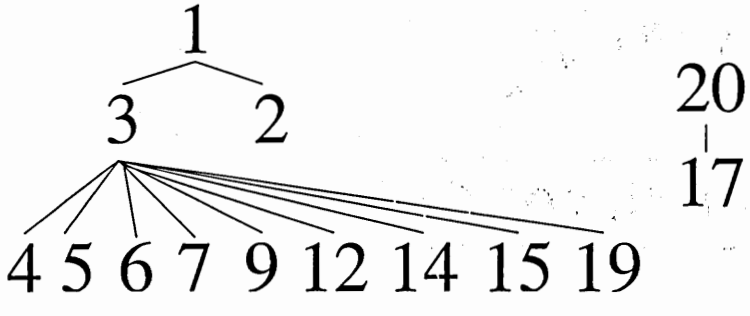

Figure 19: Partial order for the packing knapsack polytope with $n = 14$

Table 47: Measures for the packing knapsack polytope with $n = 13$

Facet	Best Case	Tight Ineq	C-G Rank	Volume	Shooting Orig.	Shooting Int.	BBT Size
0 0 0 0 0 0 1 1 1 1 1 1 1	1.857	30	1	1.012e-06	293	507	6.000
0 0 0 0 0 1 1 2 2 2 2 2 2	1.625	24	2+	4.238e-07	124	200	5.793
0 0 0 0 1 1 1 1 2 2 2 2 2	1.444	26	1	5.882e-07	144	113	5.597
0 0 0 1 1 1 2 2 2 3 3 3 3	1.300	22	1	1.885e-07	35	95	6.243
0 0 0 1 2 2 2 2 3 4 4 4 4	1.300	23	2+	4.414e-07	69	95	5.981
0 0 0 2 2 3 3 4 4 6 6 6 6	1.300	18	2+	1.865e-07	34	120	6.019
0 0 1 1 1 2 2 3 3 3 4 4 4	1.219	24	1	4.191e-07	38	69	5.478
0 0 1 1 2 2 3 3 4 4 5 5 5	1.182	18	1	1.748e-08	6	21	7.359
0 0 1 2 2 2 4 4 4 5 6 6 6	1.238	21	2+	1.750e-07	18	5	6.467
0 0 1 2 2 3 3 4 4 5 6 6 6	1.182	18	2+	5.584e-08	9	12	6.228
0 0 2 2 3 4 4 5 6 6 8 8 8	1.182	20	2+	2.483e-07	18	22	6.046
0 0 2 3 3 4 5 6 6 7 9 9 9	1.182	18	2+	1.504e-07	13	1	6.765
0 0 2 3 4 4 6 6 7 8 10 10 10	1.182	17	2+	3.705e-08	5	9	7.610
0 0 2 3 4 5 5 6 7 8 10 10 10	1.182	17	2+	3.845e-08	3	46	7.216
0 0 3 4 5 6 7 8 9 10 13 13 13	1.182	17	2+	7.047e-08	4	20	7.561
0 1 1 2 2 3 3 4 4 5 5 6 6	1.083	30	1	2.302e-06	47	370	4.913
0 1 1 2 3 3 4 4 5 6 6 7 7	1.114	24	1	3.706e-07	22	40	7.017
0 1 2 2 3 4 4 5 6 6 7 8 8	1.083	26	1	7.559e-07	15	81	5.887
0 1 2 2 4 4 6 6 8 8 9 10 10	1.156	18	2+	2.578e-08	5	9	7.212
0 1 2 3 3 4 5 6 6 7 8 9 9	1.083	22	1	1.713e-07	5	39	6.866
0 1 2 3 4 4 6 6 7 8 9 10 10	1.114	18	2+	1.840e-08	2	1	7.585
0 1 2 3 4 5 5 6 7 8 9 10 10	1.083	18	1	1.978e-08	1	38	7.177
0 2 3 4 5 6 7 8 9 10 11 13 13	1.083	26	2+	7.174e-07	18	4	7.807
0 2 3 4 6 6 9 9 11 12 13 15 15	1.114	18	2+	4.497e-08	2	4	7.567
1 2 3 4 5 6 7 8 9 10 11 12 13	1	42	0	3.281e-05	70	423	n/a

Table 48: Measures for the packing knapsack polytope with $n = 14$

Facet	Best Case	Tight Ineq	CG Rk	Volume	Shooting Ori.	Shooting Int.	BBT Size
0 0 0 0 0 0 1 2 2 2 2 2 2 2	1.750	31	2+	1.552e-07	258	477	4.245
0 0 0 0 0 1 1 1 2 2 2 2 2 2	1.556	28	2+	7.516e-08	152	114	4.116
0 0 0 0 1 1 1 1 1 2 2 2 2 2	1.400	33	1	1.824e-07	177	260	3.781
0 0 0 1 1 2 2 2 3 3 4 4 4 4	1.273	22	2+	1.078e-08	25	161	4.738
0 0 0 2 2 2 3 4 4 4 6 6 6 6	1.273	25	2+	6.522e-08	65	23	4.326
0 0 0 2 3 4 4 4 5 6 8 8 8 8	1.273	21	2+	2.047e-08	26	49	4.922
0 0 1 1 1 2 2 2 3 3 3 4 4 4	1.167	33	1	2.326e-07	74	143	4.134
0 0 1 2 2 2 3 4 4 4 5 6 6 6	1.167	27	2+	9.025e-08	37	27	4.619
0 0 1 2 3 4 4 4 5 6 7 8 8 8	1.167	21	2+	1.090e-08	4	43	5.309
0 0 2 2 4 4 5 6 6 8 8 10 10 10	1.167	22	2+	2.170e-08	11	174	5.154
0 0 3 4 5 6 7 8 9 10 11 14 14 14	1.167	21	2+	1.442e-08	11	8	5.831
0 1 1 2 3 3 4 5 5 6 7 7 8 8	1.114	23	1	1.196e-08	3	52	5.495
0 1 2 2 4 4 5 6 6 8 8 9 10 10	1.120	25	2+	3.658e-08	12	46	5.169
0 1 2 3 3 4 5 6 7 7 8 9 10 10	1.089	23	1	7.115e-09	0	15	5.817
0 2 2 4 4 6 7 8 10 10 12 12 14 14	1.111	25	2+	8.756e-08	16	197	5.275
0 2 2 4 5 6 7 8 9 10 12 12 14 14	1.091	24	2+	6.561e-08	16	31	5.523
0 2 3 4 5 6 7 8 9 10 11 12 14 14	1.077	32	2+	2.421e-07	28	10	5.912
0 2 3 4 6 6 8 10 10 12 13 14 16 16	1.094	22	2+	1.416e-08	8	44	5.695
0 2 4 4 6 8 9 10 12 14 14 16 18 18	1.089	22	2+	1.855e-08	7	15	5.752
1 2 3 4 5 6 7 8 9 10 11 12 13 14	1	49	0	6.872e-06	70	390	n/a

Table 49: Measures for the cyclic group polyhedron with $n = 7, r = 6$

Facet	Best-case Adaptation	Tight Inequalities	Volume	Shooting
1 2 3 4 5 6	0.629	9	2.505e-01	332
4 8 5 2 6 10	0.639	7	1.600e-01	245
6 5 4 3 2 8	0.645	7	8.787e-02	170
9 4 6 8 3 12	0.641	6	1.280e-01	253

Figure 20: Partial order for the cyclic group polyhedron with $n = 7, r = 6$

B.2 Cyclic Group Polyhedra

This section contains data on master cyclic group polyhedra. Polyhedra with $n = 7$ to $n = 14$ were tested. For each polyhedron, there is a table of facet measures and a diagram of the partial order. In the partial order diagrams, a purely horizontal line indicates a tie between the two facets.

Table 50: Measures for the cyclic group polyhedron with $n = 8, r = 7$

Facet	Best-case Adaptation	Tight Inequalities	Volume	Shooting
1 0 1 0 1 0 1	0.500	16	∞	303
1 2 1 2 1 2 3	0.612	8	1.003e-02	68
1 2 3 0 1 2 3	0.567	13	∞	230
1 2 3 4 5 6 7	0.592	12	8.116e-02	144
3 2 1 4 3 2 5	0.606	9	2.582e-02	92
7 6 5 4 3 2 9	0.607	9	1.563e-02	43
9 10 3 12 5 6 15	0.602	8	3.762e-02	120

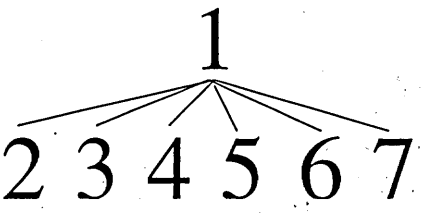

Figure 21: Partial order for the cyclic group polyhedron with $n = 8, r = 7$

Table 51: Measures for the cyclic group polyhedron with $n = 8, r = 2$

Facet	Best-case Adaptation	Tight Inequalities	Volume	Shooting
1 2 1 0 1 2 1	0.577	12	∞	367
3 6 1 4 3 2 5	0.600	10	5.526e-02	321
3 6 5 4 3 2 1	0.600	10	2.244e-03	312

Figure 22: Partial order for the cyclic group polyhedron with $n = 8, r = 2$

Table 52: Measures for the cyclic group polyhedron with $n = 8, r = 4$

Facet	Best-case Adaptation	Tight Inequalities	Volume	Shooting
1 2 3 4 3 2 1	0.603	11	3.023e-02	228
1 2 3 4 1 2 3	0.603	8	3.391e-03	259
3 2 1 4 1 2 3	0.603	8	3.003e-02	259
3 2 1 4 3 2 1	0.603	11	3.408e-03	254

Figure 23: Partial order for the cyclic group polyhedron with $n = 8, r = 4$

Table 53: Measures for the cyclic group polyhedron with $n = 9, r = 8$

Facet	Best-case Adaptation	Tight Inequalities	Volume	Shooting
1 2 0 1 2 0 1 2	0.516	20	∞	312
1 2 3 4 5 6 7 8	0.560	16	3.221e-02	170
2 1 3 2 1 3 2 4	0.577	11	5.508e-03	79
4 8 12 7 2 6 10 14	0.567	13	2.241e-02	173
8 7 6 5 4 3 2 10	0.574	13	9.321e-03	94
11 4 6 8 10 12 5 16	0.580	10	3.759e-03	57
16 5 12 10 8 15 4 20	0.570	10	1.374e-02	115

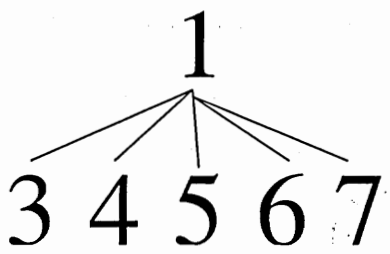

Figure 24: Partial order for the cyclic group polyhedron with $n = 9, r = 8$

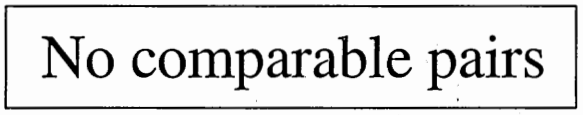

Figure 25: Partial order for the cyclic group polyhedron with $n = 9, r = 3$

Table 54: Measures for the cyclic group polyhedron with $n = 9, r = 3$

Facet	Best-case Adaptation	Tight Inequalities	Volume	Shooting
2 4 6 2 1 3 5 4	0.569	11	7.184e-03	151
2 4 6 2 4 3 2 4	0.586	10	2.738e-03	138
2 4 6 5 4 3 2 1	0.569	11	4.502e-04	159
4 2 6 4 2 3 4 2	0.586	10	2.348e-04	40
4 8 12 7 2 6 10 5	0.573	12	1.911e-03	115
5 1 6 2 4 3 2 4	0.569	11	7.124e-03	152
7 5 12 10 8 6 4 2	0.573	12	3.079e-04	116
10 2 12 4 5 6 7 8	0.573	12	4.879e-03	129

Table 55: Measures for the cyclic group polyhedron with $n = 10, r = 9$

Facet	Best-case Adaptation	Tight Inequalities	Volume	Shooting
1 0 1 0 1 0 1 0 1	0.447	28	∞	289
1 2 1 2 1 2 1 2 3	0.557	12	1.909e-04	18
1 2 3 4 0 1 2 3 4	0.516	22	∞	162
1 2 3 4 5 6 7 8 9	0.533	20	9.142e-03	118
2 4 6 3 5 2 4 6 8	0.552	13	6.387e-04	30
3 6 4 2 5 3 1 4 7	0.545	15	2.624e-03	56
4 3 2 1 5 4 3 2 6	0.548	15	1.147e-03	34
4 3 2 6 0 4 3 2 6	0.526	18	∞	121
6 2 3 4 5 6 7 3 9	0.553	12	5.010e-04	13
6 7 3 4 5 6 2 3 9	0.553	12	5.016e-04	27
9 8 7 6 5 4 3 2 11	0.547	16	1.484e-03	46
9 18 7 6 15 14 3 12 21	0.541	14	3.958e-03	86

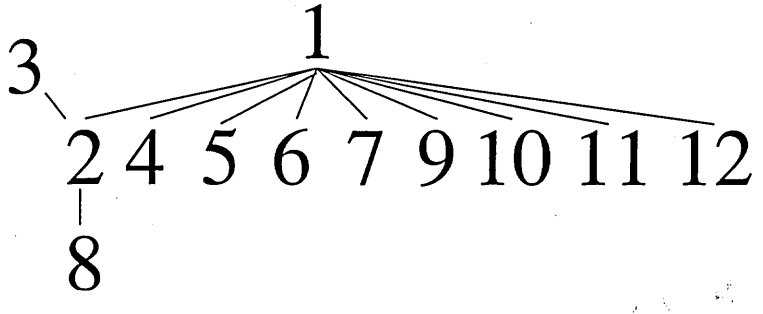

Figure 26: Partial order for the cyclic group polyhedron with $n = 10, r = 9$

Table 56: Measures for the cyclic group polyhedron with $n = 10, r = 2$

Facet	Best-case Adaptation	Tight Inequalities	Volume	Shooting
2 4 1 3 0 2 4 1 3	0.516	22	∞	198
3 6 4 2 0 3 6 4 2	0.526	18	∞	177
3 6 4 2 5 3 1 4 2	0.548	16	3.635e-04	141
4 8 2 6 5 4 3 2 6	0.552	14	9.717e-04	77
4 8 7 6 5 4 3 2 1	0.539	17	1.203e-04	199
6 12 3 4 5 6 7 8 9	0.560	11	3.521e-04	40
6 12 3 4 10 6 2 8 9	0.542	13	2.882e-03	168

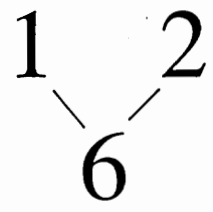

Figure 27: Partial order for the cyclic group polyhedron with $n = 10, r = 2$

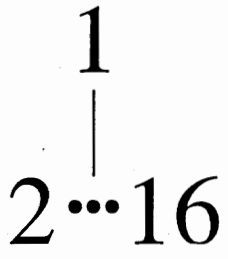

Figure 28: Partial order for the cyclic group polyhedron with $n = 10, r = 5$

No comparable pairs

Figure 29: Partial order for the cyclic group polyhedron with $n = 11, r = 10$

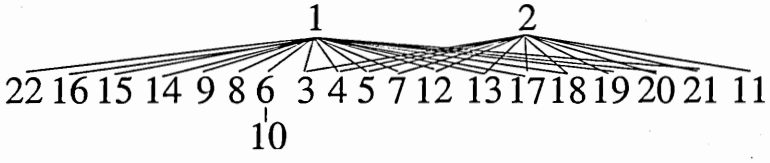

Figure 30: Partial order for the cyclic group polyhedron with $n = 12, r = 11$

Table 57: Measures for the cyclic group polyhedron with $n = 10, r = 5$

Facet	Best-case Adaptation	Tight Inequalities	Volume	Shooting
1 0 1 0 1 0 1 0 1	0.447	28	∞	271
1 2 1 2 3 2 1 2 1	0.557	12	2.172e-05	25
1 2 3 4 5 1 2 3 4	0.542	18	2.147e-03	87
1 2 3 4 5 4 3 2 1	0.542	12	1.201e-04	62
2 4 1 3 5 2 4 1 3	0.542	18	1.185e-03	91
2 4 6 8 10 7 4 6 3	0.550	12	7.555e-05	33
3 1 4 2 5 3 1 4 2	0.542	18	5.369e-04	82
3 4 1 2 5 2 1 4 3	0.542	12	1.080e-03	48
3 6 4 7 10 8 6 4 2	0.550	12	3.149e-05	35
3 6 9 12 15 8 11 4 7	0.550	13	2.662e-04	30
4 3 2 1 5 4 3 2 1	0.542	18	1.360e-04	81
4 8 2 6 10 4 3 7 6	0.550	12	2.819e-04	24
6 7 3 4 10 6 2 8 4	0.550	12	1.344e-04	36
7 4 11 8 15 12 9 6 3	0.550	13	5.029e-05	30
9 8 7 6 15 4 3 12 11	0.550	13	6.628e-04	34
11 12 3 4 15 6 7 8 9	0.550	13	4.363e-04	31

Table 58: Measures for the cyclic group polyhedron with $n = 11, r = 10$

Facet	Best-case Adaptation	Tight Inequalities	Volume	Shooting
1 2 3 4 5 6 7 8 9 10	0.510	25	2.797e-03	134
4 8 12 5 9 13 6 10 14 18	0.530	16	1.542e-04	22
4 8 12 16 9 2 6 10 14 18	0.515	21	1.989e-03	140
6 12 7 2 8 14 9 4 10 16	0.520	19	8.307e-04	69
6 12 7 13 8 3 9 4 10 16	0.526	17	3.302e-04	38
8 5 2 10 7 4 12 9 6 14	0.524	19	6.814e-04	70
9 18 5 14 12 10 19 6 15 24	0.528	14	1.344e-04	26
9 18 16 3 12 21 8 6 15 24	0.517	18	1.220e-03	89
9 18 16 14 12 10 8 6 15 24	0.536	13	7.112e-05	17
10 9 8 7 6 5 4 3 2 12	0.522	21	8.732e-04	92
13 4 6 8 10 12 14 16 7 20	0.529	16	2.245e-04	37
13 15 6 8 10 12 14 5 7 20	0.533	14	5.725e-05	12
14 6 20 12 15 18 10 24 16 30	0.534	13	1.268e-04	13
15 8 12 5 9 13 6 10 3 18	0.525	16	4.070e-04	30
16 21 4 20 14 8 24 7 12 28	0.518	16	1.138e-03	80
18 14 10 6 13 20 16 12 8 26	0.535	14	7.034e-05	15
20 7 16 14 12 10 8 17 4 24	0.525	15	2.826e-04	33
25 6 20 12 15 18 10 24 5 30	0.518	15	1.024e-03	83

Table 59: Measures for the cyclic group polyhedron with $n = 12, r = 11$

Facet	Best-case Adaptation	Tight Inequalities	Volume	Shooting
1 0 1 0 1 0 1 0 1 0 1	0.408	42	∞	239
1 2 0 1 2 0 1 2 0 1 2	0.447	38	∞	162
1 2 1 1 1 2 2 2 1 2 3	0.514	15	4.840e-06	8
1 2 1 2 1 2 1 2 1 2 3	0.514	18	7.221e-06	7
1 2 2 2 1 2 1 1 1 2 3	0.514	15	5.259e-06	10
1 2 3 0 1 2 3 0 1 2 3	0.463	35	∞	139
1 2 3 4 2 3 1 2 3 4 5	0.505	21	6.883e-05	23
1 2 3 4 5 0 1 2 3 4 5	0.477	32	∞	88
1 2 3 4 5 6 7 8 9 10 11	0.489	30	6.310e-04	94
2 1 3 2 1 3 2 1 3 2 4	0.508	20	2.063e-05	9
3 2 1 4 3 2 1 4 3 2 5	0.505	22	6.623e-05	18
3 2 3 4 1 4 1 2 3 2 5	0.505	16	2.552e-05	11
4 2 3 4 2 3 1 2 3 1 5	0.505	19	6.261e-05	13
5 2 3 4 1 6 3 4 5 2 7	0.503	19	8.128e-05	14
5 4 3 2 1 6 5 4 3 2 7	0.503	24	1.216e-04	33
5 4 3 5 1 6 2 4 3 2 7	0.503	18	5.361e-05	22
5 10 9 8 7 6 5 4 3 8 13	0.515	16	7.543e-06	6
7 2 3 4 5 6 7 8 9 4 11	0.507	19	3.062e-05	10
11 10 9 8 7 6 5 4 3 2 13	0.501	25	1.053e-04	35
11 10 9 20 7 18 5 16 15 14 25	0.510	16	1.049e-05	10
13 14 15 16 5 18 7 8 9 10 23	0.512	16	7.110e-06	6
25 14 15 28 5 30 7 20 21 10 35	0.496	18	2.012e-04	43

Table 60: Measures for the cyclic group polyhedron with $n = 12, r = 2$

Facet	Best-case Adaptation	Tight Inequalities	Volume	Shooting
1 2 1 0 1 2 1 0 1 2 1	0.471	32	∞	242
1 2 0 1 2 0 1 2 0 1 2	0.447	38	∞	220
2 4 3 2 1 0 2 4 3 2 1	0.485	27	∞	129
2 4 3 2 1 3 2 1 3 2 1	0.508	21	3.275e-06	42
5 10 3 8 7 6 5 4 3 2 7	0.509	20	2.696e-05	39
5 10 9 8 7 6 5 4 3 2 1	0.494	26	5.428e-06	146
5 10 3 8 1 6 5 4 9 2 7	0.494	26	2.671e-04	132
7 14 3 4 5 6 7 8 9 10 11	0.513	18	1.412e-05	23
7 14 9 4 11 6 7 8 3 10 5	0.513	18	2.921e-06	27

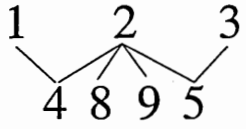

Figure 31: Partial order for the cyclic group polyhedron with $n = 12, r = 2$

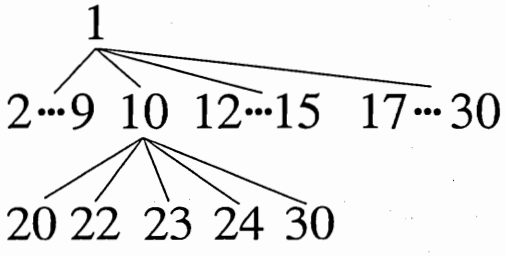

Figure 32: Partial order for the cyclic group polyhedron with $n = 12, r = 3$

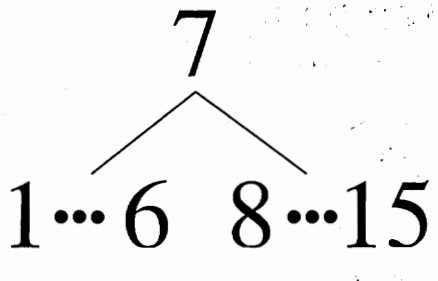

Figure 33: Partial order for the cyclic group polyhedron with $n = 12, r = 4$

Table 61: Measures for the cyclic group polyhedron with $n = 12, r = 3$

Facet	Best-case Adaptation	Tight Inequalities	Volume	Shooting
1 0 1 0 1 0 1 0 1 0 1	0.408	42	∞	224
1 2 3 2 1 1 2 1 2 2 1	0.514	14	5.145e-07	4
1 2 3 1 1 2 1 2 1 2 2	0.514	15	6.581e-06	14
1 2 3 2 1 2 2 1 1 2 1	0.514	15	1.683e-06	17
1 2 3 2 1 2 1 2 1 2 1	0.514	18	2.215e-06	20
1 2 3 2 2 2 1 2 1 1 1	0.514	14	5.639e-07	5
1 2 3 1 1 1 1 2 2 2 2	0.514	14	2.302e-06	6
1 2 3 1 2 2 1 2 1 1 2	0.514	16	7.012e-06	11
1 2 3 1 2 0 1 2 3 1 2	0.487	28	∞	63
1 2 3 0 1 2 3 0 1 2 3	0.463	35	∞	153
1 2 3 2 1 0 1 2 3 2 1	0.487	24	∞	68
2 1 3 2 1 0 2 1 3 2 1	0.487	28	∞	57
2 1 3 2 1 2 1 2 1 2 1	0.514	14	4.942e-07	5
2 1 3 2 1 2 2 1 1 2 1	0.514	16	1.642e-06	19
2 4 6 5 4 3 2 4 3 2 1	0.507	18	6.204e-07	9
3 2 5 4 3 2 1 4 3 2 1	0.505	22	2.726e-06	23
3 6 9 4 7 6 5 4 3 2 5	0.514	15	2.329e-06	9
3 6 9 8 7 6 5 4 3 2 1	0.495	22	3.514e-06	74
4 2 6 4 2 3 1 5 3 4 2	0.507	18	2.567e-06	17
5 4 9 2 7 6 5 4 3 2 7	0.508	19	8.807e-06	4
5 4 9 8 7 6 5 4 3 2 1	0.498	23	2.374e-06	42
5 10 15 8 13 6 11 4 9 2 7	0.503	22	1.078e-05	20
7 2 9 4 7 6 5 4 3 2 5	0.508	16	4.878e-06	1
7 2 9 4 5 6 7 2 3 4 5	0.508	19	4.419e-06	4
7 2 9 4 5 6 1 8 3 4 5	0.498	23	5.877e-05	33
7 2 9 4 3 6 1 8 3 6 5	0.495	22	8.930e-05	65
7 2 9 4 3 6 5 4 3 6 5	0.514	15	2.531e-06	8
7 14 21 16 11 6 13 8 15 10 5	0.512	16	3.141e-07	5
11 10 21 8 7 6 5 16 15 14 13	0.512	16	2.447e-06	4
13 2 15 4 5 6 7 8 9 10 11	0.503	22	2.641e-05	16

Table 62: Measures for the cyclic group polyhedron with $n = 12, r = 4$

Facet	Best-case Adaptation	Tight Inequalities	Volume	Shooting
1 2 3 4 2 3 1 2 3 1 2	0.508	21	1.774e-05	27
1 2 3 4 1 2 1 2 3 2 3	0.508	18	2.945e-05	37
1 2 3 4 1 2 3 2 1 2 3	0.508	21	4.566e-05	51
1 2 3 4 3 2 1 2 3 2 1	0.508	18	3.313e-06	31
1 2 3 4 3 2 3 2 1 2 1	0.508	18	2.519e-06	33
1 2 3 4 2 0 1 2 3 4 2	0.485	27	∞	146
2 1 0 2 1 0 2 1 0 2 1	0.447	38	∞	220
2 4 6 8 7 6 5 4 3 2 1	0.496	20	4.939e-06	115
2 4 6 8 4 6 5 4 3 2 4	0.514	15	4.486e-06	21
3 2 1 4 1 2 1 2 3 2 3	0.508	18	2.380e-05	23
3 2 1 4 3 2 1 2 3 2 1	0.508	21	5.054e-06	59
5 4 3 8 4 6 2 4 6 2 4	0.514	15	4.396e-06	13
5 4 3 8 7 6 5 4 3 2 1	0.502	23	2.922e-06	60
5 4 3 8 1 6 5 4 3 2 7	0.502	23	1.437e-04	67
5 4 3 8 1 6 2 4 6 2 7	0.496	20	2.378e-04	97

Table 63: Measures for the cyclic group polyhedron with $n = 12, r = 6$

Facet	Best-case Adaptation	Tight Inequalities	Volume	Shooting
1 2 1 0 1 2 1 0 1 2 1	0.471	32	∞	239
1 2 3 4 5 6 3 4 3 2 3	0.511	16	9.703e-06	17
1 2 3 4 5 6 4 2 3 4 2	0.507	19	7.420e-06	54
1 2 3 4 5 6 5 4 3 2 1	0.497	18	8.761e-06	115
1 2 3 4 5 6 1 2 3 4 5	0.497	28	2.245e-04	102
2 4 3 2 4 6 2 4 3 2 4	0.518	16	9.122e-06	36
2 4 3 2 4 6 5 4 3 2 1	0.507	19	1.897e-06	54
3 2 3 4 3 6 5 4 3 2 1	0.511	16	1.115e-06	32
3 2 3 4 3 6 1 4 3 2 5	0.511	16	2.777e-05	24
4 2 3 4 2 6 1 2 3 4 5	0.507	19	4.523e-05	36
4 2 3 4 2 6 4 2 3 4 2	0.518	16	2.207e-06	40
5 2 3 4 1 6 1 4 3 2 5	0.497	18	2.175e-04	85
5 2 3 4 1 6 3 4 3 2 3	0.511	16	1.011e-05	30
5 4 3 2 1 6 5 4 3 2 1	0.497	28	8.999e-06	92
5 4 3 2 1 6 2 4 3 2 4	0.507	19	3.028e-05	44

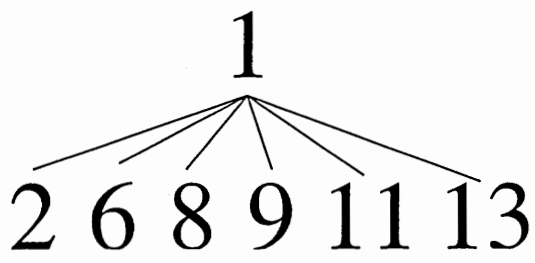

Figure 34: Partial order for the cyclic group polyhedron with $n = 12, r = 6$

No comparable pairs

Figure 35: Partial order for the cyclic group polyhedron with $n = 13, r = 12$

Table 64: Measures for the cyclic group polyhedron with $n = 13, r = 12$

Facet	Best-case Adaptation	Tight Inequalities	Volume	Shooting
1 2 3 4 5 6 7 8 9 10 11 12	0.471	36	1.698e-04	106
4 8 12 16 7 11 15 6 10 14 18 22	0.490	23	7.054e-06	20
4 8 12 16 20 11 2 6 10 14 18 22	0.475	31	1.133e-04	81
6 12 5 11 4 10 16 9 15 8 14 20	0.490	23	7.963e-06	12
6 12 5 11 17 10 3 9 15 8 14 20	0.487	24	1.205e-05	10
6 12 18 11 4 10 16 9 2 8 14 20	0.479	28	4.867e-05	51
8 3 11 6 14 9 4 12 7 15 10 18	0.487	25	1.673e-05	32
8 16 11 6 14 9 4 12 7 2 10 18	0.483	27	4.005e-05	36
9 18 14 23 6 15 24 7 16 12 21 30	0.489	20	6.181e-06	8
9 18 14 10 6 15 24 20 16 12 21 30	0.495	19	3.106e-06	7
9 18 27 10 6 15 24 20 3 12 21 30	0.476	27	7.125e-05	72
10 7 4 14 11 8 5 2 12 9 6 16	0.484	28	3.088e-05	53
10 20 30 14 24 21 18 28 12 22 32 42	0.497	17	8.823e-07	6
11 22 7 18 16 14 12 10 21 6 17 28	0.493	18	1.436e-06	7
11 22 20 18 16 14 12 10 8 6 17 28	0.495	20	2.148e-06	11
12 11 10 9 8 7 6 5 4 3 2 14	0.482	31	4.244e-05	43
14 28 16 30 18 19 20 8 22 10 24 38	0.495	18	2.042e-06	4
15 4 6 8 10 12 14 16 18 20 9 24	0.488	24	1.497e-05	34
15 4 19 8 10 12 14 16 5 20 9 24	0.485	22	1.609e-05	27
15 17 6 21 10 12 14 3 18 7 9 24	0.483	23	2.129e-05	30
15 17 6 8 10 12 14 16 18 7 9 24	0.496	19	1.931e-06	7
15 17 19 8 10 12 14 16 5 7 9 24	0.493	20	1.759e-06	8
16 19 9 12 28 18 8 24 27 17 20 36	0.494	17	1.744e-06	7
16 32 9 12 28 18 8 24 27 4 20 36	0.477	24	6.852e-05	63
17 8 12 16 7 11 15 6 10 14 5 22	0.493	20	1.670e-06	5
17 34 12 16 20 24 28 32 36 14 31 48	0.495	16	1.302e-06	2
18 10 28 20 12 17 22 14 6 24 16 34	0.494	20	2.605e-06	13
20 14 8 28 9 16 23 4 24 18 12 32	0.483	22	1.395e-05	20
20 27 8 15 22 16 10 17 24 5 12 32	0.487	20	5.575e-06	13
22 5 14 10 19 15 11 20 16 25 8 30	0.489	19	2.967e-06	6
22 18 14 23 6 15 24 7 16 12 8 30	0.488	20	6.330e-06	9
22 18 14 10 6 15 24 20 16 12 8 30	0.493	22	9.258e-06	33
24 9 20 18 16 14 12 10 8 19 4 28	0.487	22	1.156e-05	26
25 24 10 35 8 20 32 5 30 16 15 40	0.477	22	5.126e-05	44
25 24 10 22 8 20 32 18 30 16 15 40	0.493	17	2.899e-06	3
29 6 22 12 15 18 21 24 14 30 7 36	0.485	19	6.595e-06	16
30 21 12 16 33 24 15 32 36 27 18 48	0.498	16	1.260e-06	6
30 34 12 16 33 24 15 32 36 14 18 48	0.493	16	1.185e-06	2
36 7 30 14 24 21 18 28 12 35 6 42	0.478	21	5.652e-05	61
36 20 30 14 24 21 18 28 12 22 6 42	0.490	19	6.992e-06	6

Table 65: Measures for the cyclic group polyhedron with $n = 14, r = 13$

Facet	Best-case Adaptation	Tight Ineq.	Volume	Shooting
1 0 1 0 1 0 1 0 1 0 1 0 1	0.378	60	∞	2308
1 1 1 2 1 2 1 2 1 2 2 2 3	0.480	19	4.164e-08	15
1 2 1 1 1 1 2 2 2 2 1 2 3	0.480	19	3.747e-08	11
1 2 1 1 1 2 1 2 2 2 1 2 3	0.480	19	2.998e-08	11
1 2 1 2 1 1 2 2 1 2 1 2 3	0.480	18	3.914e-08	6
1 2 1 2 1 2 1 2 1 2 1 2 3	0.480	24	1.790e-07	49
1 2 2 2 1 2 1 2 1 1 1 2 3	0.480	19	4.330e-08	5
1 2 2 2 2 1 2 1 1 1 1 2 3	0.480	19	4.330e-08	16
1 2 3 4 5 6 0 1 2 3 4 5 6	0.445	45	∞	929
1 2 3 4 5 6 7 8 9 10 11 12 13	0.454	42	3.276e-05	641
2 1 1 2 2 2 1 1 1 2 2 1 3	0.480	19	3.664e-08	9
2 2 1 2 1 2 1 2 1 2 1 1 3	0.480	18	3.498e-08	14
2 2 1 2 2 2 1 1 1 2 1 1 3	0.480	19	5.913e-08	10
2 4 6 8 3 5 7 9 4 6 8 10 12	0.473	27	8.970e-07	82
2 4 6 8 10 5 7 2 4 6 8 10 12	0.468	30	3.010e-06	173
3 4 1 2 3 2 3 2 3 4 1 2 5	0.475	20	2.053e-07	28
3 6 2 5 8 4 7 3 6 9 5 8 11	0.474	26	6.499e-07	57
3 6 9 5 1 4 7 10 6 2 5 8 11	0.462	33	8.889e-06	279
3 6 9 5 8 4 7 3 6 2 5 8 11	0.474	26	4.776e-07	51
4 8 5 2 6 3 7 4 8 5 2 6 10	0.472	28	1.224e-06	95
4 8 5 2 6 10 0 4 8 5 2 6 10	0.452	37	∞	591
5 3 1 6 4 2 7 5 3 8 6 4 9	0.467	32	5.573e-06	280
5 3 8 6 4 2 7 5 3 1 6 4 9	0.467	31	1.955e-06	139
5 10 15 6 11 16 7 12 17 8 13 18 23	0.476	24	1.915e-07	20
6 5 4 3 2 1 7 6 5 4 3 2 8	0.467	34	3.695e-06	239
6 5 4 3 2 8 0 6 5 4 3 2 8	0.456	37	∞	363
6 5 11 10 2 8 7 13 5 4 10 9 15	0.471	25	6.813e-07	42
6 12 4 3 9 8 7 6 12 11 3 9 15	0.471	25	1.498e-06	91
6 12 4 10 9 8 7 6 5 11 3 9 15	0.477	21	2.690e-07	40
6 12 11 3 9 8 7 6 12 4 3 9 15	0.471	25	1.479e-06	101
6 12 11 10 9 8 7 6 5 4 3 9 15	0.477	24	7.810e-07	100
8 2 3 4 5 6 7 8 9 10 11 5 13	0.471	28	1.462e-06	124
8 9 3 4 5 6 7 8 9 10 4 5 13	0.480	22	1.500e-07	18
8 9 10 4 5 6 7 8 9 3 4 5 13	0.480	21	4.017e-08	4
8 16 3 11 12 6 14 8 9 17 4 12 20	0.469	22	8.333e-07	62
9 4 6 8 3 5 7 9 4 6 8 3 12	0.478	22	2.583e-07	43
9 4 6 8 3 12 0 9 4 6 8 3 12	0.454	33	∞	618
9 4 6 8 10 5 7 2 4 6 8 3 12	0.473	25	4.977e-07	53
9 4 13 8 3 12 7 16 11 6 15 10 19	0.470	29	1.869e-06	93
9 18 6 8 10 12 14 16 18 20 8 17 26	0.478	19	8.754e-08	22
9 18 27 8 17 12 21 16 25 6 15 24 33	0.472	23	5.906e-07	53
9 18 27 22 3 12 21 30 11 6 15 24 33	0.459	32	1.334e-05	419
9 18 27 22 17 12 21 16 11 6 15 24 33	0.477	22	3.473e-07	35

Table 65: (cont'd)

Facet	Best-case Adaptation	Tight Ineq.	Volume	Shooting
10 6 9 12 15 4 14 3 6 9 12 8 18	0.472	22	4.334e-07	28
10 13 2 12 8 4 14 10 6 16 5 8 18	0.465	26	2.714e-06	154
11 8 5 2 13 10 7 4 15 12 9 6 17	0.467	32	2.509e-06	126
11 22 5 16 13 10 21 18 15 26 9 20 31	0.475	22	2.128e-07	40
12 3 8 6 4 9 7 12 10 8 13 4 16	0.472	23	6.344e-07	50
12 24 8 20 18 9 21 12 10 22 6 18 30	0.473	18	1.915e-07	23
12 24 15 20 18 9 21 12 10 15 6 18 30	0.479	18	1.693e-07	21
13 5 11 10 9 8 7 6 5 4 10 2 15	0.471	25	6.754e-07	51
13 12 11 10 9 8 7 6 5 4 3 2 15	0.464	36	6.819e-06	374
15 16 3 18 19 6 21 8 9 24 11 12 27	0.465	27	4.123e-06	158
15 16 17 18 5 6 21 22 9 10 11 12 27	0.473	25	6.033e-07	67
15 16 17 18 5 20 7 22 9 10 11 12 27	0.475	22	1.563e-07	32
15 16 17 18 19 6 21 8 9 10 11 12 27	0.479	20	6.204e-08	14
17 6 9 12 15 18 7 10 13 16 19 8 25	0.479	21	4.257e-08	11
17 20 9 12 15 4 21 10 13 16 5 8 25	0.470	26	1.735e-06	75
17 20 9 12 15 18 7 10 13 16 5 8 25	0.477	23	2.178e-07	18
18 15 12 16 6 10 14 18 8 12 9 6 24	0.479	19	1.511e-07	12
18 15 12 16 6 17 7 18 8 12 9 6 24	0.475	19	1.438e-07	13
19 24 8 20 18 16 14 12 10 22 6 11 30	0.477	18	1.630e-07	17
25 36 5 30 27 10 35 18 15 40 9 20 45	0.460	26	1.026e-05	323
25 36 19 30 27 10 35 18 15 26 9 20 45	0.475	19	2.792e-07	36
33 24 15 34 39 30 21 12 17 36 27 18 51	0.480	19	9.547e-08	18

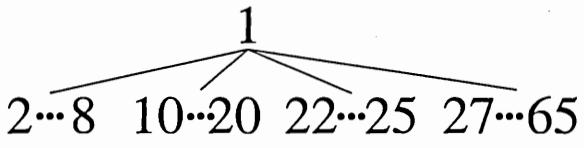

Figure 36: Partial order for the cyclic group polyhedron with $n = 14, r = 13$

Table 66: Measures for the cyclic group polyhedron with $n = 14, r = 2$

Facet	Best-case Adaptation	Tight Inequalities	Volume	Shooting
2 4 1 2 3 2 3 2 1 2 1 2 3	0.478	19	1.210e-07	50
3 6 2 5 1 4 0 3 6 2 5 1 4	0.445	45	∞	1103
4 8 5 2 6 3 0 4 8 5 2 6 3	0.456	37	∞	570
4 8 5 2 6 3 7 4 1 5 2 6 3	0.467	35	1.104e-06	550
5 10 1 6 4 2 7 5 3 8 6 4 9	0.465	32	7.057e-06	511
5 10 8 6 4 2 0 5 10 8 6 4 2	0.452	37	∞	799
5 10 8 6 4 2 7 5 3 8 6 4 2	0.472	29	1.196e-07	342
6 12 4 3 2 8 7 6 5 4 10 9 8	0.473	26	8.293e-07	224
6 12 4 3 9 8 0 6 12 4 3 9 8	0.454	33	∞	782
6 12 4 3 9 8 7 6 5 4 3 9 8	0.478	23	3.091e-07	153
6 12 4 10 2 8 7 6 5 4 10 2 8	0.468	31	2.055e-06	376
6 12 4 10 9 8 7 6 5 4 3 2 8	0.473	28	1.276e-06	342
6 12 11 10 9 8 7 6 5 4 3 2 1	0.458	37	1.915e-07	1053
8 16 3 4 5 6 7 8 9 10 11 12 13	0.475	27	9.990e-07	192
8 16 3 4 12 6 7 8 9 10 4 12 13	0.472	24	1.165e-06	172
8 16 3 11 12 6 7 8 9 10 4 5 13	0.475	22	2.701e-07	69
8 16 10 4 5 6 7 8 9 10 11 12 6	0.484	18	1.587e-08	31
8 16 10 4 5 6 14 8 2 10 11 12 6	0.469	26	3.628e-07	243
9 18 6 8 3 12 14 9 4 6 15 10 12	0.472	23	6.065e-07	169
9 18 6 8 10 12 14 9 4 6 8 10 12	0.483	18	6.656e-08	39
9 18 13 8 3 12 7 9 11 6 15 10 5	0.476	24	7.940e-08	132
9 18 13 8 3 12 14 9 4 6 15 10 5	0.469	23	1.251e-07	199
10 20 2 12 15 4 14 10 6 16 5 8 18	0.460	29	1.234e-05	662
10 20 9 12 15 4 7 10 13 16 5 8 11	0.478	22	1.951e-07	83
10 20 9 12 15 4 14 10 6 16 5 8 11	0.476	21	1.996e-07	77
12 24 15 6 4 16 14 12 10 8 20 18 9	0.474	20	1.003e-07	96
12 24 15 6 4 16 21 12 3 8 20 18 9	0.461	25	1.865e-06	665
12 24 15 6 11 16 7 12 17 8 13 18 9	0.482	18	1.481e-08	33
12 24 15 6 11 16 21 12 3 8 13 18 9	0.472	23	2.437e-07	148
12 24 15 6 18 16 7 12 17 8 6 18 9	0.475	20	5.417e-08	79
12 24 15 6 18 16 14 12 10 8 6 18 9	0.479	20	5.566e-08	56

No comparable pairs

Figure 37: Partial order for the cyclic group polyhedron with $n = 14, r = 2$

Table 67: Measures for the cyclic group polyhedron with $n = 14, r = 7$

Facet	Best-case Adaptation	Tight Inequalities	Volume	Shooting
1 0 1 0 1 0 1 0 1 0 1 0 1	0.378	60	∞	2320
1 1 1 2 2 2 3 2 1 2 1 2 1	0.480	19	3.701e-09	12
1 2 1 2 1 2 3 1 1 2 1 2 2	0.480	19	1.629e-08	13
1 2 1 2 1 2 3 2 1 1 2 2 1	0.480	19	3.701e-09	7
1 2 1 2 1 2 3 2 1 2 1 2 1	0.480	24	2.063e-08	63
1 2 1 2 1 2 3 2 2 2 1 1 1	0.480	19	5.922e-09	13
1 2 2 1 1 2 3 2 1 2 1 2 1	0.480	19	4.812e-09	12
1 2 3 2 3 4 5 4 3 2 3 2 1	0.475	20	6.066e-09	31
1 2 3 4 5 6 7 1 2 3 4 5 6	0.461	39	8.714e-06	492
1 2 3 4 5 6 7 6 5 4 3 2 1	0.461	24	1.906e-07	267
2 2 1 2 1 1 3 2 1 2 1 2 1	0.480	19	5.737e-09	12
2 4 6 1 3 5 7 2 4 6 1 3 5	0.461	39	6.156e-06	506
2 4 6 8 10 12 14 9 4 6 8 10 5	0.471	27	2.129e-07	136
2 4 6 8 10 12 14 9 11 6 8 3 5	0.468	25	3.422e-07	118
3 2 1 4 3 2 5 2 3 4 1 2 3	0.475	20	5.123e-08	21
3 4 3 2 1 2 5 2 1 2 3 4 3	0.475	20	3.989e-08	17
3 6 2 5 1 4 7 3 6 2 5 1 4	0.461	39	3.953e-06	465
3 6 5 2 1 4 7 4 1 2 5 6 3	0.461	24	1.701e-06	276
3 6 9 5 8 11 14 10 6 9 5 8 4	0.479	20	4.434e-09	10
3 6 9 12 15 18 21 10 13 16 5 8 11	0.470	28	7.122e-07	142
3 6 9 12 15 18 21 17 13 9 12 8 4	0.467	22	3.932e-08	59
4 1 5 2 6 3 7 4 1 5 2 6 3	0.461	39	2.235e-06	446
4 8 5 9 6 10 14 4 8 12 2 6 10	0.471	27	8.795e-07	112
4 8 5 9 6 10 14 11 8 5 9 6 3	0.479	20	2.833e-09	10
4 8 12 2 6 10 14 4 8 5 9 6 10	0.471	26	4.619e-07	63
4 8 12 9 13 17 21 18 15 12 9 6 3	0.467	22	2.307e-08	82
5 3 1 6 4 2 7 5 3 1 6 4 2	0.461	39	9.756e-07	471
5 3 8 6 11 9 14 12 10 8 6 4 2	0.468	25	5.761e-08	100
5 4 1 6 3 2 7 2 3 6 1 4 5	0.461	24	4.715e-06	258
5 10 8 6 4 9 14 5 3 8 6 11 9	0.479	20	1.979e-08	15
5 10 8 6 4 9 14 12 10 8 6 4 2	0.471	27	3.538e-08	131
5 10 15 6 11 16 21 12 3 8 13 18 9	0.470	28	4.900e-07	159
5 10 15 6 11 16 21 12 17 8 13 4 9	0.473	26	1.265e-07	63
5 10 15 20 25 30 35 26 17 22 13 18 9	0.471	22	3.242e-08	42
6 5 4 3 2 1 7 6 5 4 3 2 1	0.461	39	2.465e-07	452
6 5 4 10 9 8 14 6 5 11 3 9 8	0.479	20	1.804e-08	12
6 5 4 10 9 8 14 6 12 4 10 2 8	0.471	26	2.801e-07	55

Table 67: (cont'd)

Facet	Best-case Adaptation	Tight Inequalities	Volume	Shooting
6 12 4 10 2 8 14 6 5 4 10 9 8	0.471	27	5.564e-07	108
6 12 11 3 2 8 14 6 5 4 10 9 8	0.468	25	8.447e-07	112
8 2 10 4 12 6 14 8 9 10 4 5 6	0.471	26	1.699e-07	59
8 9 3 11 5 6 14 8 9 10 4 5 6	0.479	20	1.184e-08	18
8 9 10 4 5 6 14 8 2 3 11 12 6	0.468	25	4.931e-07	112
8 9 10 4 5 6 14 8 2 10 4 12 6	0.471	27	3.233e-07	144
9 4 6 8 10 5 14 2 4 6 8 10 12	0.471	26	6.497e-07	58
9 4 13 8 17 12 21 16 11 6 15 10 5	0.473	26	3.516e-08	65
9 11 6 8 3 5 14 9 4 6 8 10 5	0.479	20	6.694e-09	11
9 18 13 8 3 12 21 9 4 6 15 17 12	0.467	22	3.545e-07	69
9 18 13 8 3 12 21 16 11 6 15 10 5	0.470	28	1.503e-07	148
9 18 13 22 17 26 35 30 25 20 15 10 5	0.471	22	9.742e-09	43
10 6 2 12 8 4 14 3 6 9 5 8 11	0.468	25	1.637e-06	122
10 6 2 12 8 4 14 10 6 9 5 8 4	0.471	27	1.441e-07	136
10 6 9 5 8 4 14 10 6 2 12 8 4	0.471	26	7.322e-08	59
11 8 5 9 6 3 14 4 8 12 2 6 10	0.468	25	1.365e-06	103
11 8 5 16 13 10 21 4 15 12 9 6 17	0.473	26	4.340e-07	63
11 8 5 16 13 10 21 18 15 12 9 6 3	0.470	28	5.518e-08	159
12 10 8 6 4 2 14 5 10 8 6 4 9	0.471	26	3.649e-07	63
12 17 15 6 4 9 21 12 3 8 13 18 9	0.467	22	2.162e-07	80
13 12 4 17 9 8 21 6 12 18 3 9 15	0.467	22	6.196e-07	74
13 12 11 10 9 8 21 6 5 4 17 16 15	0.473	26	3.177e-07	61
13 12 11 10 9 8 21 6 5 18 3 16 15	0.470	28	1.347e-06	149
13 26 25 10 9 22 35 20 5 18 17 30 15	0.471	22	8.503e-08	47
15 9 3 18 12 6 21 8 9 17 4 12 13	0.467	22	4.188e-07	73
15 16 3 18 5 6 21 8 9 10 11 12 13	0.470	28	9.953e-07	154
15 16 17 4 5 6 21 8 9 10 11 12 13	0.473	26	2.340e-07	57
15 30 17 18 5 20 35 22 9 10 25 26 13	0.471	22	6.307e-08	55
17 6 9 12 15 4 21 10 13 16 5 8 11	0.473	26	1.652e-07	55
17 20 9 26 15 18 35 10 13 30 5 22 25	0.471	22	2.391e-07	36
25 22 5 30 13 10 35 18 15 26 9 20 17	0.471	22	1.201e-07	44

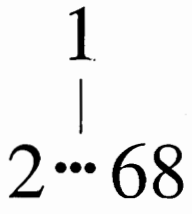

Figure 38: Partial order for the cyclic group polyhedron with $n = 14, r = 7$

REFERENCES

[1] AARDAL, K., "Capacitated facility location: Separation algorithms and computational experience," *Mathematical Programming*, vol. 81, pp. 149–175, 1998.

[2] ARÁOZ, J., EVANS, L., GOMORY, R. E., and JOHNSON, E. L., "Cyclic group and knapsack facets," *Mathematical Programming, Series B*, vol. 96, no. 2, pp. 377–408, 2003.

[3] BERTSIMAS, D. and TSITSIKLIS, J. N., *Introduction to Linear Optimization.* New York: Athena Scientific, 1997.

[4] BOLLOBÁS, B., *Random Graphs.* London: Academic Press, 1985.

[5] BRYC, W., *The Normal Distribution: Characterizations with Applications.* No. 100 in Lecture Notes in Statistics, New York: Springer-Verlag, 1995.

[6] CHERNOFF, H., "A measure of the asymptotic efficiency for tests of a hypothesis based on the sum of observations," *Annals of Mathematical Statistics*, vol. 23, pp. 493–509, 1952.

[7] CHVÁTAL, V., "Edmonds polytopes and a hierarchy of combinatorial problems," *Discrete Mathematics*, vol. 4, pp. 305–337, 1973.

[8] CHVÁTAL, V., "Hard knapsack problems," *Operations Research*, vol. 28, no. 6, pp. 1402–1412, 1980.

[9] CHVÁTAL, V., *Linear Programming.* New York: W. H. Freeman and Company, 1983.

[10] CORNUÉJOLS, G. and PULLEYBLANK, W., "A matching problem with side conditions," *Discrete Mathematics*, vol. 29, pp. 135–159, 1980.

[11] CUNNINGHAM, W. H., "Optimal attack and reinforcement of a network," *Journal of the Association for Computing Machinery*, vol. 32, no. 3, pp. 549–561, 1985.

[12] DASH, S., "Exponential lower bounds on the lengths of some classes of branch-and-cut proofs," Tech. Rep. RC22575, IBM Research Division, Sep 2002.

[13] EDMONDS, J. and JOHNSON, E. L., "Matching, Euler tours, and the Chinese postman," *Mathematical Programming*, vol. 5, pp. 88–124, 1973.

[14] EDMONDS, J., "Maximum matching and a polyhedron with 0,1-vertices," *Journal of Research of the National Bureau of Standards, Section B*, vol. 69B, pp. 125–130, 1965.

[15] EVANS, L., *Cyclic Group and Knapsack Facets with Applications to Cutting Planes.* PhD thesis, Georgia Institute of Technology, Industrial and Systems Engineering, 2002.

[16] FISCHETTI, M., GONZÁLEZ, J. J. S., and TOTH, P., "Solving the orienteering problem through branch-and-cut," *INFORMS Journal on Computing*, vol. 10, no. 2, pp. 133–148, 1998.

[17] FULKERSON, D. R., "Blocking and anti-blocking pairs of polyhedra," *Mathematical Programming*, vol. 1, pp. 127–136, 1971.

[18] GOEMANS, M. X., "Worst-case comparison of valid inequalities for the TSP," *Mathematical Programming*, vol. 69, pp. 335–349, 1995.

[19] GOEMANS, M. X. and HALL, L. A., "The strongest facets of the acyclic subgraph polytope are unknown," in *Integer Programming and Combinatorial Optimization (Vancouver, BC, 1996)*, vol. 1084 of *Lecture Notes in Computer Science*, pp. 415–429, Berlin: Springer, 1996.

[20] GOMORY, R. E., "Outline of an algorithm for integer solutions to linear programs," *Bulletin of the American Mathematical Society*, vol. 64, pp. 275–278, 1958.

[21] GOMORY, R. E., "Some polyhedra related to combinatorial problems," *Linear Algebra and Its Applications*, vol. 2, pp. 451–558, 1969.

[22] GOMORY, R. E. and JOHNSON, E. L., "T-space and cutting planes," *Mathematical Programming, Series B*, vol. 96, no. 2, pp. 341–375, 2003.

[23] GOMORY, R. E., JOHNSON, E. L., and EVANS, L., "Corner polyhedra and their connection with cutting planes," *Mathematical Programming, Series B*, vol. 96, no. 2, pp. 321–339, 2003.

[24] GRÖTSCHEL, M., LOVÁSZ, L., and SCHRIJVER, A., *Geometric Algorithms and Combinatorial Optimization.* New York: Springer-Verlag, 1988.

[25] GU, Z., NEMHAUSER, G. L., and SAVELSBERGH, M. W. P., "Lifted cover inequalities for 0-1 integer programs: Computation," *INFORMS Journal on Computing*, vol. 10, no. 4, pp. 427–437, 1998.

[26] GU, Z., NEMHAUSER, G. L., and SAVELSBERGH, M. W. P., "Lifted cover inequalities for 0-1 integer programs: Complexity," *INFORMS Journal on Computing*, vol. 11, no. 1, pp. 117–123, 1999.

[27] HOEFFDING, W., "Probability inequalities for sums of bounded random variables," *Journal of the American Statistical Association*, vol. 58, pp. 13–30, 1963.

[28] JEROSLOW, R. G., "Trivial integer programs unsolvable by branch-and-bound," *Mathematical Programming*, vol. 6, pp. 105–109, 1974.

[29] KUHN, H. W., "Discussion," in *Proceedings of the IBM Scientific Symposium on Combinatorial Problems: March 16–18, 1964*, pp. 118–121, White Plains, New York: IBM Data Processing Division, 1966. Follows the article "The Traveling Salesman Problem" by Ralph E. Gomory.

[30] KUHN, H. W., "On the origin of the Hungarian method," in *History of Mathematical Programming: A Collection of Personal Reminiscences* (LENSTRA, J. K., KAN, A. H. G. R., and SCHRIJVER, A., eds.), pp. 77–81, Elsevier Science Publishers B.V., 1991. Postscript of the article.

[31] KWAN, M.-K., "Graphic programming using odd or even points," *Chinese Mathematics*, vol. 1, pp. 273–277, 1960.

[32] MAGNANTI, T. L., MIRCHANDANI, P., and VACHANI, R., "Modeling and solving the two-facility capacitated network loading problem," *Operations Research*, vol. 43, no. 1, pp. 142–157, 1995.

[33] NEMHAUSER, G. L. and SIGISMONDI, G., "A strong cutting plane/branch-and-bound algorithm for node packing," *Journal of the Operational Research Society*, vol. 43, no. 5, pp. 443–457, 1992.

[34] NEMHAUSER, G. L. and WOLSEY, L. A., *Integer and Combinatorial Optimization.* New York: John Wiley & Sons, 1988.

[35] PADBERG, M. W., "On the facial structure of set packing polyhedra," *Mathematical Programming*, vol. 5, pp. 199–215, 1973.

[36] PADBERG, M. and RAO, M., "Odd minimum cut-sets and b-matchings," *Mathematics of Operations Research*, vol. 7, pp. 67–80, 1982.

[37] SCHRIJVER, A., *Theory of Linear and Integer Programming.* New York: John Wiley & Sons, 1986.

[38] WOLSEY, L. A., *Integer Programming.* New York: John Wiley & Sons, 1998.

VITA

Braden (Brady) Karl Hunsaker was born in Brigham City, Utah, USA on December 10th, 1974. His childhood and adolescence were spent primarily in Gainesville, Florida, though his family had previously lived in Utah, Oregon, Wisconsin, and California.

Hunsaker attended Harvard University as an undergraduate, where he graduated *magna cum laude* in 1997 with an A.B. in Mathematics. After spending a year as an intern at an international K–12 school in Stavanger, Norway, he began his graduate studies in Algorithms, Combinatorics, and Optimization at the Georgia Institute of Technology.

While in graduate school, Hunsaker married Amanda Egner in 2001.

Hunsaker earned an M.S. in Operations Research in 2001 and completed his doctoral studies in 2003. In the fall of 2003, Hunsaker joined the faculty of the University of Pittsburgh in the Department of Industrial Engineering.